Posters 6

Wednesday, August 11
17:40 – 19:00

P6-1	MEG: Motor and movement disorders
P6-2	MEG: Epilepsy
P6-3	MEG: Neurology
P6-4	MEG: Psychiatry
P6-5	Transcranial magnetic stimulation

Motor evoked response (MER) measured by MEG Utilizing MR-FOCUSS

Arcila-Londono X., [1], Bowyer S.M., [1,2,3], Mason K.M., [1], Moran J.E., [1,] Tepley N., [1,2] and Barkley G.L., [1,3]

[1]Henry Ford Health System, USA; [2]Oakland University, USA; [3]Wayne State University, USA.

ABSTRACT

MER cortex can be identified by direct cortical stimulation. Therefore, in this initial study, we set out to determine the current density mapping response using MR-FOCUSS in control subjects and patients with epilepsy. This paper suggests that a current density mapping of MER may be more useful to neurosurgeons.

KEY WORDS

Motor Evoked Response, MER, MEG, MR-FOCUSS

INTRODUCTION

There are various techniques that have been used successfully used in localizing the motor cortex, including Functional MRI [Beisteiner, 2001], Magnetic Resonace Axonography [Kamada, 2002] PET [Meyer, 2003] and MEG [Pederson , 1998]. MEG and a neuronavigational system have been used to determine the validity of the ECD localization technique for Motor mapping with MEG, where the preoperative magnetic source imaging was comparable to Electrophysiological Cortical mapping (ECM) during neurosurgery [Schiffbaur, 2002]. Those findings indicate that MEG can localize the motor cortex accurately, helping in Neurosurgical planning to avoid or decrease Neurological deficits post-procedure. To date most MEG studies have used ECD localizations. Recently a paper was published utilizing a current density mapping technique to localize the Motor Evoked Field 100 ms after electromyographic onset (MEF1) [Woldag, 2003]. MEF1 is associated with the onset of muscle movement and is usually contaminated with movement artifact. It was found that localization of MEF 1 was similar in active and passive movements: "in the region of central sulcus, directed slightly toward the precentral cortex". That establishes the localization of the readiness potential.

In contemplating the use of MEG localization information on presurgical epilepsy patients, the volume of the involved tissue is of interest to neurosurgeons. When identified, ECDs are overlaid on an MRI image, they may be misleading if the symbol locating the ECD represents a large CV. Therefore, we set out to determine if current density mapping with MR-FOCUSS is a more suitable imaging technique for brain mapping of motor cortex and investigated its routine use for the evaluation of this data. In the present study we localized the MER using an evoked finger tapping paradigm in patients with medical refractory partial epilepsy and control subjects recorded with MEG.

METHODS

Eight control subjects (4 male, 4 female) and 11 patients (7 male; 4 females) ages 7 to 60, with medical refractory partial epilepsy were monitored with 148 MEG channels (Magnes WH2500, 4D Neuroimaging). Each subject changed into a hospital gown and removed all metal articles from his/her body, except for dental work, which was demagnetized with a commercial videotape eraser. Subjects with metallic or electrical device implants were excluded. Three small coils, used to transmit subject location information to the neuromagnetometer probe, were taped to the subject's forehead with two-sided tape. One coil was located in the center of the forehead and one coil on each side, approximately 2 cm apart. Disposable ear molds of the correct size were placed in the ears and an additional localization coil was attached to each ear mold. The subject then lay comfortably on the bed inside of the magnetically shielded room, and automatic probe position routines were used to locate the head with respect to the neuromagnetometer detector coils. The neuromagnetometer helmet containing the detector array was then placed over the subject's head in close proximity to most of the cortical surface. The subject was asked to avoid both eye and body movements during data collection. Changes in the subject's position during the study were detected by changes in magnetic field locations from the coils on the forehead and ears. Runs during which the subject moved more than 0.8 cm were repeated. Data were digitized at 509 samples per second from 0.01 Hz to 100 Hz. The subject pushed a button every time he/she heard the word "on". Button pushes were performed with the middle digit. Eighty trails were averaged together to create one evoked set of data. This was performed twice on each hand.

Data analysis was carried out utilizing MR-FOCUSS [Moran, 2001] to determine location and amplitude of the cortical responses of each individual during task performance. Localizations were mapped on to each subject's MRI image. If the subject did not have an MRI scan, localizations were mapped on to a standard MRI data set of images, rescaled to fit each subject's digitized head shape [32, 33]. All MEG data was forward and backward filtered 1-50 Hz. For each subject the latency (in ms), location (x, y, z coordinates) and average amplitude of response (nAm/time point) were extracted from the MR-FOCUSS imaging results during each motor process step. The cortical regions of interest identified included: Primary and supplementary cortical areas for the motor cortex and somatosensory cortex, activation and any significant activation before or after each of these steps.

RESULTS

In our patients with focal epilepsy, the MER in 8/10 localized to the contralateral precentral gyrus. Figure 1 displays the MER localization in the in the contralateral precentral gyrus in a patient with epilepsy during a right handed finger tapping. Of the 2 that did not localize in the contralateral precentral gyrus the first was a 40 year old female patient with focal epilepsy that localized to the ipsilateral (right) precentral gyrus in both runs of right finger tapping. Her epileptic discharges were in the left fronto/parietal lobe and her seizures were associated with right arm flexion. The second was a 27-year-old male with maximal response to left hand finger tapping in the contralateral postcentral gyrus in the first run. In the second run with the same finger he had maximal response in the precentral gyrus, which also extended to the postcentral gyrus on the same side. His seizures were seen in the frontal lobe near the midline. It was not uncommon to find submaximal response in the extended area surrounding the motor cortex, such as the postcentral gyrus and middle frontal sulcus.

In our control subjects, the MER localize to the contralateral precentral gyrus in all eight. There was also submaximal response in surrounding areas, but not as widespread as with our patients with focal epilepsy.

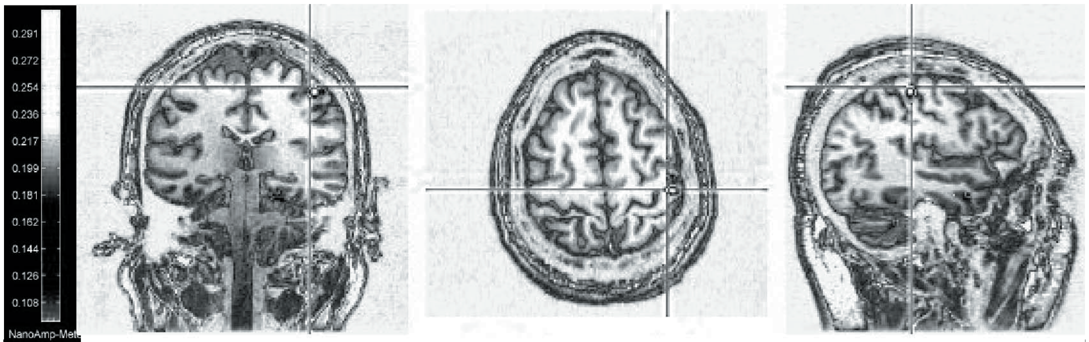

Figure1. Motor localization in the contralateral precentral gyrus in a patient with epilepsy during a right handed finger tapping.

DISCUSSION

Our goal for the last few years has been to develop ways, to measure motor response without having to resort to invasive techniques like electrocorticography. Some techniques have been useful for good temporal resolution, like somatosensory evoked potentials (from which MER is inferred), and EEG (which cannot be readily correlated with MRI). There is difficulty with functional MRI in localizing the MER if it is close to vascular lesions. SPECT and PET provide good spatial resolution, but involve radiation exposure.

In contrast, MEG measures the magnetic field produced by intracellular neuronal activity. When using ECD, it is difficult to localize the motor cortex. This technique's results represent the “center of gravity” of the source, and which is useful with stationary, non-dynamic sources (unlike movement itself). MR-FOCUSS, on the other hand is insensitive to noise and can differentiate between levels of activation. With this technique, we were able to localize the motor cortex both in patients with epilepsy and control subjects, with no significant differences in both groups

We also found that the motor evoked response usually spreads through more than one gyrus. Also the maximal response in one of our epilepsy patients corresponded to the ipsilateral precentral gyrus (with lesser activation of the contralateral precentral gyrus) and in another to the contralateral postcentral gyrus (with lesser activation of the precentral gyrus and middle frontal gyrus). That is in agreement with previous work reported by Brodal [1997] and others, and it reminds us that the motor cortex by itself is a broader area that includes, but is not limited to, the precentral gyrus. On the other hand, it lead us to think about brain plasticity, and the real availability of all the areas implicated if the one of maximal responses is affected by a lesion. Finally, with MR-FOCUSS there is the possibility of studying dynamic sources, which would allow imaging of the propagation of the signal produced by movement in real time.

ACKNOWLEDGEMENT:

Research supported by NIH/NINDS Grant RO1-NS30914.

REFERENCES

Beisteiner R, Windischberger C, Lanzenberger R, Edward V, Cunnington R, Erdler M, Gartus A, Streibl B, Moser E, Deecke L. Finger somatotopy in human motor cortex. Neuroimage. 2001 Jun;13(6 Pt 1):1016-26.

Brodal P, Bjaalie JG. Salient anatomicfetures of the cortico-ponto-cerebellar pathway. Prog. Braine Res. 1997; 114:227-249.

Kamada K, et al. Rapid identification of the primary motor area by using magneting resonance axonography. J Neurosurg. 2002; 97 (3): 558-67.

Meyer PT et al. Preoperative Motor System Brain mapping using Positron Emision tomography and statistical parametric mapping: hints of cortical reorganization. J Neurosurg Psychiatry. 2003; 74(4):471-8.

Moran JE, Bowyer SM, Tepley N: Multi-Resolution FOCUSS source imaging of MEG Data. 3rd International Symposium on Noninvasive Functional Source Imaging within the Human Brain and Heart, Biomedizinische Technik 2001; 46, 112-114.

Pedersen JR, Johannsen P, Bak CK, Kofoed B, Saermark K, Gjedde A. Origin of human motor readiness field linked to left middle frontal gyrus by MEG and PET. Neuroimage. 1998; 8(2):214- 20.

Shiffbauer H, el al. Preoperative magnetic source imaging for brain tumor surgery: a quantitative comparison with intraoperative sensory and motor mapping. J Neurosurg. 2002; 97 (6):1933-42.

Woldag H, Waldmann G, Schubert M, et al. Cortical neuromagnetic fields evoked by voluntary and passive hand movements in healthy adults. J. Clinical Neurophysiology 2003; 20:94-101.

Event Related Spectral Perturbations and Coherence in a Simple Audio-Motor Reaction Time Task

Moran, K. A., Ramirez, R. R., Jaramillo, S., Ribary, U., and Llinas, R. R.

Department of Physiology and Neuroscience, NYU School of Medicine, New York, NY 10016

ABSTRACT

Large-scale neuronal networks interact to orchestrate cognitive behavior. In this MEG study, we investigate the dynamic interactions between auditory and motor cortical activity in a simple audio-motor reaction time task. Activity was recorded with a 148-channel MEG system while subjects participated in the task. Data were analyzed with the infomax ICA algorithm. The event related spectral perturbations (ERSP), inter-trial coherence (ITC), and the inter-trial cross coherence (ITCC) of auditory and motor independent components (IC's) were computed with the wavelet transform to determine the network time-frequency dynamics. Current source density estimates were calculated with a recursive weighted minimum norm algorithm. Selected IC's localized to auditory and sensorimotor cortex. Motor component ERSPs demonstrated (1) early increases in theta power in response to onset of auditory stimulus and (2) stimulus induced suppression of alpha and beta power indicating a desynchronization followed by a resychronization of alpha, beta and gamma power. ITC showed phase locking to stimulus at theta and gamma frequency bands. ITCC identified theta band phase coherence between auditory and motor cortices. Both auditory and motor cortex exhibited simultaneous phase locking, a reset, to the auditory stimulus. Upon phase reset, motor cortex activity desynchronized in alpha and beta frequencies as a prodromic intentionality response towards movement execution. These results illustrate the complex interplay of two cortices in both synchronization and coherence of neuronal activity.

KEY WORDS

MEG, theta, gamma, somatosensory cortex, motor cortex, independent component analysis, coherence, synchronization.

INTRODUCTION

Organisms across the phylogenic span interact with their environment via sensory-to-motor transactions. A simple task such as pressing a button initiates complex brain dynamics in multiple thalamocortical regions which mediate sensory inputs and motor responses [Kansaku, 2004]. In this study, we examine the complex dynamics of auditory and motor cortices and the interactions between cortices during a simple audio-motor task.

METHODS

Seven healthy participants (four females and three males) with no known neurological or psychiatric impairments gave informed consent in compliance with a protocol approved by the local IRB. Participants ranged from 23 to 29 (mean age: 25 +/- 2.2); six participants were right handed while one was left handed. Evoked activity was recorded (bandpass filtered: 1.0 – 100 Hz, sampling rate: 508 Hz) with a 148-channel MEG system (4D Neuroimaging, San Diego) while subjects performed an audio-motor reaction time task. Participants were presented with a binaural tone and responded via an index finger button press. To ensure motivation, participants were instructed to react as fast and accurately as possible. 150-200 epochs (intertrial interval of 4000 +/- 50 ms**),** were obtained under eyes-closed conditions for left and right button press responses. Data were analyzed using the infomax ICA algorithm (EEGLAB) to isolate independent components [Delmorme, 2004]. Selection of auditory and motor components was based on time-locked averages and sensor projection vectors (Fig 1G/H, Fig.2A/C). The ERSP and the phase-locking factor (ITC) were computed with a wavelet transform [Delmorme, 2004]. The degree of cross-coherence between auditory and motor components was computed with the wavelet ITCC. The MRI of each participant was segmented into gray and white matter using the Freesurfer software package [Dale, 1999]. The sourcespace was constructed by subsampling the tessellated cortical surface. Using a recursive weighted minimum norm algorithm, current source density estimates were calculated for the selected IC's.

RESULTS

We identified a primary IC in each recording which consisted of a time-locked response to the auditory cue (Fig. 1, leftside). IC sources, displayed as sensor projection vectors, localized to auditory cortex (Fig. 2A/C). Examination of auditory time-frequency dynamics revealed an ERSP increase, synchronization in theta and alpha power (Fig. 1A). In addition, ITC calculations showed task-related phase coherence increases in theta, alpha, beta and gamma frequency bands (Fig. 1C). These results suggest that auditory cortex displays both synchronized and coherent activity (SCA) locked to the stimulus onset.

An additional class of ICs corresponding to the motor response were also identified. ICs recovered from recordings of a left-hand button-press task were localized to right sensorimotor cortex as displayed by the sensor projection vectors and the minimum-norm localization (Fig. 2B, 2D). The motor component displayed a triphasic response with prominent mu (10-12 Hz) and beta (20-30 Hz) amplitude increases (Fig. 1G). The ERSP uncovered oscillatory changes revealing an early increase in theta band power accompanied by a stimulus-induced suppression of alpha and beta power (indicating a desynchronization) followed by a rebound and resychronization of alpha, beta and gamma power (Fig. 1B). The ITC displays phase-locking to the stimulus at theta and gamma frequency bands (FIG 1D).

The interaction of motor and auditory cortices is viewed in the ITCC (Fig. 3). We observe an increased theta band phase locking between auditory and motor components immediately after stimulus presentation. This indicates a cross-cortex phase-reset to the auditory stimulus.

DISCUSSION

In this simple task, we observe SCA changes in two cortices. Gaining a better understanding of how these two cortices communicate and function will add to a greater understanding of sensorimotor transactions and their pathologies. We show that both auditory and motor cortices exhibit a simultaneous phase locking -- a reset to the auditory stimulus – which may serve as a global task-readiness signal. After this phase reset, motor cortex activity desynchronized in alpha and beta frequencies as a prodromic intentionality response towards movement execution.

Figure 1. Time-frequency analysis of auditory and motor components of one representative participant uring a left button press task. **A./B.** ERSP of selected IC's*. **C/D.** ITC of selected IC's*. **E/F.** Single trials aligned to auditory cue, amplitude of signal is represented by the colorscale. **G/H.** Average amplitude across trials; time-locked to auditory cue. *Statistically significant values (p< 0.01) were determined by the bootstrap method, all other values were set to zero.

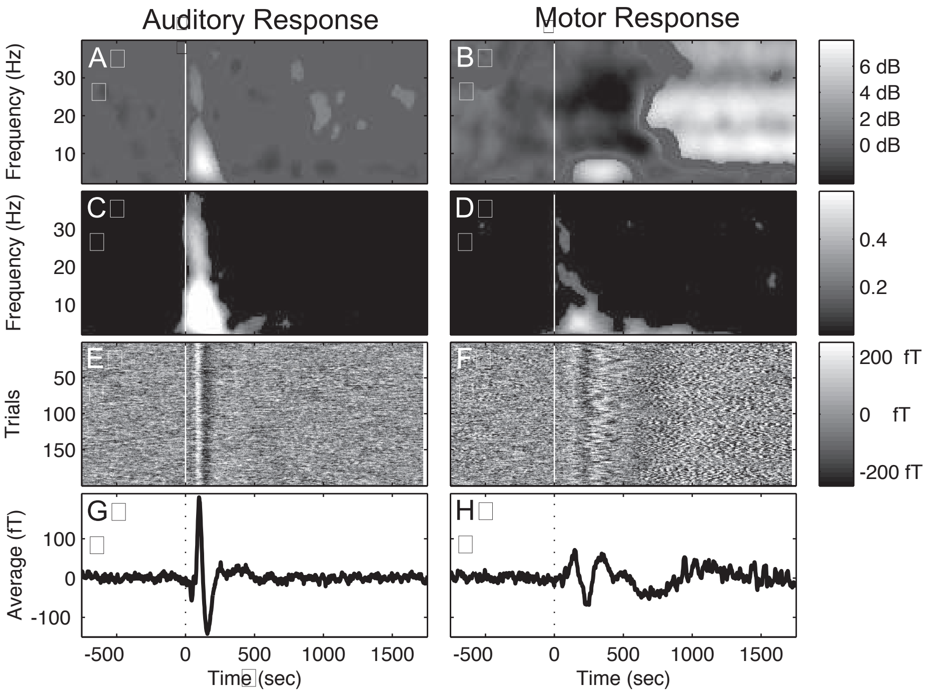

Figure 2. Spatial depiction of selected auditory and motor components. **A/B.** A two-dimensional representation of sensor projection vectors. **C/D.** Localization of selected component; displayed as an estimate of the current source density for IC, projected on inflated brain and sourcespace of participant.

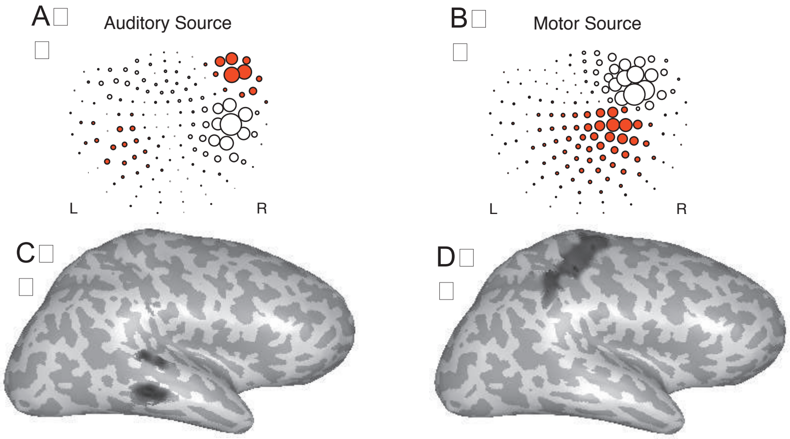

Figure 3. ITCC of selected auditory and motor components. Statistically significant values (p< 0.01) were determined by the bootstrap method, all other values were set to zero.

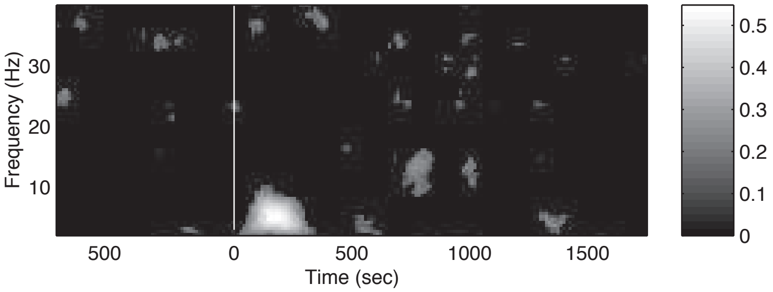

ACKNOWLEDGEMENTS

Supported by: NYUSOM GCRC (NCRR M01 RR00096) and NSF-Graduate Research Fellowship.

REFERENCES

Dale, A. M., Fischl, B. & Sereno, M. I. Cortical surface-based analysis. I. Segmentation and surface reconstruction. Neuroimage 1999; 9: 179-194.

Delorme A., Makeig S. EEGLAB: an open source toolbox for analysis of single-trial EEG dynamics including independent component analysis. J Neuroscience Methods 2004;134:9-21.

Kansaku K, HanakawaT, Wu T, Hallet M. A shared neural network for simple reaction time. Neuroimage 2004; *Article in press*.

High Resolution Neuromagnetic Imaging using Minimum-Variance Beamforming Reveals Multiple Generators of Movement-Evoked Fields in Sensorimotor Cortex

L. Bakhtazad, W. Gaetz, D. Cheyne
Neuromagnetic Imaging Lab, Hospital for Sick Children Research Institute, Toronto, Ontario, Canada

To study the role of the sensory contribution to the generation of movement-evoked fields (MEFI) and better resolve the location of MEFI generator (motor or somatosensory cortex) we recorded neuromagnetic responses during self-paced finger movements (button pressing) in six right-handed subjects using a whole-head MEG system (CTF Systems). We used a novel application of a minimum-variance beamformer algorithm (synthetic aperture magnetometry) by computing spatial filters based on the single trial data and then applying the resulting spatial filters to the averaged responses time-locked to the button press to create high resolution (2 mm) three-dimensional current source images in the hand region of the central sulcus at discrete latencies. These images were superimposed on each subject's MRI using dipole locations of the N20 median nerve response to confirm the location of primary somatosensory cortex. Images constructed for the peak of the motor field (MF) at a latency of 40 ms prior to movement onset revealed activation in the precentral gyrus hand area (MI), whereas the peak of the MEFI, 40 to 50 ms after movement onset, showed activation in the postcentral gyrus (SI) in addition to continued activation of the precentral source. This indicates that the MF and MEFI arise from multiple generators in the primary motor and somatosensory cortices, with simultaneous activation of these sources during the period of the MEFI. The latter may account for previously reported discrepancies in MEFI location based on single dipole models. In addition, we observed ipsilateral activation of precentral gyrus in 4 out of 6 subjects and occasional, weaker ipsilateral postcentral activation, confirming bilateral activation of MI prior to unilateral movements, and predominantly contralateral activation of SI following movement onset.

Supported by the Canadian Institutes of Health Research (MOP 64279) and NSERC (RGPIN 184018-02).

Impacts of fatigue on synchronization between MEG and EMG

T.W. Boonstra, A. Daffertshofer, P.J. Beek
Faculty of Human Movement Science, Vrije Universiteit, The Netherlands

In the cognitive control of action, manipulating factors like attention and fatigue influences the activity in and between different brain areas. Those factors may have an important role in action control through modulating neural dynamics in terms of neural synchronization. To investigate such modulations we recorded 151-channel whole head MEG, multi-channel bilateral EMG, and force (using MEG-compatible strain gauge meters) during rhythmic tasks that involved behavioral instabilities. In the experiment, subjects had to produce different isometric forces by adducting their thumb either between or on subsequent acoustic stimuli. When pressing between tones an increase in tempo eventually culminated in an abrupt switch to pressing in synchrony with the stimuli. Peripheral and/or central fatigue caused a decrease in transition tempos. In general, close to transitions the corresponding (kinematic and cortical) phase variability drastically increased [1,2]. Accordingly, intra-cortical and cortico-spinal synchronization (e.g., within MEG coherence and MEG/EMG coherence) was altered which was even more pronounced in the case of fatigue. If fatigue was central in origin, the enhanced fluctuations affected synchronization across a wide range of frequencies, including the movement frequency and the alpha and beta bands.

The project is financially supported by the Dutch Science Foundation (NWO, project # 051.02.050)

[1] Kaiser J, Lutzenberger W, Preissl H, Mosshammer D, Birbaumer N. 2000. Statistical probability mapping reveals high-frequency magnetoencephalographic activity in supplementary motor area during self-paced finger movements. *Neurosci. Lett.* 283; 81-84.

[2] Daffertshofer A, Peper CE, Beek PJ. 2000. Spectral analyses of event-related encephalographic signals. *Physics Lett. A* 266; 290-302.

P6-1

Mapping sensorimotor function in patients with perirolandic lesions: a comprehensive MEG protocol.

E. M. Castillo, P. G. Simos, J. W. Wheless, J. E. Baumgartner, M.E. Fitzgerald, A.C. Papanicolaou.
Vivian L. Smith Center for Neurologic Research, Department of Neurosurgery, University of Texas Houston, Medical School.

Space-occupying lesions (tumors, vascular malformations) in the vicinity of the central sulcus are often associated with the appearance of sensory and/or motor deficits. Considerable evidence supports the use of magnetoencephalography (MEG) as a valuable noninvasive tool for presurgical mapping of sensory and motor functions. In this study we test the validity and replicability of a new experimental paradigm for simultaneous sensory and motor mapping using MEG recordings. This comprehensive sensorimotor protocol (CSSMP), where external mechanic stimulation serves as a cue for voluntary movements, allows the recording of sensory and motor cortical responses during a single activation task. The stability and replicability of MEG-derived recordings during this paradigm was tested in a group of eight neurologically intact volunteers and six patients with perirolandic lesions. We found that a common sensorimotor cortical network, engaging sensory (S1, S2) and motor (M1) areas, was reliably activated in all cases and that the results remained exceptionally stable over time. Additionally, the clinical validity of the MEG-derived maps of activation was tested through intraoperative electrocortical stimulation mapping in the group of patients. The MEG-derived anatomical maps for specific sensory (S1) and motor (M1) responses were verified by direct cortical mapping and confirmed with the patient’s surgical outcome. The results of this study show that the CSSMP is a reliable and reproducible method for assessing sensory and motor areas simultaneously.

Stabilization of bimanual coordination – evidence from phase transitions

A. Daffertshofer, C.E. Peper, P.J. Beek
Faculty of Human Movement Science, Vrije Universiteit, The Netherlands

To uncover the neural basis of bimanual coordination we studied encephalographic signals (CTF 151-channel whole head MEG) during multifrequency tapping. While distinct contra- and ipsilateral cortical areas were frequency- and phase-locked to the movements, their amplitude changed markedly in the vicinity of phase transitions; frequency ratios $p{:}q \rightarrow P{:}Q$ [1]. Increases in activity locked with and ipsilateral to the slow hand can be explained in terms of an inhibitory inter-hemispheric cross-talk and phase transitions in terms of a loss of inhibition. We present a dynamical model implementing this account by assuming that macroscopic activities in bilateral primary motor cortices (M1’s) are products of self-sustained but frequency/phase-locked oscillations at the corresponding movement frequencies [2]. Both M1’s (L and R) are supposed to be linearly coupled with each other through transcallosal connections, and two bilateral (premotor) areas ($\tilde{L}$ and $\tilde{R}$) are (bi-)linearly coupled to both contra- and ipsilateral M1’s while responding (almost) instantaneously to their inputs. In turn, the activity of these units is linearly mapped to the corresponding M1. Presuming cardinal differences in time scales, we show how to formally eliminate the intrinsic dynamics of the premotor activities, at least during stable performance, yielding for the iso-frequency case the dynamics of the relative phase between the two M1’s as $\dot{\phi} = -A\sin\phi - B\sin 2\phi$. That is, besides the presence of phase transitions during multifrequency tapping, our model also provides an explanation for in- and anti-phase preferences during iso-frequency movements.

[1]Daffertshofer A, Peper CE, Beek PJ. 2000. Spatio-temporal patterns of encephalographic signals during polyrhythmic tapping. *Human Movement Science.* 19; 475-498. [2]Daffertshofer A, Peper CE, Beek PJ. submitted. Stabilization of bimanual coordination due to active inhibition – evidence from phase transitions.

Serial correlations in magneto-encephalographic recordings during voluntary rhythmic movements

A. Daffertshofer, T.W. Boonstra, P.J. Beek
Faculty of Human Movement Science, Vrije Universiteit, The Netherlands

We discuss issues of error-correction mechanisms during continued rhythmic performance. 151-channel whole head MEG (CTF) was recorded while subjects continued to tap at frequencies previously prescribed by a metronome. Voluntary rhythmic tapping is known to include eventual errors in that subjects tap at frequencies different from the one intended. On average such errors are quickly corrected within the next movement cycle. The resulting correlations between consecutive taps have been understood by splitting motor variability into a (central) 'clock variance' and a (peripheral) 'motor variance' – the latter represents an uncorrelated mapping of the motor commands to the limb with variable transfer times. On this interpretation, errors are 'corrected' without feedback in rhythmic performance. We will address questions like: Are comparable correlation functions present at the cortical level and/or along the cortico-spinal track? Do such neural areas hint at an integration of certain feedback mechanisms contrasting localized central 'clocks' for which such correlations should be absent? Explicitly, by utilizing the Hilbert transform we will show how to extract serial correlation patterns in encephalographic signals allowing for subsequent localizations of related cortical areas.

[1] Wing AM, Kristofferson AB. 1973. Response delays and the timing of motor responses. *Percept & Psychophys*, 14; 4-12.
[2] Ivry, RB., Spencer, R. M., Zelaznik, H. N., & Diedrichsen, J. 2002. The cerebellum and event timing. *Ann N Y Acad Sci, 978*, 302-317.

Neuromagnetic Imaging of Self-Initiated vs. Visually Cued Movements

W. Gaetz[1], Philippe Robaey[2], Russell Schacher[1], D. Cheyne[1]
[1]Hospital for Sick Children, Toronto, Ontario Canada;
[2]St. Justine Hospital, Montreal, Quebec Canada

Motor performance studies often employ a visual cue to initiate a response. Primate studies have shown that motor cortex is activated when a visual cue initiates a movement, but also when no movement is required. Presently, little data exists addressing this issue non-invasively in humans. We compared cortical generators activated during a self-paced motor task with a visually cued version of the same task. Neuromagnetic activity was recorded (CTF Systems Inc.) from 6 adults (M=4). For the self-paced (SP) task, subjects pressed a button with the right index finger (approx. 1 per 7 sec) for 80 trials. For the visually cued task (VC), subjects pressed the same button based on a brief (200ms) change in colour of the fixation point, where cue timing was yoked to the SP trials for each subject. The averaged MEG response for SP trials showed the expected Motor Field (MF) preceding the button press and the Movement Evoked Field (MEFI) following the button press. The VC averaged trials showed a novel time-locked activation of a Visual Cued Motor Field (VCMF; mean latency=175 ms) after cue onset, and before movement onset by 170 ms (mean RT= 347 ms) for all subjects. Responses were localized using the Synthetic Aperture Magnetometry (SAM) algorithm where spatial filter weights were calculated based on single trial data, and then applied to the peak latency observed in the averaged response (MEFI and VCMF). High res. (2mm) 3D current source images were then superimposed onto each subject's MRI. Peak VCMF activity was localized to contralateral primary motor cortex in 5 out of 6 subjects. Our MEG results are consistent with single unit studies showing cortical motor areas are activated by visual sensory input in cued motor tasks.

Supported by CIHR New Emerging Team (NET) grant.

Tomographic mapping of functional connectivity from magnetoencephalographic recordings

J. Gross, A. Schnitzler
Department of Neurology, Heinrich-Heine-University, 40225 Duesseldorf, Germany

It is well-known that specialized areas in the human brain are heavily interconnected. Recent methodological developments represent an important step towards a spatio-temporal characterization of neural interactions in the human brain. The analysis technique „Dynamic Imaging of Coherent Sources (DICS)“ has recently been introduced [1] for the tomographic mapping of power and coherence from MEG recordings in the entire brain. Coherence describes the dependence of two signals and is commonly taken as a measure of functional coupling. DICS is based on a spatial filter algorithm in the frequency domain. The forward solution is obtained from individual boundary-element models. After specification of a frequency band of interest a tomographic map of power in this frequency band is computed in the entire brain. More interestingly, a tomographic map of coherence to an external reference signal or the activity of a cerebral reference may be computed. We will demonstrate how the mapping of coherence to tremor muscle activity measured with surface electrodes allows the localization of tremor-related cerebral areas. Using these areas as cerebral reference points the cerebro-cerebral coherence may be tomographically mapped leading to the identification of frequency-specific interacting brain areas. The coupling of these areas can be further characterized by computing power or coherence spectra or phase synchronization. We will present and discuss our experiences with this methodological approach to study functional connectivity with MEG, specify the current limitations and outline ideas for future developments.

[1] Gross, J., Kujala, J., Hamalainen, M., Timmermann, L., Schnitzler, A., Salmelin, R.2001. Dynamic imaging of coherent sources: Studying neural interactions in the human brain. *PNAS U S A 98*, 694-699.

Temporal Dynamics of Ipsilateral and Contralateral Motor Activity during Voluntary Finger Movement

M.X. Huang, D.L. Harrington, K.M. Paulson, M.P. Weisend, R.R. Lee
Center for Functional Brain Imaging, New Mexico VA Health Care System, Albuquerque, NM, USA

The role of motor activity ipsilateral to movement remains a matter of debate, due in part to discrepancies among studies in the localization of this activity, when observed, and uncertainty about its time-course. The present study used magnetoencephalography (MEG) to investigate the spatial localization and temporal dynamics of contralateral and ipsilateral motor activity during the preparation of unilateral finger movements. Eight right-handed normal subjects performed self-paced finger-lifting movements with either their dominant or non-dominant hand during MEG recordings. The Multi-Start Spatial Temporal multi-dipole method [1] was used to analyze MEG responses recorded during the movement preparation and early execution stage (–800 ms to +30 ms) of movement. Three sources were consistently localized, including a source in the contralateral primary motor area (M1) and in the supplementary motor area (SMA). A third source ipsilateral to movement was located significantly anterior, inferior, and lateral to M1, in the premotor area (PMA) (Brodmann area 6). Peak latency of the SMA and the ipsilateral PMA sources significantly preceded that of the contralateral M1 source by 60 ms and 52 ms, respectively. Peak dipole strengths of both the SMA and ipsilateral PMA sources were significantly weaker than the contralateral M1 source. Altogether, the results indicated that the ipsilateral motor activity was associated with premotor function, rather than activity in M1. The time-courses of activation in SMA and ipsilateral PMA were consistent with their purported roles in planning movements.

[1] Huang, M., Aine, C.J., Supek, S., Best, E., Ranken, D., Flynn, E.R. 1998. Multi-start downhill simplex method for spatio-temporal source localization in MEG. Electroenceph Clin Neurophysiol 108:32-44.

Spatiotemporal patterns of movement-related fields in stroke patients

K. Kotani[1], Y. Kinomoto[1], M. Yamada[2], J. Deguchi[2], M. Tonoike[3], K. Horii[1], S. Miyatake[2], Kuroiwa[2]
[1]Kansai University, [2]Osaka Medical College, and [3]AIST Kansai, Japan

This study shows the analyses of the brain functions between stroke patients and normal by observing neuromagnetic fields during button pressing tasks. The measurement system included force measurement, visual stimuli presentation and MEG measurement. A 122-channel whole-head MEG system (Neuromag 122) was used in the study. A total of 18 subjects (11 post-stroke and 7 control subjects) participated in the study. The equivalent current dipoles for MRFs were estimated with the following parameters, i.e., goodness of fit (>75%), confidence volume (< 6000mm^3), and the duration of dipole (> 10msec). In addition to the single dipole analysis, Minimum Current Estimates method was applied for source estimation since neural activities for stroke patients were considered to be observed at the motor cortex of the contralateral side as well as other areas of the brain. As a result, contralateral motor cortex was activated for the normal subjects at 50msec prior to the force onset, whereas ipsilateral motor cortex was activated for some stroke patients and patients' dipole moments differed not only in their locations but also in their latencies, ranging from -150 to 50msec to the force onset. The results were in agreement with the findings by PET and f-MRI studies ([1], for example), therefore, it was implied that the compensating motor functions were shifted neighboring areas of the brain due to the recovering motor function after stroke.

Acknowledgements: This study is partially supported by the Kansai University Research Grants, 2004.

[1] Kao, Y., et al. 1998. Pilot study of functional MRI to assess cerebral activation of motor function after post stroke hemiparesis. Stroke 29, 112-122.

This poster will be also presented in Symposium 10. For the full paper, see Page 44.

Visual and Motor Cortex Interactions during a Self Paced Copy Task

F.J.P. Langheim, A.C. Leuthold, S.M. Lewis, A.P. Georgopoulos
University of Minnesota, USA

Study of a shape-copying task without visual feedback has provided insight into the temporal dynamics of mental imagery in motor output, while supporting the use of limited trial averages of motor tasks in MEG. Two subjects were presented with a fixation point, surrounded by a pentagon. After 45 seconds, the fixation point turned green cueing the subjects to begin 45 seconds of continuous pentagon copying using a joystick without feedback while fixating with eyes open. MEG data were recorded at 1017 Hz using a whole-head 248 axial-gradiometer system. Data were averaged over 7 to 17 trials after cardiac artifact removal and eye-blink exclusion. Epochs were created by averaging 1s segments centered on each of the distinct 5 corners of joystick output. Magnetic flux maps were employed to identify dipolar distributions and their relevant sensors, from which dipoles were identified in primary motor and visual cortices. Idealized source waveforms were then extracted from unaveraged data, and used for correlation analysis. This demonstrated significantly increased correlation during copy despite maintained fixation throughout the task.

(Supported by the MIND institute)

The Cerebral Network of Paced Movements

Bettina Pollok, Joachim Gross and Alfons Schnitzler
Heinrich Heine University, Düsseldorf, Germany

Even the execution of simple motor tasks involves neuronal activity in a spatially distributed network comprising cortical as well as subcortical structures. It is assumed that coherent activity between different brain areas represents functional connectivity and is essential for a successful execution of a given task. Studying the dynamic interplay between different brain areas is therefore crucial for the understanding of brain functions. The aim of the present study was to investigate brain areas associated with a unimanual auditorily paced finger tapping task and to characterize their dynamic interplay. We examined cerebro-muscular and cerebro-cerebral coupling in 7 right-handed subjects using simultaneous recordings of brain activity with a 122-channel whole-head neuromagnetometer and muscle activity of the right first dorsal interosseus with surface EMG. Our data demonstrate that task execution is associated with an oscillatory network comprising the primary sensorimotor cortex, lateral as well as mesial premotor areas, the posterior parietal cortex and thalamus contralateral and the cerebellum ipsilateral to the tapping hand. Additionally, oscillatory activity within the primary auditory cortex was observed. Connectivity and coupling direction between these areas agree well with anatomical findings. Coupling between central sources occurred predominantly at 8-12 Hz, providing evidence for the hypothesis that coupling at 8-12 Hz in a cortico-thalamic-cerebellar network represents a fundamental characteristic of the motor system.

This poster will be also presented in Workshop 14. For the full paper, see Page 141.

Cortico-muscular gamma-frequency coherence is correlated with instantaneous target probability

J.M. Schoffelen[1], R. Oostenveld[1,2], P. Fries[1]
[1]FC Donders Centre for Cognitive Neuroimaging, Nijmegen, the Netherlands
[2]Center for Sensory-Motor Interaction Aalborg University, Denmark

Oscillatory neuronal synchronization plays a functional role in information processing by the nervous system. Cortico-muscular coherence (CMC) has been found to be modulated by task parameters [1], but its functional role is still debated. Since go-cue expectancy affects spike synchronization in primary motor cortex [2], we hypothesized that CMC might be involved in motor preparation, and thus be modulated in parallel with go-cue probability in a simple reaction time task. To test this, subjects were trained to hold an isometric wrist extension until a go-cue occurred. The go-cue was a speed increase of a drifting grating that could occur between 0.05 and 3.0 s after grating onset. The instantaneous probability (hazard rate) of the go-cue was manipulated. Each subject was trained separately on two different hazard functions, i.e., linearly increasing and linearly decreasing as a function of time. CMC was assessed between the muscles involved and MEG sensors overlying contralateral motor cortex. We found reaction times to be inversely correlated with the hazard rate, indicating enhanced motor preparation during periods of high target probability. Coherence around 20 Hz was generally reduced during task performance. In contrast, CMC around 40 Hz, i.e., in the gamma-frequency range, was correlated with the hazard rate. We conclude that cortico-muscular gamma-frequency coherence may play a functional role in movement preparation.

[1] Kilner J.M. et al. 2000. Human cortical muscle coherence is directly related to specific motor parameters. J Neurosci. 8838-45.
[2] Riehle A. et al. 1997. Spike synchronization and rate modulation differentially involved in motor cortical function. Science. 1950-3.

Pathological oscillatory coupling within the human motor system in different tremor syndromes as revealed by magnetoencephalography.

Lars Timmermann, Joachim Gross, Markus Butz and Alfons Schnitzler
Department of Neurology, University Hospital Duesseldorf, Germany

Whole-head MEG-systems and the modern spatial-filter-based analysis tools recently provided new possibilities to analyze non-invasively cerebral networks of human tremor syndromes like in parkinsonian patients as well as in patients with hepatic encephalopathy (HE) with a postural tremor called “mini-asterixis”.In 6 patients with idiopathic PD we found strong coherence between the EMG of forearm muscles and activity in the contralateral primary motor cortex (M1) at tremor frequency but also at double tremor frequency. Furthermore, significant coherences were observed between M1 and medial wall areas (CMA/SMA), lateral premotor cortex, diencephalon, SII cortex, posterior parietal cortex and the contralateral cerebellum at tremor and, stronger, at double tremor frequency. In 6 patients with “mini-asterixis” and HE due to chronic liver cirrhosis excessive corticomuscular coherence occurred at the individual tremor frequency between EMG and primary motor cortex (M1) activity. Interestingly, thalamo-cortical coupling was significantly altered towards low frequencies matching the individual frequency of the mini-asterixis. Therefore, “mini-asterixis” reflects most likely a pathologically decelerated and augmented synchronized rhythmical motor cortical output possibly due to functional alterations in the motor-cortical-basal-ganglia-thalamo-cortical loops.In summary, tremor syndromes in Parkinson’s disease as well as in patients with HE and “mini-asterixis” are characterized by pathological oscillatory activity within cerebral networks of motor areas. However, the present study shows different mechanism of tremor generation in PD and HE patients.

(Supported by the Deutsche Forschungsgemeinschaft through SFB575 and the Volkswagen Stiftung)

This poster will be also presented in Workshop 14. For the full paper, see Page 144.

Applying Inverse Source Reconstruction to Investigate the Mechanisms Underlying Deep Brain Stimulation in the Treatment of Parkinson’s Disease

R.M. Webb; P. Limousin; J.C. Rothwell
Institute of Neurology, UCL, UK

Deep Brain Stimulation (DBS) via surgically implanted electrodes reduces the motor symptoms of Parkinson's disease but little is known about the mechanisms underlying its therapeutic effects. High resolution scalp EEG was recorded during 10Hz bipolar stimulation between pairs of the electrode contacts and averaged to the time of the DBS stimulus artefact. Large inter-subject variability exists in the time course and distribution of the potential. However, a positive waveform at ~20msec, distributed over the central and frontal regions ipsi-lateral to stimulation, was consistently observed. Inverse source modelling (CURRY, neuroscan) showed that in 4 of the 5 subjects the potential evoked by stimulating with the clinically effective contact was represented by single equivalent current dipole in the motor cortex. In the remaining subject the potential was well represented by a single equivalent current dipole in the sensory motor cortex. Scalp evoked potentials to DBS can be recorded and, despite the inter-subject variability, source analysis of the 20msec potential can be used as a tool to investigate the underlying physiological activations. The source models can be compared to the clinical outcomes both within subjects, by stimulating between different pairs of contacts, and between subjects. This would define whether variations in the clinical outcome are due to differences in the degree of cortical activation in specific regions or whether the exact stimulation site results in activation of different cortical regions which are associated with different clinical outcomes.

The localization of epileptic activity in the frequency and time domains using a 122-channel biomagnetometer

Anninos, P., Kotini, A., Adamopoulos, A., Pavlidis, P., Chourdakis, K.

Lab of Medical Physics, Medical School, Democritus University of Thrace, Dragana, 68100, Alex/polis, Greece

ABSTRACT

We investigated the localization of current sources for spontaneous MEG data in the frequency and time domains. MEG data are recorded as time domain signals, which have been band pass filtered. The data can been transformed from the time domain into the frequency domain by taking the fast Fourier transform of each channel of data for some epoch. This procedure gives useful information about the spatial distribution of the underlying neuronal generators. Methods: The MEG recordings were carried out in a magnetically shielded room with a whole-head 122-channel biomagnetometer. During the recordings the subject was sitting in a chair with his head covered by the helmet-shaped dewar. A head-position indicator with three small coils was fixed on the scalp. Results: Time and frequency domain analysis may be usefully combined in the analysis of data sets, which contain both transient and oscillatory components. Prominent overlapping low frequencies in the range of 2-7 Hz can be seen in the spectrum obtained from all channels whereas the alpha activities are either absent or very low. Conclusions: Time and frequency domain analysis of neuromagnetic data gives complementary information about the underlying neuronal generators. In general analysis in the time domain is appropriate for transient behavior and in frequency domain for rhythmic activity. Especially, MEG is an effective tool for localization of the epileptic zone, in some cases it can even indicates the seizure onset site and it is considered as a standard part of the diagnostic workup of most patients with epilepsy worldwide.

KEY WORDS

122-channel biomagnetometer, epilepsy, frequency domain, time domain

INTRODUCTION

Time varying electric currents, in wires or brain cells, all produce time-varying magnetic fields. Even though transmembrane, intracellular and extracellular neuronal currents each produce surrounding magnetic flux, the neuromagnetic field recordable outside of the head is a selective reflection of intracellular currents flowing in the apical dendrites of pyramidal cells oriented parallel to the skull surface. This is because of the biophysical properties of neuronal currents and the volume conduction properties of the head. The magnetic field generated by a single neuron is almost negligible; thus, when several thousands of nearby cells are synchronously active, the summated extracranial magnetic field typically achieves a magnitude of only a few hundred femto-Tesla even the strongest neuromagnetic signals-those associated with epileptic spikes are only a few thousand femto-Tesla in magnitude [Hamalainen et al., 1993; Anninos et al., 2003, 1999]. The key to successful isolation of neuromagnetic signals is to use sensors that take advantage of how the strength of a magnetic field changes as a function of distance from its source. The output of each channel of the biomagnetometer is a time varying voltage waveform that reflects local changes in magnetic flux as a function of time. The appearance of the MEG signal is very similar to that of the electroencephalogram (EEG) and both normal spontaneous rhythms and pathologic activities are readily identified in MEG waveforms. Whereas MEG signals reflect current flow in the apical dendrites of pyramidal cells oriented tangential to the skull surface, EEG reflects both tangential and radial activity [Williamson and Kaufman, 1987]. A key to locating the neuronal population that generates a neuromagnetic signal of interest is adequate sampling of the spatial pattern of the magnetic field. This is most efficiently accomplished using a multichannel biomagnetometer system [Tonoike et al., 1998; Makela et al., 1994].

METHODS

The MEG recordings were carried out in a magnetically shielded room with a whole head 122 - channel biomagnetometer [Tonoike et al., 1998; Makela et al., 1994]. The pick-up-coils of the device are shaped like figure-of-eights to make them “near-sighted”, i.e. sensitive to sources in the brain, but insensitive to the ambient noise fields. The device employs planar gradiometers, which record at each of the 61 measurement sites, the magnetic field component normal to the helmet-shaped dewar bottom surface. During the recordings the subject was sitting in a chair with his head covered by the helmet-shaped dewar. A head position indicator with three small coils was fixed on the scalp. The best-fitting equivalent current dipole (ECD) represents the location, orientation and intensity of current flow in the activated cortical source area. Typically, the whole field pattern could not be explained by one ECD and a two-dipole model was applied with one dipole located in each hemisphere. Initial guesses for the dipole locations were obtained from single-dipoles fitted to sets of channels in the neighborhood of the maximum signals. When the ECDs had been found, their locations and orientations were kept fixed while their strengths were allowed to change to explain the whole epoch. These dipole-strength vs time curves served as indicators of the temporal behavior of the active areas. Power spectra were calculated with a frequency resolution of 0.3 Hz.

RESULTS

Localization of ECD sources for alpha frequency band activity in the time domain has been performed by several groups. We use the single current dipole model applied to multi-channel MEG data to illustrate the relationship between analysis in the frequency and time domains. The spontaneous activity recorded with the 122-channel biomagnetometer (figure 1) were sampled at 400 Hz and filtered between 0.3 and 40 Hz. In figure 2 are presented the FFT transforms of the raw data for the same time period whereas in figure 3 we have the overlapping of the FFT transforms. Prominent low frequencies in the range of 2-7 Hz can be seen in the spectrum obtained from all channels whereas the alpha activities are either absent or very low. Figure 4 shows the whole-scalp distribution of the magnetic field. The arrow indicates the estimated ECD.

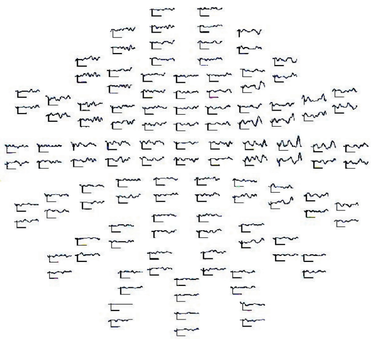

Figure 1. Spontaneous MEG activity for a specific time period.

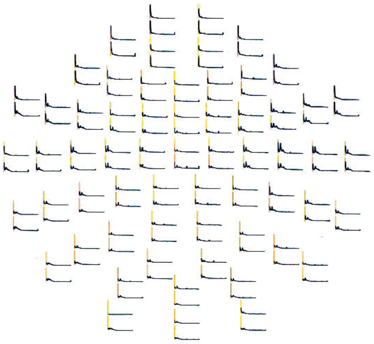

Figure 2. The FFT transform of the spontaneous MEG activity of Fig.1.

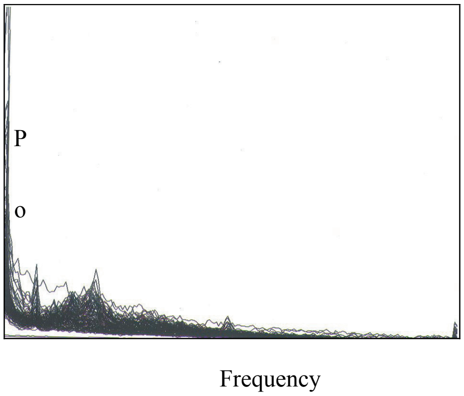

Figure 3. The overlapping of the FFT transforms of Fig.2. (Frequency range 1-20 Hz)

DISCUSSION

Time and frequency domain analysis of neuromagnetic data give complementary information about the underlying neuronal generators. In general analysis in the time domain is appropriate for transient behavior, and the frequency domain for rhythmic activity. Source localization algorithms may be applied formally for data in either domain. However, the application of a specific inversion algorithm, such as the ECD model, may or may not result in a useful inversion of the data. The utility of the algorithm depends on the goodness of fit between the structure of the sources in the model and the neuronal sources. In particular, frequency domain localization of ECD sources is useful if the underlying neuronal generators are differentiated harmonic content and spatial distribution. The existence of such sources has been demonstrated by the determination of ECD components of activity with both a sharp spectral peak and localized source volume. Both frequency and time domain analysis may be applied to the same epoch of time. The coincident occurrence of spike activity localization in the time domain and slow activity localization in the frequency domain may be an interesting tool for localization of epileptic activity. The separation of a complex set of sources underlying spontaneous activity into distinct components is an initial step in determining the functional significance of spontaneous activity.

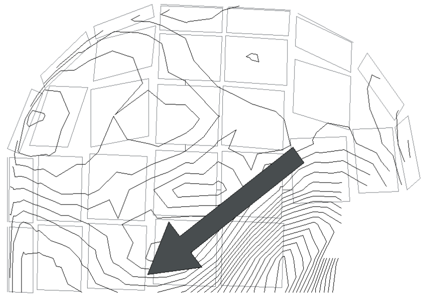

Figure 4. The MEG mapping of the scalp of the patient for the same time period.

REFERENCES

Anninos P, Kotini A, Adamopoulos A, Tsagas N. Magnetic stimulation can modulate seizures in epileptic patients. Brain Topogr 2003; 16: 57-64

Anninos P, Tsagas N, Jacobson JI, Kotini A. The biological effects of magnetic stimulation in epileptic patients. Panminerva Med 1993; 41: 207-15

Hamalainen M, Hari R, Ilmoniemi R, Knuutila J, Lounasmaa O. Magnetoencephalography -- theory, instrumentation and applications to noninvasive studies of the working human brain. Rev Mod Physics 1993; 65: 1-93

Tonoike M, Yamaguchi M, Kaetsu I, Kida H, Seo R, Koizuka I. Ipsilateral dominance of human olfactory activated centers estimated from event-related magnetic fields measured by 122-channel whole head neuromagnetometer using odorant stimuli synchronized with respirations. Ann NY Acad Sci 1998; 855:579-90

Makela JP, Hamalainen M, Hari R, McEvoy L. Whole-head mapping of middle-latency auditory evoked magnetic fields. Electroencephalogr Clin Neurophysiol 1994; 92:414-21

Congenital unilateral perisylvian syndrome: An EEG, MEG and MRI study

S. Camposano[1], A. Kotini[1], K. Hara[1], A.J. Cole[2], D. Cabello[2], PE. Grant[1], S. Stufflebeam[1], E. Halgren[1]

[1]Athinoula A. Martinos Center for Biomedical Imaging, Mass. General Hospital/Harvard Medical School, Charlestown, MA 02129, USA.

[2]Massachusetts General Hospital, Epilepsy Service, VBK-830 Fruit Street, Boston, Massachusetts 02144

ABSTRACT

We report the rare case of a 29-year-old man with congenital unilateral perisylvian syndrome (CUPS). Magnetic resonance imaging revealed extensive cortical dysplasia involving large portions of the right frontal, parietal, and temporal lobes, as well as the right insula. MEG/EEG detected spikes and a slow 3-4Hz rhythm in the right inferior frontal and insular areas. A prominent anomaly consisting of sharp 8-9 Hz activity was present in the lateral right temporal area. Auditory responses were found within the microgyric cortex in the expected location, but unexpectedly had shorter latencies and higher amplitudes in the affected hemisphere after stimulation of the ipsilateral ear. *Conclusions:* The anatomical anomaly is of greater spatial extent than the functional abnormalities. Even though it is possible to demonstrate auditory evoked potentials within the malformation, there are also abnormal contralateral effects. A part of the malformation showed clear evidence of epileptogenic and encephalopathic activity, while another part showed an abnormally exuberant alpha rhythm. Multimodal imaging is a powerful method for determining structural and functional properties of cortical malformations such as polymicrogyria.

KEY WORDS: perisylvian syndrome; polymicrogyria; EEG; MEG; frequency analysis; auditory evoked fields, epilepsy surgery.

INTRODUCTION

Congenital unilateral perisylvian syndrome (CUPS) is a rare disorder characterized mainly by the presence of a polymicrogyric cortex that affects the perisylvian region on one side. Most of the published cases of CUPS show congenital hemiparesis [Pascual-Castroviejo et al 2001, Sebire et al 1996]. Congenital bilateral perisylvian syndrome (CBPS) always shows pseudobulbar palsy with mild dysarthria, but may also present mental retardation and motor impairment [Kuzniecky et al. 1993 and1994]. CBPS is often asymmetric [Kuzniecky and Anderman1994] and it is not clear whether the unilateral form is part of a continuum that includes bilateral cases or represents a separate entity altogether. Epilepsy can be present in unilateral and bilateral cases, the reported prevalence in CBPS is up to 87% and the seizures usually begin between the ages of 4 and 12 [Kuzniecky at al 1994]. A genetic origin with different modes of inheritance has been shown for some of the bilateral forms. Intrauterine injury can produce uni- or bilateral polymicrogyria [Sebire et al 1996]. We report here a case of CUPS who was relatively asymptomatic until age 23, at which time he presented with seizures. We studied this patient with EEG, MEG, auditory and somatosensory evoked fields (AEFs and SEFs), and high resolution MRI (3T). The only previous MEG study did not address the functionality of the cortex [Tanaka et al 2000].

METHODS

Case report: The patient is a 29 year-old man with medically intractable epilepsy. His presenting event was a generalized tonic-clonic seizure at age 23, after which he continued to have frequent, stereotyped complex partial seizures in spite of aggressive pharmacotherapy. He describes a spell as a ‘weird feeling’, like a déjà vu. Afterwards he loses contact with reality. Seizure frequency has been between 2/day - 1/2month. Pregnancy, delivery and development were normal; there was no history of febrile convulsions; there were no family members with epilepsy, no head trauma, no CNS infections, and no toxic exposures. He defines himself as a ‘slow learner’ with reading problems at school, although he managed to complete high school. The neurological examination has been normal, except for a mild tremor of the left arm on extension. *Standard MRI (1.5 T)* showed extensive cortical dysplasia involving large portions of the right frontal, parietal and temporal lobes, as well as the right insula. *Fluorodeoxyglucose O^{15} PET scan* showed mild hypometabolism in the right frontal and parietal lobes and superior right temporal region, consistent with the dysplastic cortex. In the left hemisphere there was a focal area of hypometabolism within the posterior frontal/parietal region not accompanied by structural abnormalities, *LTM EEG monitoring* showed persistent, irregular slowing over the right temporal, parietal and central regions (F8, T4, T6, C4, P4), frequent sharp waves mainly in C4, with a broad field involving T4, T6, P4. Six seizures were captured, all of which were lateralized to the right hemisphere and showed maximal activity over the right paracentral, parietal and temporal regions.

PRESENT FINDINGS

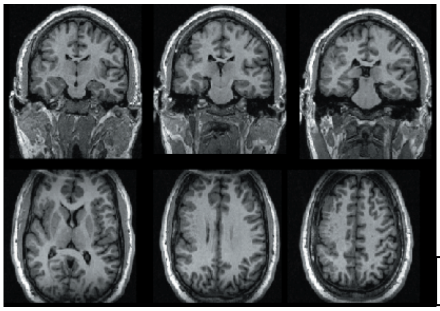

Fig 1 Coronal and axial images

The 3T MR images were partially degraded because of movement artefact and did not provide much information over and above the 1.5 T images. The reconstructed 3D image shows abnormal looking, thick gyri on the right hemisphere. The gyral folding pattern on the contralateral side could be slightly abnormal secondary to the PMG, but the gray-white junction looked normal and no PMG was present.

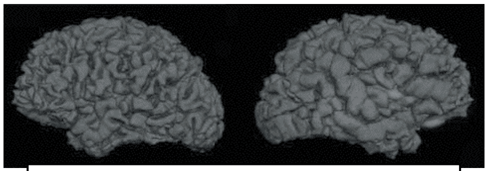

Fig 2 Reconstructed cortical surfaces

MEG/EEG PROCEDURE: 74-electrode EEG and 306-channel MEG, thirteen 4-minute sessions for recording spontaneous activity were acquired while the patient was instructed to rest or sleep. AEFs: alternating left and right beeps (ISI 0.8-1.2s, 60-75dB above hearing threshold), 70-161 trials for each ear, the responses being averaged. SEFs: median nerves were electrically stimulated (10 ms, just above motor threshold), 90-110 trials per side were averaged and stored. Equivalent current dipoles (ECDs) were estimated for interictal spikes and for evoked magnetic fields.

RESULTS: Background activity:

EEG: Asymmetric background activity was recorded on EEG and MEG, whereby a prominent, sharp 8-9 Hz rhythm with a maximal amplitude of 100 uV in T4-T6 on the right was present throughout most of the recording. The right sided 8-9 Hz rhythm did not disappear on eye opening, and did not change with drowsiness. The left side showed a smaller amplitude alpha rhythm (50uV) with normal anteroposterior gradient and reactivity. Regional right parieto-temporal, rhythmic slowing, down to 4Hz and up to 50μV in amplitude, was present during 20-30% of the recording. The distribution of spectral power can be seen on fig 3.

Fig 3. Spectral power of gradio-meters.

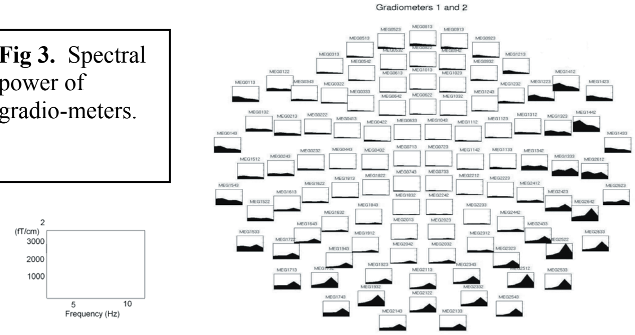

Interictal discharges (IID):

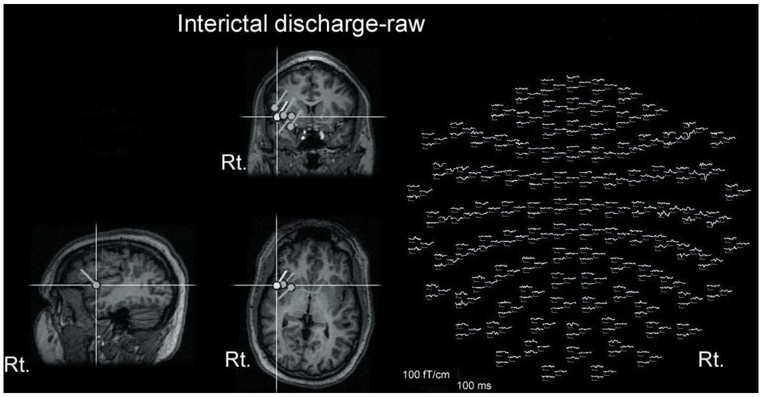

On MEG spikes were detected predominantly by the right antero- temporal sensors, including both mono- and rhythmic spikes. Many were accompanied by EEG epileptic discharges at C4, F8, although a few spikes were not accompanied by clear EEG spikes. The ECD orientations are consistently at 45 degrees between horizontal and vertical. The IID ECDs clustered around the right inferolateral frontal lobe and insula, with probable extension onto the superior portions of the temporal lobes anteriorly, an area affected by polymicrogyria. (Fig 4).

Fig 4: Example of a spike that can be recognized on the raw MEG data, and localization of the ECDs in the right inferotemporal area.

Auditory Evoked Fields (AEFs):

For both, left and right ear stimulation, the right hemispheric AEF was larger in magnitude and shorter in latency than the left AEF. The AEF ECDs were localized posterior to the epileptic discharges and lay within the area of polymicrogyria and within the expected area of the superior temporal plane (Fig.5)

Fig 5

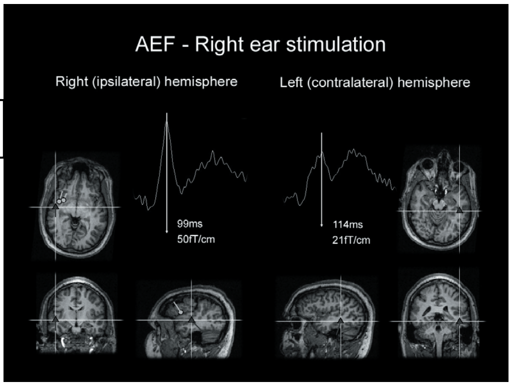
AEF - Right ear stimulation
Right (ipsilateral) hemisphere
Left (contralateral) hemisphere
99ms
50fT/cm
114ms
21fT/cm

Somatosensory evoked fields (SEFs):

Despite near maximal electrical stimulation of the median nerve at the wrists, the subject did not have a motor response of his flexor pollicis brevis, making the interpretation of the SEFs difficult. However bilateral SEFs were indeed elicited, but exhibited delayed and low amplitude N20 and P30 fields: right side: 52ms and 93ms, left side: 41ms and 67ms, both of the ECDs localized near the central sulcus. In the right side the ECD of the SEF was located at the edge of the polymicrogyria.

DISCUSSION

The epileptogenic area makes up only a part of what appears dysmorphic on the structural images. Portions of the malformation show functionality, AEFs and SEFs were present within the area of PMG. The expected contralateral AEF on the left, presumably normal hemisphere, was of lower amplitude and longer latency. This finding would suggest that the structurally abnormal hemisphere has captured some of the auditory input normally slated for the contralateral, structurally normal hemisphere. Multimodal imaging is a powerful method for determining structural and functional properties of cortical malformations such as PMG and fo great value for presurgical evaluation.

ACKNOWLEDGEMENTS: We thank Deirdre Foxe for her technical support.

REFERENCES

Kuzniecky R, Andermann F, Guerrini R. The epileptic spectrum in the congenital bilateral perisylvian syndrome. CBPS Multicenter Collaborative Study. Neurology 1994, 44: 379-85

Pascual-Castroviejo I, Pascual-Pascual SI, Viano J, Martinez V, Palencia R. Unilateral polymicrogyria: a common cause of hemiplegia of prenatal origin. Brain Dev. 2001, 23: 216-222.

Sebire G, Husso B, Dusser A, Navelet Y, Tardieu M, Landrieu P. Congenital unilateral perisylvian syndrome: radiological and clinical correlations. J. Neurol Neurosurg Psychiatry 1996; 61:52-6.

Tanaka M, Yamada K, Watanabe Y, Matsuda K, Inoue Y, Fujiwara T, Yagi K. Electroclinical and magnetoencephalographic analysis of epilepsy in patients with congenital bilateral perisylvian syndrome. Epilepsia 2000, 41: 1548-91

A comparison of the predominant lateralizations of EEG and MEG dipoles in children with intractable epilepsy

Ochi A., Otsubo H., Iida K., Elliott I., Weiss S.K., Kutomi T., Nakayama T., Sharma R., Chuang S.H., Rutka J.T., Snead O.C. III.

Division of Neurology, Diagnostic Imaging, and Neurosurgery, The Hospital for Sick Children and the University of Toronto, Toronto, Canada

ABSTRACT

We studied interictal magnetoencephalographic (MEG) and EEG dipoles to evaluate whether concordance in the predominant lateralizations of EEG and MEG dipoles can identify surgical candidacy. We selected 42 children with intractable localization-related epilepsy who had undergone video-EEG monitoring, magnetic resonance imaging (MRI), and MEG. We defined predominant lateralization as >50% of EEG or MEG dipoles localized in an ipsilateral hemisphere. The predominant lateralization of MEG and EEG dipoles was concordant in 35 patients (83%) and discordant in 7 (17%). In 35 patients with concordant lateralization, 24 patients had lateralized ictal onset, 22 had lateralized MRI lesions, and 20 patients underwent focal resection. Sixteen of 20 patients showed good surgical outcome. In 7 patients with discordant lateralization, lateralized ictal onset and MRI lesions were seen in one each, and none of them underwent focal resection. Concordance between lateralized EEG and MEG dipoles indicates a unilateral epileptogenic lesion. Discordance between EEG and MEG dipole lateralizations indicates complex epileptic regions in bilateral hemispheres.

KEY WORDS

MEG dipoles, EEG dipoles, lateralization, intractable epilepsy, children

INTRODUCTION

Patients with intractable localization-related epilepsy, secondary bilateral or multilobar interictal discharges, and a single epileptogenic zone now have better opportunities for seizure control (Malow 1999, Hufnagal 2000). Variability in interictal epileptiform discharges is likely to reflect this propagation (Hufnagal 2000). Equivalent current dipole analyses applied to scalp-EEG and magnetoencephalographic (MEG) data reveal this variability by quantifying interictal epileptiform discharges and localizing their sources in the brain. Since EEG and MEG dipole analyses visualize the orientations, phases, and extents of epileptic discharges differently, their results are complementary (Ochi 2001a). A combination of the two methods may help to elucidate the behaviour of interictal epileptiform discharges.

We analyzed EEG and MEG dipoles for interictal epileptiform discharges from children with intractable localization-related epilepsy. We identified predominant lateralization of dipoles that clustered predominantly in one region or hemisphere. We compared the EEG and MEG dipoles with ictal onset discharge distributions from prolonged video-scalp EEG recordings and with magnetic resonance images (MRI). Our objectives were 1) to evaluate the concordance or discordance between the predominant lateralizations of EEG and MEG dipoles; and 2) to evaluate whether combining lateralization data from EEG and MEG dipole analyses can identify surgical candidacy.

METHODS

We retrospectively studied 42 children (24 girls and 18 boys; mean age, 9.0 years; range, 5 months - 16 years) who presented with intractable, possible localization-related epilepsy and who underwent prolonged video-EEG recordings. All patients had MRI studies, MEG spikes, and prolonged video-EEG recordings.

We recorded video-EEG telemetry (BMSI 5000, Nicolet, Madison, WI) using 19 or 25 scalp electrodes placed according to the International 10-10 system (subtemporal electrodes; F9, F10, T9, T10, P9 and P10). Sampling rate was 200 Hz. We archived interictal periods from video-EEGs for several hours and detected interictal epileptiform discharges using a spike detection program (Insight, Persyst Development, Prescott, AZ). Thereafter, we visually selected focal interictal epileptiform discharges with high signal-to-noise ratio for EEG dipole analyses (Ochi 2000, Ochi 2001b). We used a single moving dipole inverse-solution algorithm, a three-shell spherical head model, and standard electrode-positioning data (SynaPointPro, NEC, Tsukuba, Japan) (Ochi 2000, Ochi 2001b). A dipole model fit was calculated every 5 ms. We analyzed the dipole localizations of individual interictal epileptiform discharges without averaging. For each epileptiform discharge, we performed dipole calculations from spike onset to the maximum negative peak at each time point, and chose one dipole that had a goodness of fit greater than 95%.

Thirty-eight of 42 patients had MEG studies that were performed at The Hospital for Sick Children, in Toronto, using a whole-head gradiometer Omega system (151 channels, CTF, Port Coquitalam, BC, Canada). Sampling rate was 625 Hz. The remaining 4 patients had MEG studies that were performed at the Scripps Clinic and Research Foundation in San Diego, CA, using a whole-head Magnes 2500 WH (148 channel) magnetometer (4D Neuroimaging, San Diego, CA). Sampling rate was 300 Hz. MEG epileptic events, spikes and sharp waves (referred to as spikes), were visually identified by examining the MEG recordings and were cross-referenced with the simultaneous EEG recording. At times, we identified MEG epileptic spikes without corresponding EEG spikes. We selected the earliest spike component of the interictal epileptiform discharges for EEG and MEG dipole analysis. We applied a single moving dipole analysis with a single-shell, whole-head, individually-created spherical model for a period of 50 ms before and after the peak of each spike. We defined the MEG dipole for each spike as a single dipole fit with the criteria of a residual error of less than 30%.

We defined predominant lateralization as >50% of EEG or MEG dipoles localized in an ipsilateral hemisphere. When the predominantly lateralized EEG and MEG dipoles localized in the same hemisphere, we considered the dipole distribution to be **concordant**; when the predominantly lateralized EEG dipoles localized in the hemisphere contralateral to the predominantly lateralized MEG dipoles, we considered them to be **discordant.**

RESULTS

For EEG dipole analysis, we identified from 23 to 161 interictal epileptiform discharges (mean, 76 discharges) per patient from prolonged video-EEG studies, from which we obtained 7 to 81 dipoles (mean, 33 dipoles). We identified from 19 to 493 interictal MEG epileptic discharges (mean, 143 discharges) per patient, from which we obtained 4- to 323 MEG dipoles (mean, 70 dipoles).

Predominant lateralization of EEG and MEG dipoles were concordant in 35 (83%) of the 42 patients (Group A). Predominant lateralization of EEG and MEG dipoles were discordant in 7 patients (17%, Group B).

In Group A, ictal onset EEG discharges lateralized in 24 (69 %) patients, including 9 with regional and 15 with hemispheric distributions, but did not lateralize in 11 consisting of 6 bilateral and one multiple distributions, and 4 generalized voltage attenuations. MRI lesions were found in 26 (74%) patients and lateralized in 22 (63%), including 12 with regional and 10 with hemispheric distributions. Lesions consisted of cortical dysplasia in 15, mesial temporal sclerosis in 5 (including dual pathology in 2), cyst, tumor or atrophic hemisphere in 2 each, tuberous sclerosis complex or gliosis in one each. Lesions were not lateralized in 4, including 1 with bilateral and 3 with multiple distributions. MRI findings were nonspecific in 3 and normal in 6. Twenty patients in Group A underwent focal resection using intra- or extra-electrocorticography. Sixteen patients (80%) showed good surgical outcome.

In Group B, 4 patients had generalized ictal onset EEG discharges, 2 with bilateral and 1 with regional discharges. MRI showed multiple cortical tubers in 3 patients and cortical dysplasia in one. Three patients had normal MRI. None of the 7 patients underwent focal resection.

Table 1, Correlation of predominant lateralization of MEG and EEG dipoles, ictal EEG dishcharges and MRI lesions in 42 patients

	Concordant lateralization (Group A)	Discordant lateralization (Group B)
# of patients(%)	35 (83%)	7 (17%)
Lateralized ictal discharges	24 [69%]	1 [14%]
Lateralized MRI lesions	22 [63%]	1 [14%]
Focal resection	20 [57%]	-
Good surgical outcome	16/20(80%)	NA

DISCUSSION

Two-thirds of the patients in Group A had lesions in a hemisphere with concordant EEG and MEG lateralization. Concordant EEG and MEG dipole localizations probably delineate a tightly connected unifocal epilepsy network. Gilliam et al. (Gilliam 1997), reporting on patients with mesial-basal temporal lobe epilepsy, found that patients with concordantly lateralized interictal EEG and MRI abnormalities had a better surgical outcome than patients with concordantly lateralized MRI lesions and ictal EEG results with nonlateralizing interictal EEG spikes.

We selected and analyzed the earliest spike component of the interictal epileptiform discharges for EEG and MEG dipoles. Hufnagel et al. (Hufnagal 2000), using a computer program for automatic detection of interictal spikes, analyzed intracranial EEG data and reported that the zones of the earliest spike and seizure origin were highly correlated. The first detectable peak of both MEG and EEG had a high topographic correlation with the epileptic generator eliciting the seizures. The concordance between lateralized EEG and MEG dipoles indicates a unilateral epileptogenic lesion which is surgically resectable.

When the predominant EEG and MEG dipoles were localized in opposite hemispheres, the ictal EEG discharges tended to be bilateral or generalized. In our study, patients with discordant predominant lateralizations of EEG and MEG dipoles had no lesion or multiple lesions. Siegel et al. (Siegel 2001) studied 43 patients with intractable localization-related epilepsy and normal MRIs. From noninvasive video- and scalp-EEG monitoring studies, they concluded that invasive monitoring should be avoided in patients with evidence of multifocal seizure origin. Malow et al. (Malow 1999) reported that all subjects with bilateral temporal interictal epileptiform discharges and normal MRIs or widespread abnormalities on MRI had postoperative residual seizures. The opposite lateralization of EEG and MEG dipoles supports their conclusions and indicates bilaterality in epileptic regions without a specific epileptogenic lesion.

A comparison of the predominant lateralizations of EEG and MEG dipoles allows us to understand the behaviour of epileptic activities in the abnormal neural networks of children with intractable localization-related epilepsy.

REFERENCES

Gilliam F, Bowling S, Bilir E, et al. Association of combined MRI, interictal EEG, and ictal EEG results with outcome and pathology after temporal lobectomy. *Epilepsia* 1997;38:1315-20.

Hufnagel A, Dümpelmann M, Zentner J, et al. Clinical relevance of quantified intracranial interictal spike activity in presurgical evaluation of epilepsy. *Epilepsia* 2000;41:467-78.

Malow BA, Selwa LM, Ross D, Aldrich MS. Lateralizing value of interictal spikes on overnight sleep-EEG studies in temporal lobe epilepsy. *Epilepsia* 1999;40:1587-92.

Ochi A, Otsubo H, Shirasawa A, et al. Systematic approach to dipole localization of interictal EEG spikes in children with extratemporal lobe epilepsies. *Clin Neurophysiol* 2000;111:161-8.

Ochi A, Otsubo H, Sharma R, et al. Comparison of electroencephalographic dipoles of interictal spikes from prolonged scalp video-electroencephalography and magnetoencephalographic dipoles from short-term recording in children with extratemporal lobe epilepsy. *J Child Neurol* 2001a;16:661-7.

Ochi A, Otsubo H, Chitoku S, et al. Dipole localization for identification of neuronal generators in independent neighboring interictal EEG spike foci. *Epilepsia* 2001b;42:483-90.

Siegel AM, Jobst BC, Thadani VM, et al. Medically intractable, localization-related epilepsy with normal MRI: presurgical evaluation and surgical outcome in 43 patients. *Epilepsia* 2001;42(7):883-8.

Epileptic discharges of MEG using synthetic aperture magnetometry: Comparison to intracranial epileptic discharges over the epileptogenic zone

Otsubo H., Oishi M., Suyama Y., Iida K., Ochi A., Weiss S. K., Xiang J., Gaetz W., Cheyne D., Chuang S.H., Rutka J.T., O.C. Snead III.

Divisions of Neurology, Diagnostic Imaging, and Neurosurgery. The Hospital for Sick Children, Canada

ABSTRACT

We conducted this study to identify the reliability of synthetic aperture magnetometry (SAM) for epileptic spikes at virtual intracranial sites. We retrospectively simulated SAM analysis for preoperative MEG data of 10 children with neocortical epilepsy. We compared the interictal discharges on SAM-virtual sensor (SAM-VS) with identically located cerebral sites on electrocorticography (ECoG) in individual patients. In 9 out of 10 patients, the main features of interictal activities on both SAM-VS and ECoG correlated well in morphologic features and distributions. In addition, SAM-VS showed the deep-seated epileptiform discharges in 3 patients. SAM-VS is comparable to ECoG in revealing interictal epileptiform discharges.

KEY WORDS

Magnetoencephalography, Synthetic aperture magnetometry, Children, Neocortical epilepsy, Intracranial EEG, Virtual sensor, Epileptogenic zone

INTRODUCTION

Surgical treatment for neocortical epilepsy (NE) is challenging due to the difficulties in determining the exact epileptic cortical areas to be resected. A long-term electrocorticography (ECoG) using implanted intracranial electrodes is invasive, but is often performed for patients with NE to localize the precise epileptic cortex.

Magnetoencephalography (MEG) is one of the neuroimaging tools and can localize the source of a brain activity by calculating inverse and forward problems from weak magnetic fields generated by the intraneuronal current (Otsubo 2001a). The equivalent current dipole (ECD) analysis has been recognized as the simplest and the most convenient way to analyze MEG data of epilepsy patients. MEG is expected to reduce the necessity of the invasive ECoG recording. Previous authors have described that the ECDs for interictal epileptic discharges detected the seizure focus in NE patients (Minassian 1999, Otsubo 2001b). However, this method shows the cortical activity at one location, called a center of gravity. Unless the ECDs are clustering, the characteristics and distributions of the epileptic activity cannot be provided by a single ECD.

Synthetic Aperture Magnetometry (SAM) is a new method to analyze MEG data (Robinson 1998). This spatial filtering technique based on a minimum-variance beamformer uses the specific mathematical algorithms. It theoretically shows the time-course of estimated source activity at any locations (SAM-virtual sensor, SAM-VS) in the brain as if an intracranial electrode was recording cortical activity. Therefore, SAM has the possibility to provide supplement information to overcome the current ECD results. Our purpose of this study is to identify the reliability of SAM-VS for intracranial activities in NE patients, comparing with ECoG data.

METHODS

We retrospectively studied 10 children (six boys, four girls; age 7-17 years, mean 11.9), who underwent the long-term ECoG recording using intracranial electrodes and surgical treatment for their intractable NE between June 2001 to November 2003 at the Hospital for Sick Children, Toronto, Canada.

A whole-head MEG system (Omega; CTF Systems Inc., Port Coquitalam, BC, Canada) was used to collect MEG data in all patients. During the recording, the patients were placed in a supine position under sleep deprivation or general anesthesia. We collected 2-minute minimum 15 data sets.

Subdural grid electrodes were implanted to record ECoG. The recordings started from the same day of implantation and lasted for 4 to 5 days. After obtaining of minimum 3 seizures and functional mapping, we determined and resected the epileptic areas.

We retrospectively analyzed patients' MEG data (5 data sets, 2-minute each) using SAM software (CTF System Inc.). On the patient's brain MRI, 20 to 30 positions on the cerebral surface were manually marked for SAM-VS, as covering the areas where subdural grids were actually placed. The calculated activities on those positions were visualized as the waveform (nAm) along with time course (sec).

We compared between SAM-VS and ECoG data in individual patients, which both were 10-minute data with most interictal epileptiform discharges and without artifacts. For ECoG analysis, we used an automatic spike cluster analysis (Insight; Persyst, USA) to define morphologic features of interictal discharges and distributions of each clustering discharges. For SAM-VS analysis, we visually evaluated all epileptic discharges to compare with result of ECoG analysis in morphologic features and distributions.

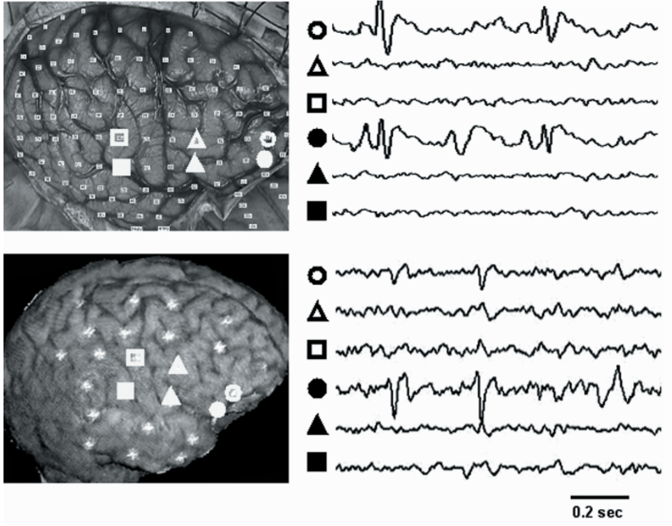

Fig.1. Wave form examples of ECoG (Upper) and SAM-VS (Lower) in patient No.1
Open and closed circles, triangles, and squares represent the positions of electrodes in right inferior frontal region for both ECoG and virtual sensors of SAM. This patient shows focal epileptiform discharges over the same right frontal pole and basal region on both ECoG and SAM-VS.

RESULTS (Table 1)

Main morphologic features of epileptic discharges on ECoG in 10 patients consist of focal discharges in 4, focal rhythmic (sharp) train in 2, multiple independent spikes in 2, widely distributed spike discharges in 1, and focal discharges and low-amplitude fast activities in 1.

Then SAM-VS demonstrated the similar results to ECoG classifications, focal discharges in 4 out of 4, focal rhythmic (sharp) train in 2 out of 2, multiple independent spikes in 2 out of 2, and widely distributed spike discharges in 1 out of 1. In 1 patient (case No.10), only focal discharges were observed on SAM-VS. In 6 patients, additional minor findings of focal discharges, were identified on ECoG. Three of them were observed on SAM-VS.

We obtained total 22 locations of frequent epileptiform discharges in 10 patients from ECoG clustering analysis. SAM-VS showed the same distributions in 16 regions.

DISCUSSION

The present study showed that the epileptiform discharges on SAM-VS in NE patients are comparable to those of ECoG in their morphologies and distributions. The main interictal ECoG findings of individual patients were identically presented on SAM-VS, instead of separated recording sessions.

SAM-VS can have some advantages to the classical ECD method. First, SAM-VS can reveal the spike morphologies of intracranial activities, which ECDs do not provide. We can distinguish the characteristics in morphologies of each epileptiform discharges. Second, SAM-VS shows the distribution pattern of discharges such as focal, widespread, or multi-focal, compared to the each ECD which shows only the center of the gravity.

On the other hand, the ECD method has the great advantage in simply showing the location of the active source on the co-registered brain MRI. The latest SAM-kurtosis analysis is now being to visualize SAM results on the patient's MR images. Thus, establishing SAM makes MEG data analysis more objectively than present ECDs analysis.

The final goal of our investigation is that MEG replaces the invasive ECoG monitoring in surgery for NE patients. The ictal onset region plays the important role to determine the areas to be resected. MEG has the limitation to collect interictal data in most of the studies. Some studies, however, indicated that the spatial extent of interictal discharges on ECoG predicted the primary epileptic area (Hufnagel 200, Asano 2003). According to those results, SAM-VS analysis of interictal discharges may have a potential to replace the invasive monitoring, since the further analysis of virtual interictal zone on the SAM-VS may provide the real epileptogenic zone.

TABLE 1. Summary of the morphologic features and distributions of ECoG and SAM-VS

Patient's number	ECoG		SAM-VS			
	spike clustering ananlysis	locations	spike clustering ananlysis	locations		
1	focal discharges^{M}	basal-polar F	focal discharges^{M}	basal-polar F		
2	focal discharges^{M}	perisylvian	focal discharges^{M}	intrasylvian	(+)	
	focal discharges	C	focal discharges	C		
3	focal discharges^{M}	basal T-O	focal discharges^{M}	basal T-O		
	focal discharges	lateral P	focal discharges	lateral P		
	focal discharges	lateral O	focal discharges	lateral O		
4	focal discharges^{M}	perisylvian	focal discharges^{M}	intrasylvian	(+)	
	focal discharges	lateral P				E^{1}
5	focal rythmic (sharp) train^{M}	lateral F	focal rythmic (sharp) train^{M}	lateral F	(+)	
	focal discharges	C	focal discharges	C		
	focal discharges	lateral P				E^{2}
6	focal rythmic (sharp) train^{M}	perisylvian	focal rythmic (sharp) train^{M}	intrasylvian	(+)	
	focal discharges	C				E^{3}
	focal discharges	lateral P				E^{4}
7	multiple independent spikes^{M}	lateral F ~ lateral P	multiple independent spikes^{M}	lateral F ~ lateral P		
8	multiple independent spikes^{M}	lateral F	multiple independent spikes^{M}	lateral F		
	multiple independent spikes^{M}	lateral T-O	multiple independent spikes^{M}	lateral T		
	multiple independent spikes^{M}	basal F				E^{5}
9	widely distributed discharges^{M}	C	widely distributed discharges^{M}	C	(+)	
	focal discharges	lateral F	focal discharges	lateral F		
10	focal discharges^{M}	C	focal discharges^{M}	C		
	low-amplitude fast activities^{M}	lateral P				E^{6}

^{M},main features: F,frontal; T,temporal; C,central; O,occipital; P,parietal;
(+), SAM-VS in a deep fissure or sulcus: E, ECoG specific

REFERENCES

Asano E, Muzik O, Shah A, et al. Quantitative Interictal Subdural EEG Analyses in Children with Neocortical Epilepsy. Epilepsia 2003;44:425-434.

Hufnagel A, Dumpelmann M, Zentner, et al. Clinical relevance of quantified intracranial interictal spike activity in presurgical evaluation of epilepsy. Epilepsia 2000;41:467-478.

Minassian BA, Otsubo H, Weiss S, et al. Magnetoencephalographic localization in pediatric epilepsy surgery: Comparison with invasive intracranial electroencephalography. Ann Neurol 1999;46:627-633.

Otsubo H and Sneed OC. Magnetoencephalography and Magnetic source Imaging in Children. J Child Neurol 2001a;16:227-235.

Otsubo H, Ochi A, Elliott I, et al. MEG predicts epileptic zone in lesional extrahippocampal epilepsy: 12 pediatric epilepsy surgery cases. Epilepsia 2001b;42:1523-1530.

Robinson SE and Vrba J. Functional Neuroimaging by Synthetic Aperture Magnetometry (SAM). Recent Advances in Biomagnetism Sendai, Japan. Sendai express;1998.

Localization of Interictal Spikes using SAM(g_2) and Dipole Fit

Robinson, S.E.[1], Nagarajan, S.S.[2], Mantle, M.[2], Gibbons, V.[2], and Kirsch, H.[2]

[1]VSM MedTech Ltd., CTF Systems, Canada
[2]University of San Francisco, U.S.A

ABSTRACT

SAM(g_2) is an automated analysis that transforms the MEG data into a functional image of spike-like activity, giving the source waveforms for those locations. Since the source waveforms estimated by SAM have higher signal-to-noise ratio (SNR) than does the raw MEG data, it is possible to automatically mark the location and timing of each spike for comparisons with dipole fit procedures. Both SAM(g_2) and equivalent current dipole (ECD) fits were used to analyze MEG interictal spike recordings in 10 patients with cortical dysplasias and medial temporal lobe epilepsy. The ECD fit locations obtained by manual spike classification and latency marking were compared with those found by automated SAM(g_2) procedures. When the SNR of interictal activity was high (compared to the background) with a clear single focus, there was excellent agreement between the ECD cluster location and the SAM(g_2) maximum. However, when the SNR of spikes was low, manual single ECD location scatter was larger than SAM(g2) reconstructions. When multiple independent interictal spike loci were present, there was some disagreement between SAM(g_2) and ECD scatter in the cases of low SNR spikes. When SAM(g_2) indicated multiple coupled spike loci, the residual variance for the dipole fit was high and its scatter unacceptably large – even for multiple dipole models. This study demonstrates that SAM(g_2) is equivalent to ECD fit for localizing interictal spikes when there is a single locus and good SNR. Further studies are required to validate cases in which there are multiple spike loci or poor SNR.

KEY WORDS

MEG, epilepsy, interictal spike, localization, minimum-variance beamformer, dipole fit.

INTRODUCTION

The traditional approach to MEG interictal spike localization is the equivalent current dipole fit. However, that procedure is difficult to automate, and generally requires manual identification of spikes. Furthermore, the model order (number of dipoles to fit) may vary among spikes. SAM(g_2) was developed to automate epilepsy data analysis, freeing it from model-order considerations [Robinson, 2002]. SAM(g_2) represents the MEG data in two forms: a three-dimensional functional image of g_2 (excess kurtosis – a measure of "spikiness"), and SAM virtual sensors estimating the source waveforms at the coordinates identified in the functional image. Because the signal-to-noise ratio of the spikes is greater in the virtual sensors than in the raw MEG data, the spikes are easily marked by adaptive threshold detection, and classified by source location. Thus, dipole fit can be automated following SAM(g_2). In this study, we compared the localization of interictal spikes by SAM(g_2) and by dipole fit. The objective of this comparison was two-fold: 1) to determine if SAM(g_2) and dipole fit are equivalent for cases in which there appears to be a single spike locus, and 2) to determine how they differ when multiple spike loci are present.

METHODS

MEG epilepsy data recordings from 10 patients with diagnoses of cortical dysplasia and medial temporal lobe epilepsy were analyzed using SAM(g_2) and automated dipole fit. This was a retrospective study, as data from all patients had previously been subjected to manual spike marking and dipole fit. Several minutes of data were recorded from each patient in a passband of dc – 75 Hz (300 Hz sample rate) using a CTF 275-channel whole cortex MEG helmet. These data were divided into one-minute segments for our analysis.

The SAM(g_2) algorithm begins with computing SAM coefficients for estimating the source waveforms at coordinates within the region of interest (ROI). The source waveform for any coordinate θ is simply the weighted sum of measurements (referred to as a "virtual sensor"): $\hat{S}_\theta(t) = \mathbf{W}_\theta^{\mathrm{T}}\mathbf{M}(t)$, where $\mathbf{W}_\theta = \mathbf{C}^{-1}\mathbf{B}_\theta / \mathbf{B}_\theta^{\mathrm{T}}\mathbf{C}^{-1}\mathbf{B}_\theta$, **C** is the covariance matrix of MEG measurements **M**, and $\mathbf{B}_\theta$ is the lead field (forward solution for a unit current dipole at θ). Excess kurtosis (g_2) is used as a measure of spikiness at each coordinate. It is computed from each source waveforms as: $g_2 = \sum_T \left[S(t) - \bar{S}\right]^4 / \left(\sigma^4 T\right) - 3$, where σ is the standard deviation and T is the number of time samples. A functional image is made up from the g_2 values at each coordinate.

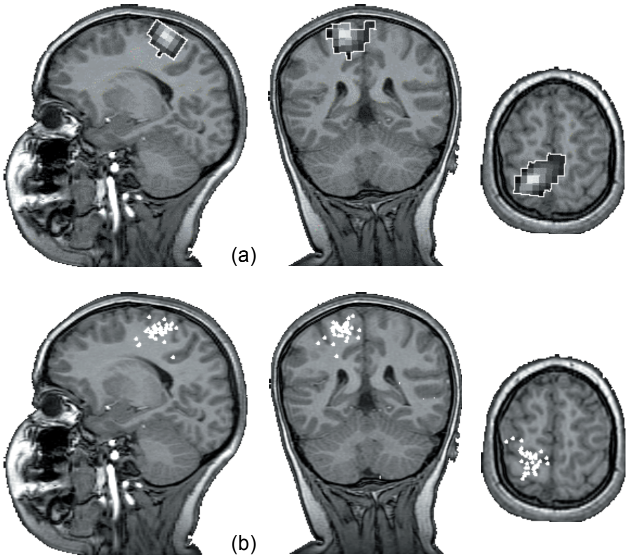

Figure 1. A single interictal spike locus is seen in both SAM(g_2) (a) and dipole fit (b). The dipole fit scatter is small (for dipoles with < 10 % residual variance). However, its centroid is slightly deeper than that indicated by SAM(g_2).

The SAM(g_2) images were computed for a ROI of x = {-10.0, 10.0 cm}, y = {-9.0, 9.0 cm}, z = {0.0, 14 cm}, relative to the head frame, in 5 mm steps; this ROI enclosed the entire head, in all cases. Epileptic activity was imaged by SAM(g_2) for the 20 to 70 Hz frequency range which provided optimal image contrast for interictal spike activity. A list of the local maxima in the SAM(g_2) images was saved, and SAM virtual sensors were computed for each location for viewing source waveforms in the dc – 75 Hz range. The same list of maxima was used to generate virtual sensors for the 20 – 70 Hz activity. The peak of each spike in the 20 – 70 Hz source time series was marked using an adaptive threshold-crossing algorithm, and a best-fit current dipole computed for ± 2 samples around each marker (5 samples). Dipoles having greater than 10% residual variance were rejected. In cases for which spikes appeared correlated among several loci, a two dipole fit was applied in addition to the single dipole fit. The SAM(g_2) image and dipole markers were then co-registered with the corresponding MRI of each patient. The presence and number of interictal spikes was confirmed by viewing the dc – 75 Hz virtual sensors. We then compared the relative location of the SAM(g_2) maxima to the centroid of the dipole scattergram. Spikes were also marked manually for subsequent dipole fit. These results were compared with the fits from automated dipole marking.

RESULTS

These 10 patients exhibited a variety of spike patterns. The automated SAM(g_2) and dipole fit methods were successful, with no user intervention. In 7 out of 10 patients, excellent correlation was found between the SAM(g_2) results and prior manual spike localization. In the remaining 3 cases, manual data analysis failed to localize MEG abnormalities (including one patient where magnetic dental work interfered with standard dipole analysis). The interictal spike loci found by SAM(g_2) for these 3 patients was concordant with the other clinical findings.

One example of a patient with a single interictal spike locus is shown in Figure 1. A single maximum was found in the SAM(g_2) image near the left central sulcus (Figure 1a). There is little difference between the two methods other than that the corresponding dipole fit scattergram (Figure 1b) indicates a slightly deeper source. Another patient presented with multiple spike loci. The coronal views are shown in Figure 2. In the top row, each of three spike loci are shown – labeled V0 and V1 in the left hemisphere, and V2 in the right hemisphere. The virtual sensor waveforms for these sites are shown in Figure 3. These appear to be independent regions of interictal spiking. That is, the source waveforms have little correlation with one another, although several spikes are coincident in time. The scattergram for single dipole fits to markers derived from each of the three source waveforms is shown in the bottom row of Figure 2. All fits shown have less than 10% residual variance. Although the residual variance was reduced when fitting this data to two dipoles, this had little effect on the scattergram. The dipole fits appear in the same region indicated by SAM(g_2), but were unable to discern three distinct loci from these plots. The automated spike markers were usually placed earlier than the corresponding manually placed markers. Dipole scatter was greater for the manually-marked data than for the SAM(g_2) analysis.

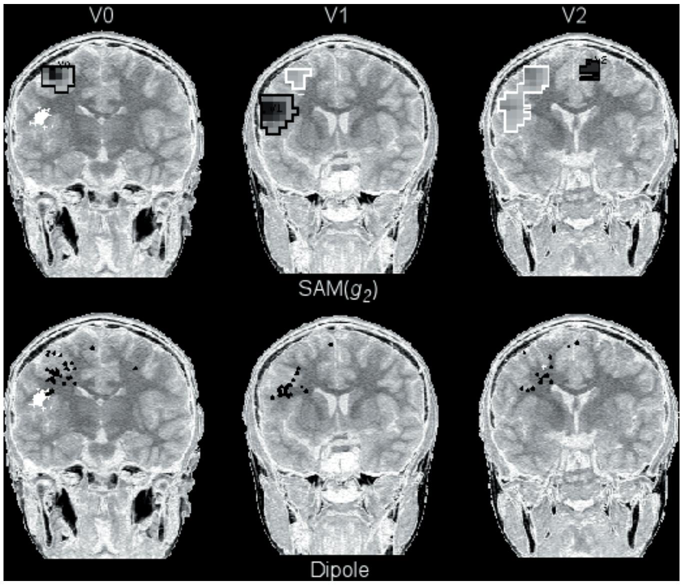

Figure 2. In one of the patients, SAM(g_2) found three spike loci, labelled V0, V1, and V2 (top row). Spikes were marked in each source waveform for these loci. Single dipole fits were then computed around each spike. The scatterplots (residual variance < 10 %) for spikes corresponding to each source are shown in the bottom row. The dipole scatterplots are unable to resolve the different loci.

DISCUSSION

This study demonstrates that SAM(g_2) is equivalent to the ECD fit for localizing MEG interictal spikes when there is a single spike locus and good SNR. We were able to obtain good quality ECD fits using SAM(g_2) for automated spike detection. When multiple independent interictal spike loci were present, there was some disagreement between SAM(g_2) and ECD scatter in the cases of low SNR spikes. When SAM(g_2) indicated multiple coupled spike loci, the residual variance for dipole fit was higher and its scatter larger – even for multiple dipole models. The difference between dipole scatter for the automated and manually-placed spike markers is attributable to the SAM virtual sensors emphasizing the earliest portion of the spike, before excitation has spread. The placement of manual markers were based upon the MEG sensor waveforms, in which the spike peaks appear later than those seen in the virtual sensors. The increased scatter of dipole fits to manual markers results from the spread of excitation as the spike progresses. The automated spike marking procedure, using the SAM virtual sensors is not only faster than manual marking, it is also more accurate in that it shows where the spikes have originated and not where they have spread.

The multifocal example (Figures 2 and 3) suggests that selection of model order for dipole fit could vary from spike to spike. Some spikes were independent while others were correlated. Had we examined the spectrum of singular values, it would have explained these data by a three source model. This is precisely what was found using SAM(g_2). However, the three-source model does not necessarily apply to all spikes, as not all sources are active simultaneously. Hence, model order needs to be determined for each individual spike (or perhaps for each sample). This could be done by coincidence of the SAM(g_2) automated markers.

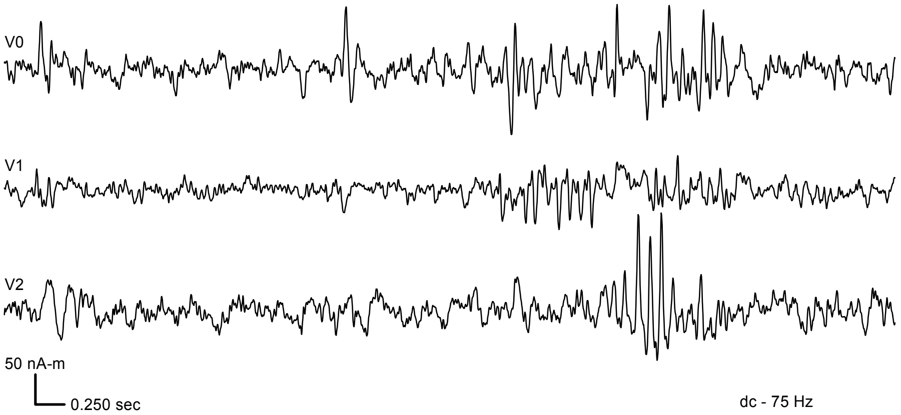

Figure 3. Three SAM virtual sensors, corresponding to the three maxima in the SAM(g_2) image, show independent source waveforms with some spike correlation.

Examination of these results calls to question whether dipole fit is truly necessary. SAM(g_2) localization compared favorably with dipole fit in cases with a single interictal spike locus. In multi-focal cases, SAM(g_2) consistently yielded a sharper representation of each site of spike generation. SAM(g_2) has the advantage of being automated as well. Nonetheless, further testing will be necessary to determine the sensitivity and specificity of SAM(g_2) analysis in single and multiple focus cases.

REFERENCES

Robinson, SE., Vrba, J, Otsubo, H, Ishii, R. Finding epileptic loci by nonlinear parameterization of source waveforms. Proceedings of the 13th International Conference on Biomagnetism 220-222, 2002.

SAM(g2) analysis for detecting spike localization: a comparison with clinical symptoms and ECD analysis in an epileptic patient

Ukai S.[1], Kawaguchi S.[1], Ishii R.[1], Yamamoto M.[1], Ogawa A.[1], Mizuno-Matsumoto Y.[1],
Robinson S.E.[2], Fujita N.[3], Yoshimine T.[4], Shinosaki K.[5], and Takeda M.[1]

Departments of [1]Psychiatry and Behavioral Science, [3]Radiology, [4]Neurosurgery, Osaka University Graduate School of Medicine, Japan, [2]CTF Systems Inc., Canada, [5]Department of Neuropsychiatry, Wakayama Medical University, Japan

ABSTRACT

SAM(g2) analysis, a combination of synthetic aperture magnetometry (SAM) and excess kurtosis (g2) method, is a novel epilepsy analysis procedure based on a spatial filtering technique. By producing a three-dimensional image of the g2 values and superimposing them onto a patient's MR images, this analysis can automatically estimate spike localization from raw MEG epilepsy signals without prior selection of spikes. The aim of this study is to examine SAM(g2) analysis using MEG signals of an epileptic patient, whose clinical symptoms of colored elementary visual auras had ceased in accordance with the changes of the estimated localizations of the equivalent current dipoles (ECDs) of the interictal spikes. His visual auras were experienced in 1997, while they ceased in 1999 with effective medication. The patient provided written informed consent for the experimental procedures. The MEG signals were recorded in 1997 and 1999, and were analyzed using both ECD and SAM(g2) analyses. For the MEG signals of 1997, ECD analysis estimated most of the interictal spikes in the right fusiform and inferior temporal gyri, which subserve human color processing. SAM(g2) analysis also estimated them in the same areas. For those of 1999, both ECD and SAM(g2) analyses estimated them in the right transverse gyrus of Heschl. As well as ECD analysis, SAM(g2) analysis successfully estimated the changes of the localizations of the interictal spikes in accordance with the changes of the patient's clinical symptoms, indicating that SAM(g2) analysis is useful for detection of interictal spike localization in epileptic patients.

KEY WORDS

MEG, epilepsy, spatial filter, equivalent current dipole, spike, synthetic aperture magnetometry (SAM)

INTRODUCTION

Robinson et al. proposed a novel epilepsy analysis procedure, SAM(g2) analysis [Robinson, 2002], which is a combination of synthetic aperture magnetometry (SAM) [Ishii, 1999] [Taniguchi, 2000] [Ukai, 2002] and excess kurtosis (g2) method based on a spatial filtering technique. This analysis is distinguished for ability to automatically estimate spike localization from raw MEG signals including spikes without prior selection of them, different from equivalent current dipole (ECD) analysis.

The aim of this study is to examine SAM(g2) analysis using MEG signals of an epileptic patient, whose characteristic colored elementary visual auras had gradually ceased in response to effective pharmacotherapy, in accordance with the changes of the estimated ECD localizations of the interictal spikes [Kawaguchi, 2003].

METHODS

Patient: In 1995, a male had suddenly suffered from colored elementary visual auras lasting several seconds and following generalized tonic clonic seizures (GTCS) at the age of 25. He described many unformed sparkling blobs with various colors moving in the bilateral visual fields. His past clinical history was unremarkable. He had normal intelligence and showed no abnormal neurological signs. MRI revealed hypoplasia of the bilateral cerebellar cortices. EEG found interictal spikes in the right temporal region. We made his diagnosis of localization-related epilepsy with secondarily GTCS and started pharmacotherapy. The frequency of his visual auras had gradually decreased and he experienced visual auras every 2 months in 1997, until he had neither visual auras nor secondarily GTCS in 1999.

MEG recording: The patient gave written informed consent for the experimental procedures. The MEG signals analyzed in this study were obtained in 1997 and 1999 using a whole head helmet-shaped 64-channel SQUID sensor array (CTF Systems Inc., Canada). MEG signals were low-pass filtered at 80 Hz and notch filtered at 60 Hz and then digitized with a sample frequency of 250 Hz. During each MEG measurement, all 10 sec epochs including interictal spikes were manually recorded on disks and analyzed off-line.

ECD analysis: After MEG signals were filtered with a band-pass of 1-50 Hz, an ECD model was estimated at each time-point within the encompassing signal segment of each spike using a single-dipole model with a dipole-fit software (CTF Systems Inc., Canada). For each individual spike, the ECD with the best correlation coefficient was taken to represent the spike. ECD locations were considered valid if the correlation coefficient was ≥ 0.90.

SAM(g2) analysis: For each image voxel, time-series of source activity are estimated from the entire 64-channel MEG signals by SAM, which is a spatially constrained minimum-variance beamformer for MEG, and excess kurtosis (g2) is computed. The presence of spike activity yields a large positive kurtosis, whereas normal cortical activity has a small kurtosis. A three-dimensional image of the g2 values (SAM(g2) image) is produced by mapping all kurtosis values. SAM(g2) image is superimposed onto individual MR images to be examined in relation with anatomical structure. A location of spike activity is determined by searching the volumetric SAM(g2) image for positive maxima. In this study, all recorded 10 sec MEG signals including interictal spikes of 1997 and 1999 were respectively submitted to SAM(g2) analysis. Voxel resolution was set with 5 mm.

RESULTS

Table 1 shows the frequency of colored visual auras, the numbers of all spikes recorded and the localizations of the spikes estimated by ECD analysis. ECD analysis estimated six of the nine spikes in the right fusiform and the right inferior temporal gyri in 1997, and four of the five spikes in the right transverse gyrus of Heschl in 1999 (Table 1, Fig. 1). SAM(g2) analysis estimated the localizations of the interictal spikes in the right fusiform and the right inferior temporal gyri and their surrounding areas in 1999, and in the right transverse gyrus of Heschl and its surrounding areas in 1999 (Fig. 1).

DISCUSSION

Colored elementary visual auras were frequently experienced in 1997 and they ceased in response to effective pharmacotherapy in 1999. Simultaneously, ECD analysis estimated most of the interictal spikes in the right fusiform and inferior temporal gyri in 1997, while most of them in the right transverse gyrus of Heschl in 1999. These results suggest that the right fusiform and inferior temporal gyri subserved symptomatogenic zone of the colored elementary visual auras of epileptic-positive symptoms in this patient. In addition, these results were in agreement with the previous findings that the fusiform gyrus and the inferior temporal cortex are involved in human color processing using PET [Zeki, 1991], visual evoked potentials [Allison, 1993] and electrical cortical stimulation [Lee, 2000]. In this clinical study, as well as ECD analysis, SAM(g2) analysis also successfully estimated the changes of the localizations of the interictal spikes in accordance with the changes of the patient's clinical symptoms of colored elementary visual auras.

	MEG measurement	
	1997	1999
Frequency of colored visual auras	6/year	-
No. all spikes recorded	34	15
No. spikes valid for ECD localization	9	5
ECD localization		
Right fusiform gyrus	3	
Right inferior temporal gyrus	3	
Right middle temporal gyrus	3	
Right transverse gyrus of Heschl		4
Right inferior parietal lobule		1

Table 1. Frequency of colored visual auras, the number of spikes and the localizations of the spikes valid for ECD localization in 1997 and 1999.

For estimation of epileptic spike localization, SAM(g2) analysis has following advantageous characteristics compared with conventional ECD analysis: 1) SAM(g2) analysis combines the steps of spike localization and spike identification, 2) It can automatically analyze MEG signals including spikes, 3) It is considerably faster than the conventional ECD analysis requiring manual spike marking and dipole fit. In conclusion, these advantageous characteristics of SAM(g2) analysis and the results of this clinical study showing the relationship between the changes of the clinical manifestations and the spike localizations by ECD and SAM(g2) analyses indicate that SAM(g2) analysis is clinically useful for detection of interictal spike localization in epileptic patients.

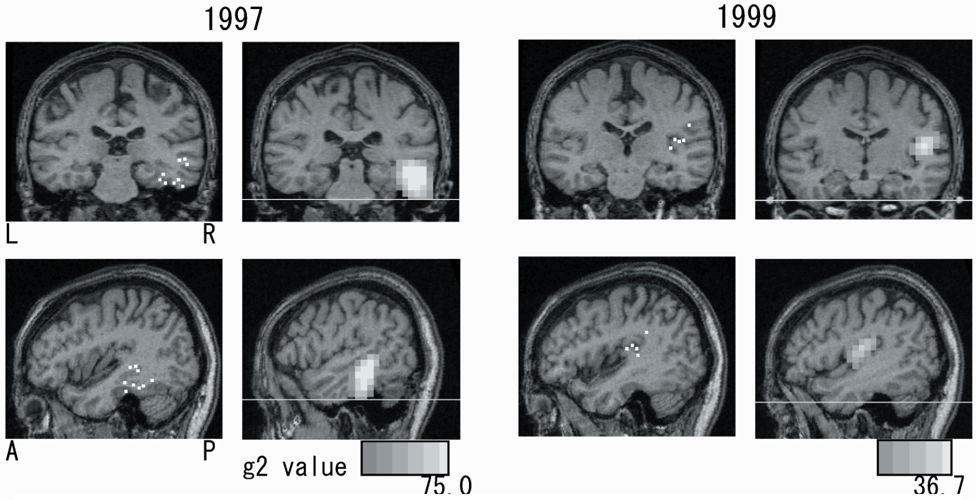

Figure 1. ECD localizations of the interictal spikes (left) and SAM(g2) image (right) in 1997 and 1999.

REFERENCES

Allison T, Begleiter A, McCarthy G, Roessler E, Nobre AC, Spencer DD. Electrophysiological studies of color processing in human visual cortex. Electroencephalogr Clin Neurophysiol 1993;88:343-355.

Ishii R, Shinosaki K, Ukai S, Inouye T, Ishihara T, Yoshimine T, et al. Medial prefrontal cortex generates frontal midline theta rhythm. Neuroreport 1999;17: 675-679.

Kawaguchi S, Shinosaki K, Ukai S, Ishii R, Yamamoto M, Ogawa A, et al. Interictal spikes in the fusiform and inferior temporal gyri of an epileptic patient with colored elementary visual auras: a 5-year longitudinal MEG ECD study. Neuroreport 2003;14:637-640.

Lee HW, Hong SB, Seo DW, Tae WS, Hong SC. Mapping of functional organization in human visual cortex: electrical cortical stimulation. Neurology 2000;54:849-854.

Robinson SE, Vrba J, Otsubo H, Ishii R. Finding epileptic loci by nonlinear parameterization of source waveforms. In Nowak H, Haueisen J, Giebler F, Huonker R, editors. Biomag 2002. Proceedings of the 13th International Conference on Biomagnetism; 2002 Aug 10-14; Jena, Germany. Berlin: VDE VERLAG GMBH; 2002. p. 220-222.

Taniguchi M, Kato A, Fujita N, Hirata M, Tanaka H, Kihara T, et al. Movement-related desynchronization of the cerebral cortex studied with spatially filtered magnetoencephalography. Neuroimage 2000;12:298-306.

Ukai S, Shinosaki K, Ishii R, Ogawa A, Mizuno-Matsumoto Y, Inouye T, et al. Parallel distributed processing neuroimaging in the Stroop task using spatially filtered magnetoencephalography analysis. Neurosci Lett 2002;334:9-12.

Zeki S, Watson JD, Lueck CJ, Friston KJ, Kennard C, Frackowiak RS. A direct demonstration of functional specialization in human visual cortex. J Neurosci 1991;11:641-649.

Effect of Sodium Valproate on Neuromagnetic Responses to Chromatic Flicker: Implication to Photosensitivity

[1]Watanabe, K., [2]Sayres, R., [3,4]Shimojo, S., [5,6]Imada, T., and [7]Nihei, K.

[1]National Institute of Advanced Industrial Science and Technology, Japan; [2]Stanford University, USA; [3]CalTech, USA; [4]NTT CS Lab., Japan; [5]University of Washington, USA; [6]Tokyo Denki University, Japan; [7]National Center for Child Health and Development, Japan

ABSTRACT

The effect of oral administration of sodium valproate in normal subjects was evaluated using whole-scalp magnetoencephalography, with results compared to the effect of sodium valproate in photosensitive children. Neuromagnetic responses to 10 Hz equiluminant red-green and red-blue flicker were measured before and after 5 days of sodium valproate administration. For the red-green flicker, relative power spectra at the stimulus frequency (10 Hz) were attenuated with medication in most brain regions. However, for the red-blue flicker, the 10-Hz power in the occipital region was enhanced with medication, while it was reduced in other regions. These results qualitatively resembled those in photosensitive children. The present findings suggest that (1) combinational chromatic sensitivity can be a critical factor for cortical excitability, that (2) the effect of sodium valproate is qualitatively similar in normal and photosensitive subjects, and that (3) the effect of sodium valproate on cortical excitability is not simply to suppress the stimulus-synchronized occipital activity, but rather to inhibit the spread of cortical activity from the occipital region to other region.

KEY WORDS: Photosensitive, Epilepsy, Magnetoencephalography, Color, Flicker

INTRODUCTION

Photosensitive epilepsy (PSE) is a common type of stimulus-induced epilepsy, and the increasing use of television and computer games has been boosting the incidence of PSE [Harding, 1994] [Wilkins et al., 1979]. Chromatic sensitivity is now recognized as an important factor of PSE [Takahashi et al., 1999]. In addition to sensitivity to single color, researchers have investigated the possible role of color combinations for photosensitivity (eg red-blue flicker being more provocative than monochromatic flicker) in patients [Tobimatsu et al., 1999] and in normal adult subjects [Watanabe et al., 2002]. Sodium valproate (VPA) is widely used as the first-choice drug against PSE because of its efficacy and good behavioral profile [Loscher, 1999]. However, its mechanism of action in the human brain is not fully known [Davis et al., 1994]. Given the wide spectrum of PSE, it is crucial to examine the effects of VPA on cortical excitability under various visual stimulation paradigms. To this end, we recorded magnetoencephalographic (MEG) responses to equiluminant red-green and red-blue flicker in normal adults and examined the acute effect of VPA. Results were then compared to those in normal and photosensitive children with and without VPA treatment.

METHODS

Two types of equiluminant (1.6 cd/m^2), 10 Hz square-wave flicker were presented on a viewing window (13.4 x 17.7 deg) at a 30-cm viewing distance: Red-Green (R/G) and Red-Blue (R/B). [CIE; red, $x = 0.496$, $y = 0.396$; green, $x = 0.308$, $y = 0.522$; blue, $x = 0.153$, $y = 0.122$]. A flickering stimulus was presented for 2 s and followed by a 3-s dark interval. We studied three male adults (age range 22-47 years) who had no personal or family history of photosensitive epilepsy to examine the acute (5 days) effect of VPA. Two photosensitive female child patients also were tested, including one 13 year-old who had been under VPA treatment for 19 months (400 mg/day), and one 14 year-old with no history of pharmacological treatment. In addition, two normal age-matched female children were tested. All subjects (and children's parents) gave their informed consent. Subjects sat in a magnetically-shielded room and passively observed visual stimuli without moving their eyes. Experiment for normal adults: The control experiment (2 sessions: R/G and R/B) was conducted prior to VPA administration in order measure baseline neuromagnetic responses to chromatic flicker. Following the control experiment, the adult subjects received 100 mg of VPA orally three times daily (total of 300 mg) for 5 consecutive days. The experimental phase of the study (2 sessions: R/G and R/B) was conducted on the last day of VPA administration. Experiment for child patients and normal children: To minimize potential risk, each child was tested only once (2 sessions: R/G and R/B). The photosensitive 13-year old child had been administered her usual dose of VPA, while the three other children (including the photosensitive, but non-VPA treated child) did not receive VPA. A pediatric neurologist, who continuously monitored MEG activity online, and the parents of the child participating in the study observed the experiment. The experiment was to be terminated if either the physicians or the parents suspected the child's safety was at risk, or if the child felt ill, but no such incident occurred. The experimental procedure was approved by the ethics committee of National Children's Hospital in Japan. Neuromagnetic responses were measured with a Neuromag-122 neuromagnetometer. MEG signals were analog-filtered (bandpass frequency 0.03-100 Hz) and digitized at 500 Hz from 100 ms prior to stimulus onset to stimulus offset. At least 80 artifact-free responses (without eye movement, blink, or excessive neuromagnetic signal) were averaged for each color combination. Averaged MEG signals were then digitally lowpass-filtered at 40 Hz, and the DC-offset during the baseline (-100 to 0 ms) was removed. Waveform amplitudes were normalized within each subject with respect to the subject's maximum amplitude. Based on normalized MEG amplitudes, relative power spectra were computed at each channel using a multitaper method of spectral analysis [Mitra & Pesaran, 1999]. We focused on stimulus-synchronized (10 Hz) power spectra. To clarify differences among brain regions, the power spectra were pooled within 7 classified regions (Fig. 2 & 3).

RESULTS

In the normal adult subjects, the R/B flicker produced more pronounced stimulus-synchronized activity in the occipital areas than the R/G flicker (Fig. 1), despite the fact that all the colors were equiluminant. For the R/G flicker, the relative power were attenuated after VPA medication in most brain regions. However, for the R/B flicker, the 10-Hz power in the occipital areas was enhanced with VPA medication, while it was reduced in the other regions (Fig. 1 & 2). For the R/G flicker, an ANOVA (Time x VPA x Color) indicated that there were main effects of VPA in all brain regions ($p < 0.05$), except for the right temporal and bilateral occipital regions. For the R/B flicker, significant main effects of VPA were observed in the left parietal, vertex, right parietal, and bilateral occipital regions ($p < 0.05$). Neither a main effect of Time nor any significant interactions were present. Fig. 3 shows the results of the child subjects. During the R/G stimulation, the stimulus-synchronized responses were generally higher in the non-treated patient than in the treated patient and the two age-matched control children. Additionally, the stimulus-synchronized responses were generally highly suppressed in the treated patient. In contrast, during the R/B stimulation, the MEG response at the occipital region in the treated patient showed enhanced activity relative to those in the non-treated patient and the control children. However, in the other regions, the MEG power was lower in the treated patient.

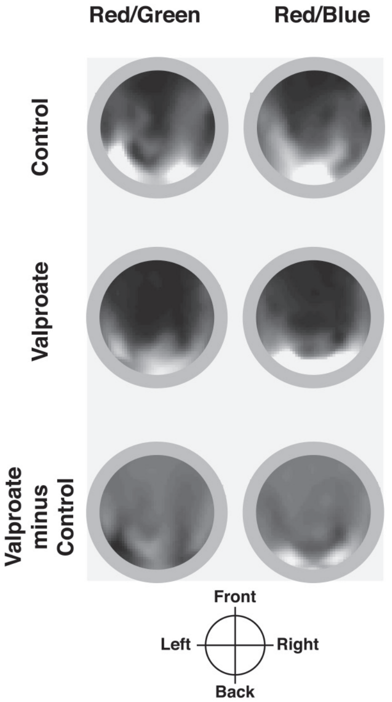

Figure 1. Spatial distribution of relative 10-Hz power of MEG signals in normal adult subjects (normalized and averaginged across all subjects; white designating larger power).

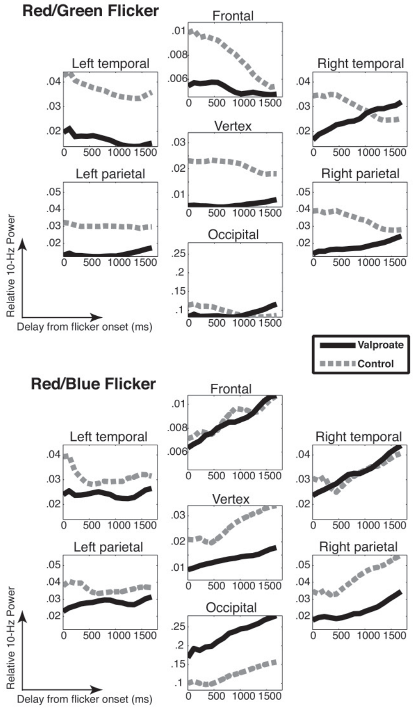

Figure 2. Relative 10-Hz power as a function of delay from the flicker onset (averaged across the adult subjects).

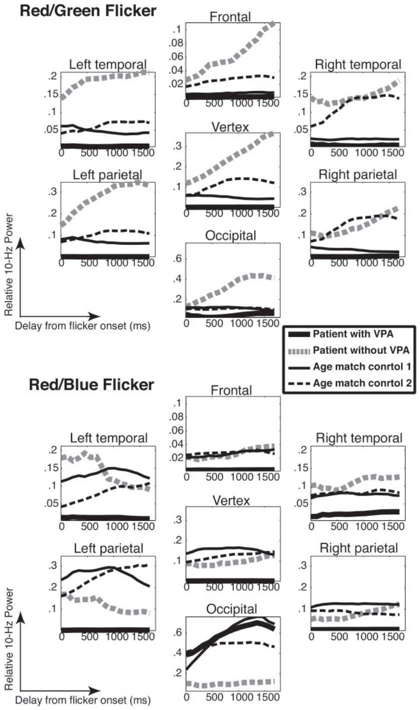

Figure 3. Relative 10-Hz power as a function of delay from the flicker onset (individual child subjects).

DISCUSSION

The results of the present experiment support the idea that color combination of flickering stimulus can be a crucial factor in cortical excitability [Tobimatsu et al., 1999] [Watanabe et al., 2002], and point to the possibility that VPA medication may interact with a subject's chromatic sensitivity. The results also imply that the action of VPA may be not only to simply suppress overall cortical activity, but also to prevent the spread of cortical activity from the occipital region (depending on visual stimulation). This implication could be related to the clinical observation that VPA effectively eliminates the generalized photoconvulsive response (spike and wave discharges) in more than one third of patients, while it has little effect on the occipital spikes [Harding et al., 1978]. Because VPA is effective for various types of seizure, it is suggested that several mechanisms are involved in its anticonvulsant effects. One major mechanism, the potentiation of GABAergic functions, seems to be more pronounced in some specific brain regions, such as the substantia nigra [Herrick & Hgarding, 1980], which may underlie the inhibition of spread of excessive stimulus-synchronized neuronal activity.

ACKNOWLEDHEMENTS: Supported by NTT CS Lab., NHK Broadcasting and Culture Foundation, and AIST, Japan.

REFERENCES

Davis R, Peters DH, McTravush D. Valproic acid: A reappraisal of its pharamacological properties and clinical efficacy in epilepsy. Drugs 1994; 47: 332-72.
Harding GFA, Herrick CE, Jeavons PM. A controlled study of the effect of sodium valproate on photosensitive epilepsy and its prognosis. Epilepsia 1978; 19: 555-65.
Harding GFA, Jeavons PM. Photosensitive Epilepsy. London: MacKeith Press; 1994.
Herrick CD, Harding GFA. The effect of sodium valproate on the photosensitive VEP. In Barber C, editor. Evoked potentials. Lancaster: MTP Press; 1980. p. 539-47.
Loscher W. Valproate: A reappraisal of its pharamacodynamic properties and mechanisms of action. Prog Neurobiol 1999; 58; 31-59.
Mitra PP, Pesaran B. Analysis of dynamic brain imaging data. Biophys J 1999; 76: 617-708.
Takahashi, Y, Fujiwara, T, Yagi, K, Seino, M. Photosensitive epilepsies and pathophysiologic mechanisms of the photoparoxysmal response. Neurology 1999;53: 926-32.
Tobimatsu S, Zhang YM, Tomoda Y, Mitsudome A, Kato M. Chromatic sensitive epilepsy: A variant of photosensitive epilepsy. Annal Neurol 1999; 45: 790-93.
Watanabe K, Imada T, Nihei K, Shimojo S. (2002). Neuromagnetic responses to chromatic flicker: Implication for photosensitivity. Neuroreport 2001; 13: 2161-5.
Wilkins AJ, Darby CE, Binnie CD. Neurophysiological aspects of pattern-sensitive epilepsy. Brain 1979; 102: 1-25.

Automatic localization of epileptic zones using magnetoencephalography

Jing Xiang[1], Stephanie Holowka[1], Yang Jiang[2], Hui Qiao[3], Bo Sun[3], Daniel Wilson[1], Sylvester Chuang[1]

[1]MEG Laboratory, Department of Diagnostic Imaging, The Hospital for Sick Children, Toronto, ON, M5G 1X8, CANADA;
[2]Laboratory of Neuropsychology, National Institute of Mental Health, Bethesda, MD, 20892, USA; [3]MEG Laboratory, Beijing
Tiantan Hospital, Beijing, 100050, CHINA

ABSTRACT

Conventional visual identification of epileptic spike and sharp wave is a challenging problem in the clinical application of magnetoencephalography (MEG). More importantly, the convention method has problems of detecting other abnormalities such as high frequency oscillation in the human epileptic brain. The objective of this study was to develop a new approach using magnetic spectral analysis and spatial filtering. Twelve patients with seizure have been studied with a whole cortex MEG system. Fifteen trials were recorded for each patient; each trial was 120 seconds. Neuromagnetic spectrum was analyzed using a new method called accumulated spectrogram. Focal increases of spectral power were localized using synthetic aperture magnetometry (SAM). The MEG results were then compared with clinical findings. Focal increases of spectral power have been identified in all patients (12/12, 100%). The locations of the focal increases of spectral power were in agreement with dipole locations of spikes in 9 patients (9/12, 75%). A comparison between MEG results and clinical findings indicated that SAM revealed focal epileptic activities in two patients when dipole fitting had failed. The results suggest that epileptic regions could be quantitatively identified and accurately localized using accumulated spectrogram and SAM. In comparison to visual identification of spike, the new approach is objective and sensitive, and provides the possibility of analyzing much wider frequency bands.

KEY WORDS

Magnetoencephalography (MEG), epilepsy, synthetic aperture magnetometry (SAM), spectrogram, spike

INTRODUCTION

MEG is one of the most important advances made in the past decade in the management of seizure disorders and has developed to the point that it has now entered routine clinical application [Barkley, 2003]. The combination of functional data derived from magnetoencephalographic recordings co-registered with structural magnetic resonance imaging (MRI) is called Magnetic Source Imaging (MSI). MSI decreases the risk of morbidity associated with epilepsy surgery and enhances the probability of postsurgical seizure control. In current practice, MEG epileptiform signals are visually identified. After representative epileptic spikes have been marked, they are localized by fitting to on equivalent current dipoles (ECD) model. This method is labor-intensive, time-consuming, subjective and requires considerable skills to minimize errors. Newly developed multichannel and high sampling rate MEG recording techniques have provided the ability to ask and partially answer questions that were previously beyond our capability. Our previous studies have showed that focal increases of spectral power can be accurately localized with magnetic spatial filtering technique, such as SAM [Xiang, 2003]. Therefore, it would be very interesting to use spectral analysis and spatial filtering technique to study epileptiform activities. The objective of this study is to combine two new methods, magnetic frequency transform and spatial filtering techniques, to form a new systematic approach to identifying the neuromagnetic activation associated with epilepsy. Building on our previous studies, this study focuses on the localization of pediatric seizures.

METHODS

Twelve children with epilepsy (6 girls and 6 boys, aged 6 – 17 years, with a mean age of 10 years) were studied. A 151-channel whole cortex CTF OMEGA system was used for recordings (CTF Systems Inc., Port Coquitlam, Canada). MEG measurements were performed in a magnetically shielded room (MSR) with a total system white noise level below 10 fT/√Hz. The localization of the subject's head relative to the sensor array was measured using three small coils affixed to the nasion and pre-auricular points. Sleep deprivation was used to provoke epileptic discharges. Data were recorded with noise cancellation of third order gradients. The sampling rate of data acquisition was 625 Hz. Each trial was 120 seconds; fifteen trials were recorded for each patient. The head position was measured before and after each trial. To ensure accurate source localization, the movement of the patient's head was limited in 5 mm. If patient's head moved more than 5 mm during the recording, the datum set was marked as bad and another additional trial would be recorded. Three-dimensional MRI, 3D-SPGR sequence, was obtained for each subject using a Signa Advantage (GE Medical System, Milwaukee, USA).

Magnetic spikes were identified and classified by an experienced MEG expert and a neurologist using the CTF DataEditor program. The dipole source location corresponding to each spike was estimated individually using the CTF DipoleFit program with the single dipole model. All recorded MEG data were transformed to spectrogram with Fourier Transform. Since each trial only has 120 seconds and may have no spike, all fifteen trials (total of 30 minutes) from each patient were accumulated as one accumulated spectrogram (ASM). The accumulation procedure included two steps. The first step was to normalize each channel for each frequency band according to the averaged spectral power from all measuring channels [Xiang, 2002]. The second step was to recursively add all data from one patient onto one spectrogram.

A real head model was produced from each subject's MRI, and multiple spheres were used in SAM analysis. The region of interest (ROI) was set to include the whole brain with a 2.5 mm voxel resolution. SAM Z value was calculated from the changes in spectral power in each voxel of all 120 seconds recording and normalized by the variance. We calculated one SAM image for each trial (one datum set); total of 15 SAM images were computed and an averaged SAM image was produced. The volume of an epileptic region was calculated by using a software called magnetic source locator (MSL) [Xiang, 2003]. The distribution of spectral power was displayed on individual MR images. A SAM peak was defined when a focal Z value was higher than 5.

RESULTS

Focal increases of spectral power have been identified in all patients (12/12, 100%). All 15 datasets with spikes were found in 8 children, 9 to 14 datasets with spikes were found in the other 4 children. Therefore, all the children in this study had MEG spikes in at least 9 datasets. In spectrogram, we identified focal increases of spectral power. All 15 datasets with a focal increase of spectral power were found in 9 children; 9 to 14 datasets with focal increase of spectral power were found in 3 children. In comparison with time-domain waveform, spectrogram has similar sensitivity but showed more focal abnormalities in the MEG data. One focal increase of spectral power was identified in 7 children; two focal increases were identified in 4; and more than two focal increases were identified in the other 2. In comparison with single trial spectrogram (or spectrogram), accumulated spectrogram showed much clearer focal increase of spectral power. Figure 1 shows an example of spikes and focal increases of spectral power in a typical case. The accumulated spectrogram showed a focal increase of spectral power in all children.

All 15 SAM images (each trial had one SAM image) showed a focal increase of spectral power were found in 6 children; 9-14 SAM images showed a focal increase were found in the other 6. To enhance the focal increases of spectral power across all SAM image, an averaged SAM image was produced for each patient. In comparison to single SAM image, the averaged SAM image showed much clearer focal increase of spectral power. The exact location of focal increase of spectral power was defined by overlapping averaged SAM image onto individual MRI. The locations of SAM peaks were in agreement with the dipoles in 9 children (9/12, 75%). One child did not have a clear dipole cluster, but averaged SAM image showed a clear epileptic focus. Interestingly, dipoles around the center of SAM peak were found in 4 children who had single epileptic focus. In three children who had multiple epileptic foci, the SAM showed more foci than dipole clusters and the dipole clusters tending to be in the middle of two SAM peaks. The comparison of MEG results and clinical findings indicated that SAM accurately localized epileptic regions in 91% (11/12) of children with localization related seizures. There were one or more additional focal increases of spectral power in SAM images did not have corresponding clinical evidences in 2 children.

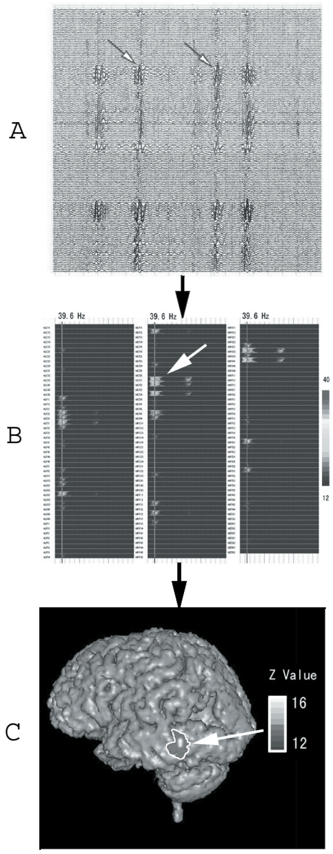

Figure 1. Flowchart of the developed method for localization of epileptic regions. **A:** Time domain waveforms show epileptic spikes. **B:** Spectrogram shows focal increases of spectral power. **C:** Magnetic source image (MSI) shows an epileptic region defined bv SAM.

DISCUSSION

The primary results indicate that accumulated spectrogram is a new approach, which can quantitatively describe the epileptiform paroxysms. In comparison with conventional visual identification of spikes, accumulated spectrogram provides a quantitative way to identify the increase of spectral power including conventional spike (15 – 70 Hz). Our results have demonstrated that channel normalization could cancel most of the background activity and highlight focal increases of spectral powers. However, channel normalization is not enough to produce a good spectrogram with high correlation between focal increase of spectral power and spike. Therefore, we further developed accumulated spectrogram to accumulate more than one spectrogram together. Once focal increase of spectral power was found, spatial filtering technique was applied to localize the focal increases of spectral power. To get the whole picture of the entire recording for each patient, we developed a new tool to average SAM image for all 15 trials. Our results indicate that averaged SAM image provides a better solution for identifying epileptic foci.

The present method yielded very plausible equivalent sources for the patients that showed a structural lesion on MRI. Our previous study indicates that SAM can delineate the functional area of somatosensory cortex [Xiang, 2003]. According to the data from this study, SAM has the potential to localize and delineate the epileptic region. According to our data, using accumulated spectrogram and averaged SAM image, subtle epileptic activity could be identified. In comparison with the conventional visually identifying spikes, the current method has the following advantage: (1) it is objective. The focal increases of spectral power can be quantitatively described; (2) the current method opens a door to analyze much more wider frequency range. The high frequency can be as high as 500 Hz, which goes beyond the convention spike and sharp wave analysis (15 – 70 Hz). (3) According to our data, the shape and extent of the epileptic foci can be visualized. We consider that spectral analyses and spatial filtering techniques have the potential to bring a breakthrough in the clinical application of MEG in epilepsy.

ACKNOWLEDGEMENTS

We thank Dr. Paul Babyn for insightful theoretical discussions and many practical suggestions during the course of the experiments. This study was supported by a Research Grant from Savoy Foundation, Quebec, Canada.

REFERENCES

Barkley,G.L. & Baumgartner,C. MEG and EEG in Epilepsy. J. Clin. Neurophysiol. 2003; 20: 163-15.

Bragin A, Wilson C L, Staba RJ, Reddick M, Fried I, Engel J. Interictal high-frequency oscillations (80-500 Hz) in the human epileptic brain: entorhinal cortex. Ann. Neurol. 2002; 52: 407-8.

Xiang J, Holowka S, Sharma R, Hunjan A, Otsubo H, Chuang S. Volumetric localization of somatosensory cortex in children using synthetic aperture magnetometry. Pediatr. Radiol. 2003; 33, 321-6.

MEG clarified the source of epilepsia partialis continua (EPC) in a patient with previously non-diagnostic EEG, Video-EEG, SPECT and MRI Studies

A. Bagic[1], M. Balish[1], R. Bonwetsch[2], W.H. Theodore[2], T. Holroyd[3], R. Coppola[3], and S. Sato[1]
[1]EEG and [2]Clinical Epilepsy Sections, NINDS; [3]MEG Core Facility, NIMH; NIH; Bethesda, MD 20892

We evaluated the usefulness of MEG in a 40-years-old female with EPC involving the left arm and hand, whose previous routine EEG, 24-hour video EEG, SPECT and MRI studies were negative.

A CTF 275-channel whole-head MEG System with 600 Hz and 6 KHz acquisition rates was used to acquire simultaneously MEG, EEG (21 and 64 channels) and EMG from representative muscles of the left arm and hand. Muscle activity was used as a marker for identifying and averaging cortical events. The origin of cortical events was localized using dipole analysis and the data were co-registered into a 3D-reconstructed 3T MRI using the CTF software.

Several different types of events were identified including those involving the extensor digitorum communis (EDC), abductor pollicis longus (APL) and first dorsal interosseous (FDI) muscles without biceps involvement, those involving the biceps only, and those with biceps as well as APL and FDI involvement. The EMG bursts were brief (events averaged 20 ms), with a 5-7 ms delay between biceps and APL and FDI contraction, and a 3-5 ms delay between EDC and APL and FDI contraction. Averaged cortical waveforms were found to precede each type of event starting between 6-10 ms prior to the EMG event. The dipole localized in the right precentral gyrus corresponded anatomically as expected, with slight variation seen among the different events. The significance of the localization of these cortical events and the potential etiology of the lesion is discussed.

These observations clearly show the usefulness of MEG in identifying the source of EPC, leading to a possible curative surgical intervention for this patient's medically intractable condition.

Differences in MEG/EEG epileptic spike yields explained by regional differences in signal to noise ratios

J.C. de Munck[1] , A. de Jongh[1], P. Ossenblok[2]
1. VU University medical center, Department of Clinical Physics, The Netherlands Physics
2Epilepsy Center Kempenhaeghe, Heeze, The Netherlands

There still is controversy concerning the preferred modality in clinical applications: MEG or EEG. There are multiple studies comparing interictal spike rates of EEG and MEG that do not yield conclusive results. The overall picture is that in patients with temporal lobe epilepsy the spike yields for MEG and EEG are comparable, and that for frontal lobe epilepsy the MEG spike yields may significantly exceed that of EEG. Differences between MEG and EEG can be explained by several factors: 1) the number of sensors, 2) differences in depth dependency, 3) differences in background activity and 4) differences in smearing of the potential fields due to skull resistivity. To quantify these factors, we assumed that spike detection is proportional to signal-to-noise (SNR). For two subjects 1.) a forward model was constructed using MR, 2.) realistic subject specific conductivity values were derived by EIT measurements, and 3.) spontaneous M/EEG recordings were made. On a regular 1 cm mesh, for both MEG and EEG the SNR at the sensors was computed using the dipole field as signal and the spontaneous M/EEG as noise. This way, systematic differences in SNRs of EEG and MEG were mapped for the whole brain. The results of that model are consistent with indications found in the literature: at temporal areas the SNRs of MEG and EEG are comparable, and at frontal areas the SNR of MEG is significantly higher. Our model-based approach indicates that SNR mapping clarifies differences between EEG and MEG findings that are difficult to understand from patient studies alone.

Dipole Density Analysis Of Spikes And Slow Waves Improves MEG Resolution In Temporal Lobe Epilepsy

A. Fernández [1], LF Quesney[1-2], C Amo[1], A Turrero [3], P Zuluaga [3], F Maestú [1] , P Campo[1], Tomás Ortiz[1]
[1]Centro de Magnetoencefalografía Universidad Complutense de Madrid, España [2]McGill University, Dept. Neurology and Neurosurgery., Montreal, Canada [3]Departamento de Bioestadística, Facultad Medicina, UCM, España

Mesial temporal sclerosis is the pathogenic and epileptogenic substrate in approximately 70% of patients with temporal lobe epilepsy. MEG´s resolution in interictal spiking involving mesial temporal structures is limited . We studied whether MEG´s localizing effectiveness is enhanced by performing dipole density analysis of spikes and slow waves.Methods :We compared conventional visual and dipole MEG density analysis on spikes and slow waves recorded in 26 patients with temporal lobe epilepsy (11 females, mean age: 30 years) who underwent surgery. One year follow up was available Surgical outcome included 24 patients class I and 2 patients class II (Engel's classification). Results from dipolar density readings for MEG spikes and slow waves in ten different anatomical regions were submitted to a logistic regression analysis. Three logistic models were calculated to respectively study interictal spikes, slow waves and a combination of both. Measuring temporal lobe interictal spikes and slow waves , correctly lateralized all patients in comparison with MRI data. Logistic regression analysis predicted an exclusive unilateral manifestation of temporal lobe epileptogenesis in 24/26 patients (92.3 %), which is only slightly inferior to the results obtained by long term video-EEG monitoring with foramen oval electrodes. The prediction in the remaining two patients was compatible with a predominantly unilateral damage. The clinical implication of this data and its correlation with the localizing / lateralizing effectiveness of MRI, SPECT and PET will be presented. MEG dipole density analysis of slow waves and spikes significantly improves MEG lateralizing effectivenessin temporal lobe epilepsy. We believe that this is largely due to the inclusion of patients with slow waves and without spikes in our data , thus minimizing the category of otherwise " negative findings " . The slow wave activity may be due to the lesion or to surrounding inhibition.

Utilization of MEG results to obtain more favorable outcomes in neurosurgical resection in epilepsy patients

M.J.M. Fischer, G. Scheler, H. Stefan
Department of Neurology, University of Erlangen-Nuremberg, Germany

Magnetoencephalography (MEG) is providing an insight about the distribution of interictal spike localizations in patients with epilepsy during presurgical evaluation. To achieve comparability to other methods and portability to neuronavigation MSI results were represented by an ellipsoidal 3D model. However, the neurosurgeon has to meet more criteria than results provided by MEG, therefore MSI results are evaluated in respect to the actual resection volume by the clinical outcome.

Patients (n=24) from the last 5 years, who had epilepsy surgery at the University of Erlangen, an available pre- and postoperative MRT, a preoperative MEG registering epileptic activity and a postoperative observation period of at least 6 month were included. A 3D model of the resection volume was generated from pre- and postoperative MRT data. Clinical approved MSI results, evaluated by an experienced diagnostician, were represented in 3D by ellipsoids. A principal component analysis provided the axis to fit the ellipsoids to the localizations, the parameters we chose on each axis contain 95% of the variance. Clusters of localizations were represented separately. The coverage of the ellipsoidal representation of MSI results by the resection volume was determined at 1,3µl/voxel resolution.

It was demonstrated that a higher coverage of the localizations of interictal spikes is correlated ($p = 0.019$) with a better Engel outcome 6 month after surgical treatment. Following preliminary results [1] this is the first validation of MSI results by postoperative outcome on a sufficient number of cases. The described method to represent MSI localizations was evaluated and provides the foundation for better comparability to other results in the future. [1] Genow, A. et al., Epilepsy surgery, resection volume and MSI localization in lesional frontal lobe epilepsy. Neuroimage 2004 (1):444-9.

Neuromagnetic Imaging of Cortical Sensorimotor Oscillations in Pediatric Epilepsy: A Case Report

W. Gaetz, E.W. Pang, H. Otsubo, W. J. Logan, I. Elliott, S.K. Weiss, J.T. Rutka, O.C. Snead III, D. Cheyne
Hospital for Sick Children, Toronto, Ontario, Canada

Functional mapping of eloquent cortex is important for minimizing neurological deficits subsequent to epilepsy surgery. Conventional methods of activating sensory cortex include the presentation of electrical stimulation to superficial nerves, which produces robust activity of limited functional significance. Using normal control subjects, our MEG lab has recently demonstrated that: 1) characteristic sensory and motor cortical oscillations (event-related desynchronization (ERD) and synchronization (ERS)) can be observed following a motor or sensory event, and 2) synthetic aperture magnetometry (SAM) spatial filtering methods can localize both ERD and ERS in sensory and motor cortex. We present a case where we applied the SAM technique to localize facial motor and sensory areas by modulating the inherent cortical oscillations using a motor (self-paced tongue protrusion/retraction) and tactile/sensory (transient brushing of the left and right cheek) paradigm. A 17-yr old girl with complex partial seizures secondary to left frontal cortical dysplasia had a prior excision of left frontal cortex with multiple subpial transections over left facial motor areas. She continued to have seizures involving right mouth pulling, and a second surgery was planned. Pre-surgical mapping using SAM localized facial motor and sensory control to right cortex only, regardless of side of stimulation. The left hemisphere facial motor cortex was removed and the patient is seizure-free with no deficits in facial motor control. We have demonstrated a novel application of a new non-invasive technique for successfully localizing eloquent cortex and tracking cortical reorganization often reported in pediatric epilepsy.

Supported by the Canadian Institutes of Health Research (MOP 64279).

MEG vs. EEG measurements of right-left propagation of interictal spikes in a patient with partial epilepsy

K. Hara[1], D.M. Foxe[1], S. Camposano[1], P. E. Grant[1], E. Halgren[1], S. Stufflebeam [1]
[1]MGH/MIT/HMS Athinoula A. Martinos Center for Biomedical Imaging, Massachusetts General Hospital / Harvard Medical School, Charlestown, MA, USA

Introduction: It is often difficult to lateralize partial epilepsy when there are bilaterally independent interictal spikes (IIS) on electroencephalography (EEG). We report the use of magnetoencephalography (MEG) to suggest laterality in a patient with bilateral frontal spikes on EEG. Method: Patient was an 11 years old RH girl with refractory partial seizures. She was investigated using a 306-channel MEG with simultaneous 70-channel EEG to define the location of the IIS based on the single-dipole model for pre-surgical evaluation. We visually searched, classified and compared IIS on MEG with EEG. Results: EEG showed independent left and right or bilateral frontal lobe IIS. MEG showed independent right and left frontal lobe spikes, too. But MEG detected spikes that propagated from the right frontal lobe to left frontal lobe over a 15-30ms interval. This MEG result suggests that her primary epileptic region might be the one in the right frontal lobe. Conclusion: In epilepsy patients with bilateral IIS on EEG, MEG might show the more accurate lateralize and indentify moving epileptic activity. Thus, this result suggests that MEG might be able to determine the laterality of epileptic activity in patients candidates for surgery.

Opercular to Interhemispheric Source Distribution of Benign Rolandic Spikes of Childhood

M. Ishitobi[1], N. Nakasato[2], K. Yamamoto[3], K. Iinuma[1]
[1]Department of Pediatrics, Tohoku University School of Medicine;
[2]Department of Neurosurgery, Kohnan Hospital;
[3]Department of Pediatrics, Sendai City Hospital, Sendai, Japan

Objective: To determine the source distribution of benign rolandic spikes of childhood along and across the central sulcus. *Methods*: Subjects were 15 patients, aged between 7 and 15 years old, suffered from seizure disorders. All had no major abnormalities on brain magnetic resonance imaging, no neurological deficits, and centrotemporal spikes by previous routine EEG. The equivalent current dipoles of the magnetoencephalographic (MEG) spikes measured by the whole-head system were compared to the spike distributions detected by simultaneous scalp EEG according to the international 10-20 system. *Results*: Locations and orientations of the MEG spikes corresponded to the EEG spike distribution as follows: superiorly oriented spike MEG dipoles in the opercular area with T3/4 negative peaks (8 spike groups in 6 patients); anteriorly oriented spike dipoles in the mid-rolandic area with C3/4 or P3/4 negative peaks (17 spike groups in 13 patients); and laterally oriented spike dipoles in the interhemispheric area with Cz/Pz negative peaks (4 spike groups in 3 patients); and others (4 spike groups in 4 patients). *Conclusions*: Based on the ECD location from the opercular to the interhemispheric areas, three spike types were considered as rolandic spikes in a broader sense than in previous reports. Precentral theory of the rolandic spike source was proposed to explain all the three spike types.

Whole head MEG and EEG in the presurgical evaluation of epilepsy patients: a prospective study

S.Knake[1,2], S. M. Stufflebeam[1], Hideaki Shiraishi[1], P. Ellen Grant[1], Keiko Hara[1], Thomas Witzel[1], Valerie Carr[1], Deirdre Foxe[1], Evelina Busa[1], Matti S. Hämäläinen[1], Seppo Ahlfors[1], Susana Camposano[1], Donald L. Schomer[3], Edward B. Bromfield[4], Barbara A. Dworetzky[4], Joseph R. Madsen[5], Reese G. Cosgrove[6], Peter L. Black[4], Blaise F. Bourgeois[5], Pal G. Larsson[7], Andrew J. Cole[6], Elizabeth Thiele[6],
Anders M. Dale[1] and Eric Halgren[1]

Purpose:To evaluate the clinical impact of a combined 306-channel MEG / 70-EEG-recording on the presurgical evaluation of epilepsy patients.

Methods: Sixtyseven patients were prospectively evaluated by simultaneously recorded MEG and EEG. MEG and EEG were evaluated by two independent reviewers. All patients were surgical candidates and had undergone Video-EEG-Monitoring. Two source modelling techniques were used: Equivalent current dipole fitting (ECD) and dynamic statistic parametric mapping (dSPM).

Results: The overall sensitivity to detect interictal epileptiform discharges was 72% (48 / 67 pts) for MEG and 61 % for EEG (41 / 67 patients). The combined sensitivity was 75%. The simultaneous MEG/EEG investigation has induced a change in clinical management in 13 of 67 patients (19%).

Conclusion: MEG and simultaneously acquired EEG are complementary and an enrichment in the presurgical evaluation. The MEG/EEG results impacted the clinical management in this selected group of the patients. The combined evaluation improved the selection of candidates for epilepsy surgery. Large prospective studies on the impact of MEG on the postsurgical outcome have to follow.

Wavelet-based Spectral Spatiotemporal Map Predicts Propagation of Epileptic Spikes

Fa-Hsuan Lin, Keiko Hara, John W. Belliveau, Eric Halgren, Steven M. Stufflebeam
MGH-MIT-HMS Athinoula A. Martinos Center for Biomedical Imaging, Massachusetts General Hosptial, Charlestown, MA USA

Introduction: We introduce a wavelet-transformed MEG method to predict the propagation of epileptic spikes on the cortical surface [1]. Specifically, we obtain spatiotemporal maps of spectral power and phase relationships, quantified by the phase locking value (PLV). PLV is the trail-by-trial phase relationship at a particular frequency between the two areas of the cortex. **Method:** An epilepsy patient was placed in the magnetically shielded room in during a 306-channel MEG measurement of spontaneous activity. Using a single equivalent current dipole (ECD) method, epileptic spikes were identified and divided into spatial clusters. Some spikes were seen to propagate across hemispheres. Wavelet analysis in 5-40 Hz activity of these spikes revealed the oscillation frequency of the maximal power. Using minimum-norm estimate (with and without noise normalization) we calculated both the spectral power and PLV onto the cortical surface. **Result:** A PLV at 10 Hz revealed a high PLV at between the right and left frontal lobe, which predicted the location of trans-hemispheric spike propagation. **Conclusions:** This wavelet-based spectral spatiotemporal mapping technique can predict the propagation of epilepsy spikes, possibly leading to a more accurate method to detecting epileptogenic cortex from propagated spikes.

Supported by the MIND Institute

References [1] Lin, F-H et. al. 2004. “Wavelet-based Spectral Spatiotemporal Mapping in the Human Brain”, NeuroImage, under revision.

Relative merits of MEG for identification of the epileptogenic zone as compared with invasive EEG

Ekaterina Pataraia, Eduardo M. Castillo, Panagiotis G. Simos, Rebecca Billingsley-Marshall,Michele Fitzgerald, Shirin Sarkari, Joshua Breier , Andrew C. Papanicolaou
Department of Neurosurgery, University of Texas - Health Science Center, Houston, Texas, USA

The purpose of the present study was to determine whether magneto-encephalography (MEG) can provide additional, helpful information towards the localization of epileptogenic zone in comparison with invasive EEG. 48 patients with focal, drug-resistant epilepsy were evaluated at the Epilepsy Monitoring Unit in the University Texas Comprehensive Epilepsy Program from 1997 to 2001 and underwent epilepsy surgery. Recordings were performed with a 148-channel whole-head MEG system concurrently with 24-channel surface EEG. Follow-up information was available for up to 12 months postoperatively. Only the patients with interictal changes during the MEG-recordings were included in the present study. The interictal spikes in MEG were identified visually, while estimation of the location of their intracranial sources was performed using the single equivalent dipole model (ECD). ECD locations were then superimposed on the patients' high resolution MRI. The epileptogenic zone in MEG and in invasive EEG was defined in relation to resected area as perfectly overlapping, partially overlapping and non-overlapping. Further analyses included the classification of MEG- and invasive EEG results with respect to postoperative seizure outcome. The results were classified as (a) correct if the localized area was perfectly overlapping with resected area and the patient was seizure-free postoperatively, (b) incorrect if the localized area was the same as resected area, but the patient was not seizure free postoperatively, or the localized area was different from resected area and the patient was seizure-free postoperatively, and (c) indeterminate if the localized zone differed from the resected zone and the patient was not seizure-free postoperatively. Based on MEG alone, the epileptogenic zone was perfectly overlapping with resected area in 34 patients (70.8%), partially overlapping in 9 patients (18.8%) and non-overlapping in 5 patients (10.4%). The results for invasive EEG did not differ significantly from MEG-localization (32 (66.7%), 13(27.1%) and 3 (6.3%) patients respectively). In regard to postoperative outcome, the localization was correct in 27 of 34 patients (79.4%) with perfectly overlapping areas in MEG and correct in 25 of 32 patients (78%) with perfectly overlapping areas in invasive EEG. In patients with frequent interictal spikes the epileptogenic zone with MEG did not significantly differ from the results of invasive EEG, which suggests that MEG could replace invasive EEG in the future if additional studies corroborate these findings. Furthermore, resection of the epileptogenic zone as defined by MEG seems to have prognostic implications on postoperative seizure control.

Paramount Role Of Cingular Cortex In Generalized Epilepsy: MEG Evidence

LF Quesney 1-2, C Amo 1, F Maestú 1, A Fernández 1, T Ortiz 1.
1Centro de Magnetoencefalografía Universidad Complutense de Madrid, España 2 McGill University, Dept. Neurology and Neurosurgery., Montreal, Canada

PURPOSE: Two pathophysiological mechanisms may explain the genesis of generalized spike-and-wave discharges, namely : thalamo-cortical synchronization and cortico-callosal propagation. We studied the synchronization mechanism of generalized spike-wave discharges (SWs) in patients with pharmaco- resistant generalized epilepsy undergoing MEG recordings, technique which also allowed us to perform dipole source localization on MRI. METHODS: Small time difference was measured in 63 MEG generalized SWs with an interhemispheric asynchrony ranging from 0 to 30 msec. recorded in 5 patients (mean age: 38 years). A total of 1208 dipoles corresponding to spikes underwent source localization and superimposition on MRI. All patients underwent simultaneous MEG (148 channels Magnes) and EEG (32 channels) recordings. Digitizing frequency ranged from 678 to 4000 samples/second. Minimum requirements for dipole selection included: correlation > 0.90, GOF > 0.90 confidence volume < 15 cm3. RESULTS: Only148 SWs (12%) were bilaterally synchronous (0-3 msec inter-hemispheric asynchrony) and this probably represents thalamo-cortical synchronization. Cortico-callosal propagation (12-30 msec. inter-hemispheric asynchrony) was documented in 240 SWs (20%). A total of 820 SWs (68%) showed an inter-hemispheric asynchrony of 3-12 msec. Dipole source analysis showed that 714 of these SWs (74%) were localized in the cingular cortex bilaterally, although asymmetrically. The anatomical source localization of 1208 dipoles obtained in 63 SWs , was as follows: cingular cortex = 945 (78%), frontal mesial = 87 (7%) and frontal lateral = 176 (15%). CONCLUSION: Contrary to established views, our study shows that a thalamo-cortical and a cortico-callosal mechanisms of synchronization are only minimally represented in the genesis of generalized SWs in patients with pharmaco-resistant generalized epilepsy. Our findings demonstrate a paramount role of the cingular cortex in the synchronization of generalized SWs. The clinical implications of our findings will be discussed.

Variation of MEG and EEG Localisations Due to Different Volume Conductors

Scheler G, Fischer M, Hummel C, Genow A, Stefan H
Centre Epilepsy, Dept. of Neurology, University of Erlangen

Purpose: Defining the area eliciting the seizure precisely is essential for decision making in surgical epilepsy therapy. The aim of this study was to compare the accuracy of MEG and EEG results using two different volume conductor models in epilepsy patients. Methods: Simultaneous MEG and EEG investigations were performed in 85 patients during presurgical epilepsy evaluation. MEG was recorded with a 74 channel dual unit biomagnetometer (Magnes II, 4D-Neuroimaging). EEG was recorded simultaneously using 31 scalp electrodes positioned according to the international 10/20 system. Electrocardiogram (ECG) was recorded to track cardiac artefacts. Co-registered magnetic resonance tomography (MRT) data were available for all patients. Results: Localizations of about 4000 interictal spikes from MEG and EEG each were performed according to a single equivalent dipole source model. As volume conductors (a) a 3 spherical shells and (b) a realistic shaped head model (Boundary Element Method, BEM) segmented from MR-scans were used. Spatial distances between best fitting dipoles calculated with both volume conductor models and both modalities were assessed. In a preliminary calculation from 9 EEG spikes the mean distance between localisations between both volume conductor models was 19.4 mm (± 6.7 mm sd), from 14 MEG dipoles 10.1mm (± 5,0 mm sd), respectively. Conclusion: A calculation on a more realistic head model allows better confirmation of MEG results, because EEG source localisations are more influenced by the volume conductor model. Source localisations based on MEG are less dependent of the chosen volume conductor model and provide stable information for epilepsy surgery, especially in patients with lesions, malformations or tumors.

Differentiability of simulated hippocampal, parahippocampal and lateral temporal sources

J.M. Stephen[1], D. Ranken[3], C.J. Aine[1, 2], M.P. Weisend[2], J. Shih[1]
[1]University of New Mexico and [2]New Mexico VA Healthcare System, Albuquerque, New Mexico, USA, [3]Los Alamos National Laboratory, New Mexico, USA

Previous MEG studies have provided significant evidence that MEG can measure signals generated from the hippocampus, despite the cylindrical shape and deep location in the brain. The current study extended this work by examining the ability to differentiate the hippocampal subfields, parahippocampal cortex, and lateral temporal sources using simulated interictal epileptic activity. A model of the hippocampus was generated from the MRIs of five subjects. CA1, CA3 and dentate gyrus of the hippocampus were activated as well as entorhinal cortex (EC), presubiculum (PS) and lateral temporal cortex. In addition, pairs of sources were activated sequentially (5 ms offset) to emulate various hypotheses of mesial temporal lobe seizure generation. The simulated MEG activity was added to real background brain activity from the five epilepsy patients and the waveforms were compared to determine differentiability of the generators at the sensor level. In addition, the MEG simulated data was modeled using an automated multi-dipole spatio-temporal modeling technique [1]. The waveforms and source locations/orientations for all hippocampal and parahippocampal sources were differentiable from lateral temporal sources. In addition, hippocampal and parahippocampal sources were differentiable to varying degrees. For example, CA3 was differentiable from DG but not from CA1, whereas CA3 was differentiable from both EC and PS. This suggests that a similar simulation approach may be useful for determining the specific generators of real spike activity in patient data. This study was supported by NIH COBRE grant 5-P20-RR15636-02.

[1] Ranken, D.M., et al. 2002. MEG/EEG Forward and inverse modeling using MRIVIEW. Proceedings of Biomag 2002, 785-787.

The advantages of interictal MEG compared to EEG in case of Frontal Lobe Epilepsy.

[°]P. Ossenblok, ['] J.C. de Munck, [2] F.S.S. Leijten, [°]W. Drolsbach, [°3]P. Boon.
[°]Epilepsy Centre Kempenhaeghe, Heeze, Netherlands; [']MEG Centre, VUmc, Amsterdam, Netherlands;
[2] University Medical Centre, Utrecht, Netherlands; [3]University Hospital Gent, Gent, Belgium

A necessary step towards epilepsy surgery is the preoperative localization of the brain area that is responsible for the seizures of the patient in relation to eloquent cortex, preferably with non-invasive methods. In case of frontal lobe epilepsy (FLE) advanced source analysis of MEG proved to be a strong, non invasive tool for the identification of both the epileptic focus and the sensorimotor cortex.Visual inspection of the simultaneously recorded MEG and EEG of 20 patients revealed interictal epileptiform discharges (IEDs) with varying morphology and topography. Cluster analysis was used to classify these discharges on the basis of their spatial distribution followed by equivalent dipole analysis of the spike sub-averages, taking into account the realistic shape of the head. This fully automated analysis procedure yielded the brain areas involved during the IEDs. Spatio-temporal analysis of single spike events was used to identify the brain area responsible for the epilepsy of each of the patients studied. Cluster analysis based on the orientation of the equivalent dipoles obtained for the magneto-encephalographic median nerve responses provided us, furthermore, with a reliable tool for the localization of the sensorimotor cortex. For patients with FLE the yield of interictal spikes is much higher in the MEG than in the simultaneously recorded EEG. Also, the localizability of MEG is much better than for EEG, thus in general yielding a better “goodness of clinical fit“ compared, either to an epileptogenic lesion at MRI (n=18) and/or compared to intracranial recordings (n=10). Visualizing the source reconstruction results relative to the anatomy obtained from 3D-MRI, especially, appeared to be useful for guiding these intracranial recordings, and thus contributed to successful resective surgery, while minimizing the risk of sensorimotor deficits.

Comparison of Single Dipole Model with Adaptive-Beamformer Technique in Magnetoencephalograpy of temporal lobe epilepsy

Naohiro Tsuyuguchi (1), Hideji Hattori (2), Tsuyoshi Tsutada (3), Masahiro Shimogawara(4) Kensuke Sekihara(5) ,Mitsuhiro Hara(1)
(1) Department of Neurosurgery, (2)Pediatrics, (3)Geriatrics and Neurology, Osaka City University Graduate School of Medicine (4) Yokogawa Electronics Ltd. MEG center (5) Department of Electronics & Systems Engineering, Tokyo Metropolitan Institute of Technology

PURPOSE We evaluated source localization of interictal magnetoencephalography(MEG) in patients with intractable temporal lobe epilepsy(TLE) by single dipole model and adaptive-beamformer technique [1]. **METHODS** We performed spike recording simultaneously with EEG and MEG on ten patients with TLE. Scalp or subcortical EEG was recorded from 12 channels, whereas MEG was recorded from 160 channels. We compared neural activated area of a magnetic field in these two methods. **RESULTS** In four cases in ten cases, activated area caluculated by beamformer was larger than distribution of dipoles. In other six cases, we could not detect epileptogenic region by both methods. Dipole is sometimes distributed over white matter, because it only shows the center of activated area. On the other hand, the distribution by beamformer shows neurergic spatial spread and gives other information with dipole method. **CONCLUSIONS** adaptive-beamformer technique can present useful information in TLE.

[1] Sekihara K, Nagarajan SS, Poeppel D, Marantz A, Miyashita Y. 2001. Reconstructing Spatio-Temporal Activities of Neural Sources Using an MEG Vector Beamformer Technique. IEEE Transactions on Biomedical Engineering Vol.48, No.7, 760-771

Cortical thickness in a case of Congenital Unilateral Perisylvian Syndrome

Kotini, A., Camposano, S., Hara, K., Salat, D., Cole, A., Stufflebeam, S., Halgren, E.

Athinoula A. Martinos Center for Biomedical Imaging, Massachusetts General Hospital / Harvard Medical School, Charlestown, MA 02129,USA

ABSTRACT

In congenital perisylvian syndrome, there is polymicrogyric cortex distributed in variable extensions around the sylvian fissure. Unilateral cases usually present with congenital hemiparesis, while bilateral cases have pseudobulbar paralysis of the oropharingoglossal region. Both unilateral and bilateral cases have a high rate of epilepsy. Polymicrogyric cortex is characterized by too many small convolutions. Often there are no intervening sulci, and almost no white matter can be seen under them. On MRI they appear to have increased thickness. Bilateral and symmetric polimycrogiria can be hard to recognize on standard MRIs. Accurate and automated methods for measuring the thickness of cerebral cortex are available. They have mainly been used to study a variety of disorders with diminished cortical thickness. We studied a case of right perisylvian polymicrogyria, who presented in adult life with epilepsy and had a normal neurological exam. Fischl and Dale's automated cortical thickness analysis rendered a very clear picture of increased cortical thickness with values up to 9 mm in the affected areas (normal cortical thickness varies between 1 and 4.5 mm). The thickest areas were seen over grossly abnormal gyri on the reconstructed cerebral cortex. On MEG he presented a prominent and monotonous 9 Hz activity that was located within the limits of a thick gyrus. There was a significant difference of thickness between homologous hemispheric areas. To our surprise some areas of the left hemisphere also appeared to have increased thickness, raising the question of a bilateral asymmetric case.

KEY WORDS

Cortical thickness, automated MRI segmentation, polymicrogyria, perisylvian syndrome

INTRODUCTION

The thickness of the cortex is of great interest in both normal development as well as a wide variety of neurodegenerative and psychiatric disorders. Changes in the gray matter are manifested in Alzeimer's disease [Frisoni et al., 1996], Huntington's disease [Vonsattel and DiFiglia M., 1998], corticobasal degeneration [Boeve et al., 1999], schizophrenia [Pfefferbaum and Marsh, 1995] etc. The cortical thinning is frequently regionally specific and the progress of the atrophy can therefore reveal much about the evolution and causative factors of a disease. Congenital unilateral perisylvian syndrome is a rare disorder characterized mainly by the presence of a unilateral cerebral malformation that affects the perisylvian region and is often accompanied by a reduction in the size of the ipsilateral hemisphere, including the thalamus [Sebire et al., 1996]. Epilepsy can be present in unilateral and bilateral cases. The reported prevalence in congenital bilateral perisylvian syndrome is up to 87% and the seizures usually begin between the ages of 4 and 12 [Kuzniecky and Andermann, 1994]. The etiology of the unilateral cases is known less, but there is the suspicion that they are more commonly acquired *in utero* [Sebire et al., 1996]. We estimated the cortical thickness in a case of congenital unilateral perisylvian syndrome, who was relatively asymptomatic until age 23 evaluating the cortical atrophy in the affected areas.

CASE REPORT

The patient is a 29 year-old man with medically intractable epilepsy, who was referred for pre-surgical evaluation for an MEG and a high-resolution phased-array surface coil MRI. His presenting event was a generalized tonic-clonic seizure at age 23, after which he continued to have frequent stereotyped complex partial seizures in spite of an aggressive program of pharmacotherapy. He describes a spell as a ‘weird feeling’, which he cannot describe more accurately or specifically, although it, resembles déjà vu. At times he will see his right hand moving involuntary, and then he will lose contact with reality, which he refers to as ‘black-out’ and other witnesses describe as staring spells and disorientation. He has up to 2 of these episodes each day but can also be seizure free for a whole month. His mother's pregnancy and delivery were described as normal, and he reported no history of febrile convulsions or head trauma. There were no known CNS infections or toxic exposures. His early developmental milestones were stated to be normal, but he described himself as being a ‘slow learner’ and having reading problems at school, although he managed to complete high school. He reported no family history of epilepsy or any other neurological disease. His actual neurological exam was normal, except for some mild tremor on left arm extension and mild dysmetria on left finger to nose examination. For the estimation of cortical thickness we used the Fischl and Dale's [2000] automated cortical thickness analysis. The measurement of the thickness is enabled by a procedure for generating highly accurate models of both the gray/white and pial surfaces. The distance between these two surfaces then gives the thickness of the cortical gray matter at any point. They construct an estimate of the gray/white boundary by classifying all white matter voxels in an MRI volume. The surface of the connected white matter voxels then is refined to obtain subvoxel accuracy in the representation of the gray/white boundary and subsequently deformed outward to find the pial surface [Dale et al., 1999]. The automated cortical thickness analysis rendered increased cortical thickness values up to 9 mm in the affected areas (normal range: 1-4.5 mm). The thickest areas were seen over grossly abnormal gyri on the reconstructed cerebral cortex. Some areas of the left hemisphere also appeared to have increased thickness, raising the question of a bilateral asymmetric case (Figure 1). On MEG the spikes were detected predominantly by the right anterio- temporal sensors, including both mono- and rhythmic spikes. The equivalent current dipole (ECD) orientations are consistently at 45 degrees between horizontal and vertical. The ECDs clustered in the right infero-lateral frontal lobe and insula, with probable extension onto the superior portions of the temporal lobes anteriorly, an area affected by polymicrogyria. On MEG he presented also a prominent and monotonous 9 Hz activity that was located within the limits of a thick gyrus.

DISCUSSION

Our patient shows very clearly that the epileptogenic area is only a part of what appears dysmorphic on the images. The only other report of MEG in perisylvian syndrome [Tanaka et al., 2000] describes patients with focal epilepsy, in which the ECD clusters overlaid the perisylvian dysplasia, some patients exhibited more than one cluster. In the only patient with generalized epilepsy the ECDs didn't cluster, they did not localize primary cortices. Malformations of cortical development are known to be closely associated with partial seizures, but polymicrogyria is less frequently associated with epilepsy, as compared to focal cortical dysplasias, heterotopias, or agyria-pachigyria [Jansky et al., 2003]. The results presented in this study were achieved by combining a number of techniques including methods for constructing and transforming models of the human cerebral cortex, which are a part of a freely available software package. Furthermore, the pattern of cortical folds, in the form of mean curvature, Gaussian curvature, or average convexity, can be used to characterize geometric differences between populations in much the same manner as cortical thickness, a capability that may be useful in studying disorders associated with abnormalities in cortical folding patterns, such as polymicrogyria [Fischl and Dale, 2000]. The combination of these tools yields a set of powerful techniques for analyzing morphometric properties of the human cerebral cortex, with important applications in the study of the patterns of geometric changes associated with specific diseases.

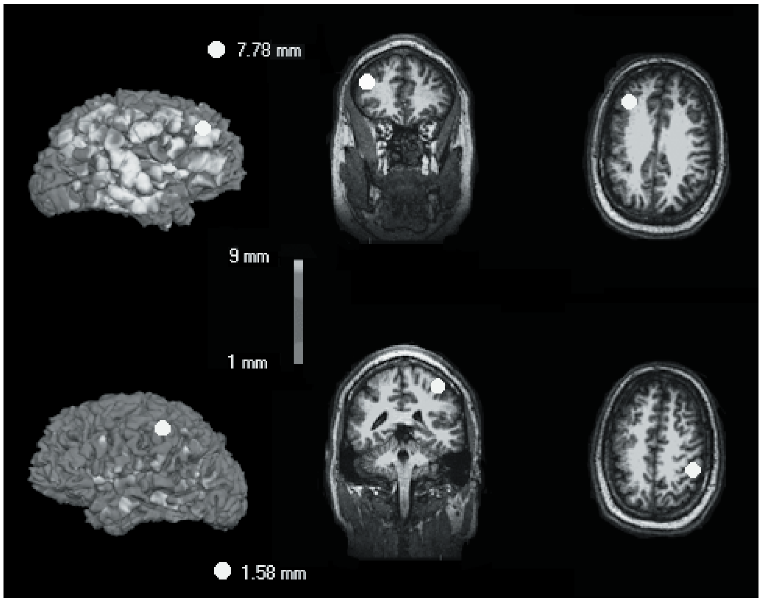

Figure 1. Reconstructed cortical surface with superimposed thickness. On the right side the white dot shows example of thick cortex in the frontal region. The left side shows normal thickness over most of the hemisphere.

REFERENCES

Boeve B, Maraganore D, Parisi J, Ahlskog J, Graff-Radford N, Caselli R, et al. Pathologic heterogeneity in clinically diagnosed corticobasal degeneration. Neurology 1999; 52:795–800

Dale AM, Fischl B, Sereno MI. Cortical surface-based analysis. I. Segmentation and surface reconstruction. Neuroimage 1999; 9:179-94

Fischl B, Dale AM. Measuring the thickness of the human cerebral cortex from magnetic resonance images. Proc Natl Acad Sci U S A. 2000; ;97:11050-5

Frisoni GB, Beltramello A, Weiss C, Geroldi C, Bianchetti A, Trabucchi M. Am J Neuroradiol 1996;17: 913–23

Janszky J, Ebner A, Kruse B, Mertens M, Jokeit H, Seitz R, et al. Functional organization of the brain with malformations of cortical development. Ann Neurol 2003; 53:759-67

Kuzniecky R, Andermann F. The congenital bilateral perisylvian syndrome: imaging findings ina multicenter study. CBPS Study Group. Am J. Neuroradiol 1994; 15: 139-44

Pfefferbaum A, Marsh L. Structural brain imaging in schizophrenia. Clin Neurosci 1995; 3: 105-11

Sebire G, Husso B, Dusser A, Navelet Y, Tardieu M, Landrieu P. Congenital unilateral perisylvian syndrome: radiological and clinical correlations. J. Neurol Neurosurg Psychiatry 1996: 61:52-6

Tanaka M, Yamada K, Watanabe Y, Matsuda K, Inoue Y, Fujiwara T, et al. Electroclinical and magnetoencephalographic analysis of epilepsy in patients with congenital bilateral perisylvian syndrome. Epilepsia 2000, 41: 1548-91

Vonsattel JP, DiFiglia M. Huntington disease. J Neuropathol Exp Neurol 1998; 57: 369-84

Predictor of cognitive deterioration in elderly subjects by auditory-evoked magnetic signal using magnetoencephalography

[1]Oe H., [2]Kandori A., [1]Miyashita K., [2]Ogata K., [2]Miyashita T., [3]Tsukada K., [4]Sakoda S., [1]Naritomi H.
[1]Department of Cerebrovascular Medicine, National Cardiovascular Center, Osaka,
[2]Central Research Laboratory, Hitachi Ltd., Tokyo, [3]Okayama University, Okayama
and [4]Osaka University, Osaka, Japan

ABSTRACT

Our previous auditory-evoked magnetic fields (AEFs) study has suggested that auditory impulses originated from the unilateral ear first arrive at the contralateral temporal cortex and later reach the ipsilateral temporal cortex presumably through interhemispheric neural connections. Such a conduction manner of auditory impulses enables us to measure interhemispheric neural conduction time (INCT). Our recent study showed the significant correlation between INCT and cognitive impairment in elderly subjects. In the present study, we estimated INCT and mini-mental state examination (MMSE) score in 11 elderly subjects with normal cognitive function yearly for consecutive 4 years. In 6 of 11 subjects (Group A), the cognitive function remained unchanged during the follow-up period showing 4 or less MMSE score reduction. In the other 5 subjects (Group B), the cognitive function deteriorated significantly during the follow-up period showing 5 or more MMSE score reduction. Changes in INCT and MMSE scores were compared between the two groups. In Group A, the baseline MMSE scores were 29.2±1.3, and the baseline INCT was 7.5±7.8msec. During the follow-up period, MMSE scores and INCT remained unaltered. In Group B, the baseline MMSE scores were normal showing 27.4±1.1, however, the baseline INCT was prolonged as compared with Group A showing 30.4±11.6msec. At the first and second follow-up years, MMSE remained unchaged showing 27.4±1.1 and 28.0±1.7, respectively, while INCT increased gradually to 31.2±11.6 and 34.2±14.6 msec, respectively. At the third follow-up year, MMSE scores began decreasing to 23.6±2 in association with further increase of INCT. MMSE score reduction and INCT increase became more remarkable at the fourth follow-up year. Thus, the prolongation of INCT occurred 2-3 years prior to the development of cognitive deterioration in elderly subjects. The measurement of INCT with AEFs may be useful for early detection of cognitive impairment in elderly subjects who may later develop dementia.

KEY WORDS

Auditory evoked magnetic fields; N100m peak latency; Mini-mental state examination; Cognitive deterioration: Interhemispheric neural conduction time.

INTRODUCTION

Auditory impulses originated from the unilateral ear reach the temporal auditory cortex bilaterally, although detailed neural pathways have remained unclarofied. MEG studies have indicated that the latency of auditory-evoked neuronal action peak (N100m peak) detected at the temporal cortex ipsilateral to the auditory stimulation is always delayed as compared with that deteced at the contralateral side [Pantev, 1998]. Regarding this phenomenon, our recent MEG study has suggested that auditory impulses originated from the unilateral ear first arrive at the contralateral temporal cortex and later reach the ipsilateral temporal cortex through interhemispheric neural connections, thus, leading to the delay of ipsilateral N100m peak latency [Oe, 2002]. Such a conduction manner of auditory impulses enables us to measure INCT with MEG. Our recent study showed the significant correlation between INCT and cognitive impairment in the elderly subjects [Naritomi, 2003] [Oe, 2004]. In the present study, we estimated changes in INCT and MMSE scores longitudinally for 4 years in 11 elderly subjects with normal cognitive function to see whether MMSE scores decrease during the follow-up period and whether the prolongation of INCT precedes the decrease of MMSE scores.

METHODS

11 normal cognitive elderly subjects complaining of unstable gait and dizzy sensation (MMSE score > 26, mean age: 68±8 years) who had otherwise no focal neurological abnormality were subjected. MEG studies were performed in all the subjects using a superconducting quantum interference device system (MC-6400, Hitachi Ltf.). Auditory stimuli with 90 dB in intensity and 1,000 Hz tone-burst were provided in the right ear, and N100m peak latency was measured at both temporal cortices. The INCT was calculated from the right and left N100m peak latencies. Cognitive function was evaluated using MMES scores. Following the measurements of the baseline INCT and MMSE scores, the measurements were repeated yearly for the consecutive 4 years in all the subjects. They were later classified to two groups according to the changes in MMSE scores, such as Group A with 4 or less MMSE score reduction during the follow-up period and Group B with 5 or more MMSE score reduction during the follow-up period. Longitudinal changes of INCT and MMSE scores were compared between the two groups.

RESULTS

Longitudinal changes of MMSE scores (♦) and INCT (■) are shown in Fig.1 and Fig. 2. There were 6 subjects in Group A. Their mean age was 73.8±8.4 years. The baseline MMSE scores were 29.2±1.3, and the baseline INCT was 7.5±7.8msec. At the fourth follow-up year, MMSE scores remained unchanged showing 29.7±0.5, and INCT increased slightly to 12.0±6.7msec (Fig. 1). There were 5 subjects in Group B. Their mean age was 70.6±8.9 years. The baseline MMSE scores were normal showing 27.4±1.1, while the baseline INCT was 30.4±11.6 msec which was significantly prolonged as compared with that in Group A. At the first follow-up year, MMSE score showed no change (27.4±1.1), and INCT showed also no remarkable change (31.2±11.6 msec). At the second follow-up year, MMSE scores remained unchanged at the normal levels (28.0±1.7), while INCT increased slightly to 34.2±14.6 msec. At the third follow-up year, MMSE scores decreased suddenly to 23.6±2.1, and INCT increased further to 38.3±10.1 msec. At the fourth follow-up year, MMSE scores were markedly reduced to 18.0±1.3, and INCT was prolonged definitively to 45.0±13.0 msec.

DISCUSSION

There have been several reports concerning the correlation between the delay in N100m latency in AEFs and the cognitive dysfunction [Pekkonen, 1999] [Naritomi, 2003] [Oe, 2004]. However, none has ever reported longitudinal changes of INCT before and after the development of cognitive dysfunction. We performed a follow-up study of cognitive function and AEFs in 11 elderly subjects with normal cognitive function who complained of unstable gait. The unstable gait is known to be one of predictors of non-Alzheimer's type dementia. As we anticipated, 5 of 11 subjects began to show the deterioration of cognitive function at the third follow-up year. In these 5 subjects, INCT was significantly prolonged at the baseline measurement at which time MMSE scores were normal. Our results suggest that the prolongation of INCT occurs 2-3 years prior to cognitive deterioration in elderly subjects with unstable gait. The cognitive function works under rapid interactions of multiple cerebral regions interconnected with neurons. The conduction velocity of interhemispheric neurons may play an important role for maintaning normal cognitive function. The degeneration or loss of interhemispheric neurons in elderly subjects may cause reduction of interhemispheric neural conduction velocity and prolongation of INCT and may culminatingly bring about the deterioration of cognitive function. The longitudinal measurements of INCT with AEFs can be carried out easily in elderly subjects repeatedly. The measurment may be useful to predict the development of cognitive impairment in elderly subjects and may greatly contribute to the preventive medicine of dementia.

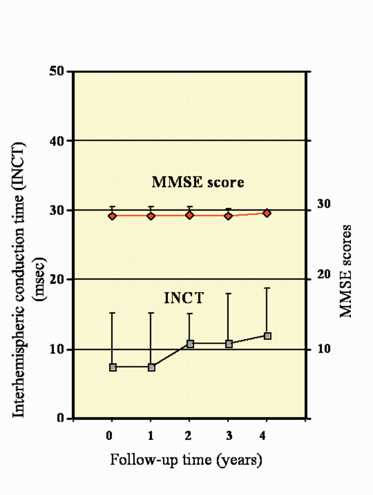

Figure 1 Longitudinal changes of interhemispheric neural conduction time (INCT) and mini-mental state examination (MMSE) scores in Group A

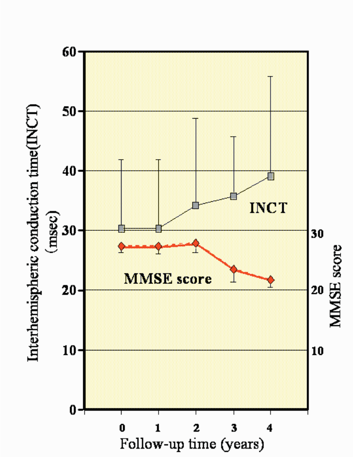

Figure 2 Longitudinal changes of interhemispheric neural conduction time (INCT) and mini-mental state examination (MMSE) scores in Group B

REFERENCES

Naritomi H, Oe H, Kandori A, Yamada N, Miyashita T, Tsukada K. Interhemispheric neural conduction time estimated by auditory-evoked magnetic fields is prolonged correlating with the degree of cognitive dysfunction in elderly subjects with unstable gait. J Cereb Blood Flow Metab 2003, 23: 597.

Oe H, Kandori A, Yamada N, Miyashita T, Tsukada K, Naritomi H. Interhemispheric connection of auditory neural pathways assessed by auditory evoked magnetic fields in patients with fronto-temporal lobe infarction. Neurosci Res 2002; 44:483-488.

Oe H, Kandori A, Miyashita T, Ogata K, Yamada N, Tsukada K, et al. Prolonged interhemispheric neural conduction time evaluated by auditory-evoked magnetic signal and cognitive deterioration in elderly subjects with unstable gait and dizzy sensation. International Congress Series, 2004; in press.

Pantev C, Ross B, Berg P, Elbert T, Rockstroh B. Study of the human auditory cortices using a whole-head magnetometer: left vs. right hemisphere and ipsilateral vs. contralateral stimulation. Audiol Neurootol 1998, 3; 183-190.

Pekkonen E, Jääskeläinen IP, Hietanen M, Huotilainen M, Näätänen R, Ilmoniemi RJ, et al. Impaired preconscious auditory processing and cognitive functions in Alzheimer's disease. Clin Neurophysiol 1999, 110; 1942-1947.

Neuromagnetic Study of Auditory Processing in Williams syndrome

Pekkonen, E.,[1,2,3] Osipova, D.,[2,3,4] Sauna-Aho, O.[5], and Arvio, M.[6]

[1]Department of Neurology, University of Helsinki, Finland; [2]BioMag laboratory, Helsinki University Central Hospital, Finland
[3]Cognitive Brain Research Unit, University of Helsinki, Finland; [4]Helsinki Brain Research Center, Helsinki, Finland
[5]Päijät-Häme Central Hospital, Lahti, Finland; [6]Pääjärvi Centre, Pääjärvi Inter-Municipal Association, Lammi, Finland

ABSTRACT

Williams syndrome (WS) is a rare congenital disorder, and mental retardation occurs in approximately 75 % of patients. Electroencephalographic (EEG) studies have found abnormalities of visual processing in WS. To study whether preattentive auditory processing is divergent in WS, we examined with magnetoencephalography (MEG) four WS patients and eight healthy controls. The patients with WS had delayed auditory P50m response over the hemisphere ipsilateral to the ear stimulated, whereas the amplitudes of P50m and N100m responses did not differ between the groups. Present results tentatively suggest that preattentive auditory processing contributing to stimulus detection is not attenuated, but partly delayed in WS.

KEY WORDS

Williams syndrome, EEG, MEG, Auditory evoked fields, Event related potentials

INTRODUCTION

Williams syndrome (WS) was first recognized as a distinct entity in 1961. WS is a rare congenital disorder affecting males and females equally, and it is associated with a microdeletion in the chromosomal region 7q11.23. It occurs in all ethnic groups and has been identified in countries throughout the world. WS is a complex developmental disorder comprising intellectual disability with a peculiar cognitive profile, impulsive and outgoing (excessively social) personality, limited spatial skills and motor control [Morris, 1988]. Besides cognitive abnormalities, impairment of visual processing have been found in EEG-studies [Grice, 2003]. MRI studies have revealed overall decrease of brain volumes, and increased cortical gyrification [Reiss, 2000]. It has not been previously studied whether early auditory processing is impaired in WS.

METHODS

Four patients with WS and eight healthy controls participated in the study. Institutional ethical committee approval was obtained prior the study. Monaural sinusoidal tones were presented to all subjects with interstimulus interval of 1 s, and the auditory evoked fields (AEF) were measured using a 306-channel whole-head MEG-system (Neuromag®). The recording passband was 0.03-100 Hz, with a sampling rate of 397 Hz. Vertical and horizontal electro-oculograms (EOG) were recorded to exclude blinking artifacts. Peak latency and amplitude values of the P50m and N100m were measured from the channel pair showing the largest responses over each hemisphere. The data analyses were accomplished using unpaired two-tailed *t*-tests.

RESULTS

There were not significant differences of the P50m and N100m amplitudes between the groups. The P50m was delayed in the auditory cortex ipsilateral to the ear stimulated in the WS group (Figs 1 and 2), whereas no significant differences of the N100m latencies were found between the groups.

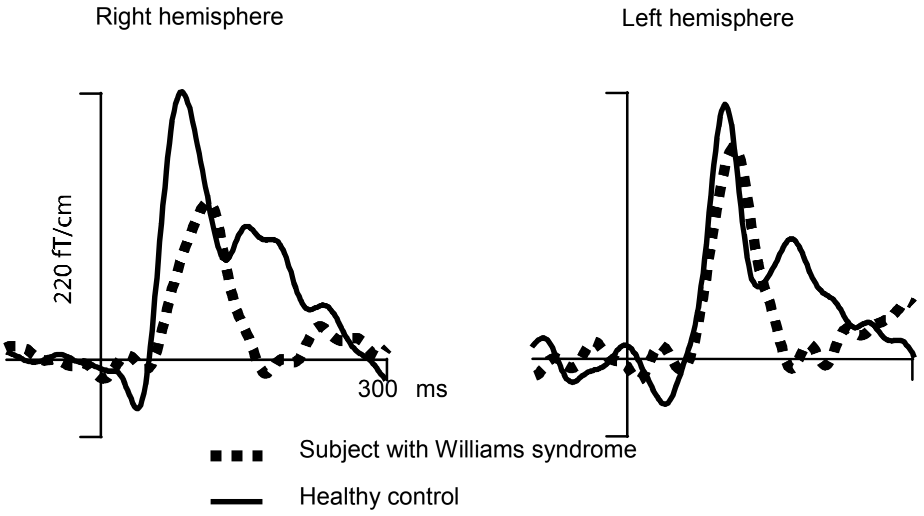
Right hemisphere

Left hemisphere

Figure 1 shows the AEFs of one patient with WS and one healthy control subject. The patient had delayed P50m bilaterally, although the group analysis showed a significant P50m delay only ipsilaterally to the ear stimulated.

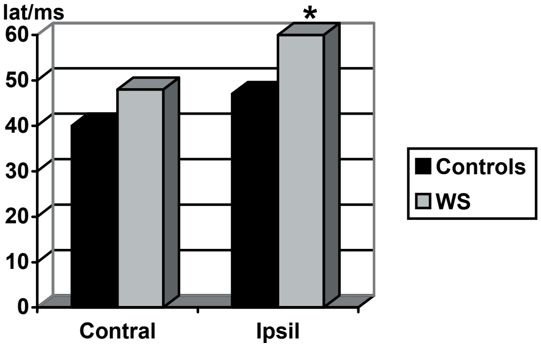

Figure 2. The P50m was significantly delayed in WS patients over the hemisphere ipsilateral to the ear stimulated. Contral: Contralateral hemisphere; Ipsil: Ipsilateral hemisphere. * $p < 0.05$.

DISCUSSION

Present results suggest that, unlike impaired visual processing [Grice, 2003], preattentive auditory processing contributing to stimulus detection is not attenuated in WS patients. Based on insignificant differences of AEFs amplitudes, the refractoriness of the P50m and N100m generators appears not to be affected by WS pathology, although reduced activation in the temporal lobes has been shown by fMRI in WS [Levitin, 2003]. Present results tentatively suggest that functional integrity of the smaller ipsilateral auditory pathway is more vulnerable to neuropathological changes in WS than that of the larger contralateral pathway.

ACKNOWLEDGEMENTS

We thank Mrs. Suvi Heikkilä, Mrs. Liisa Åstedt, and Mrs. Mari Ajasto for their assistance during the MEG measurements.

REFERENCES

Grice SJ, Haan MD, Halit H, Johnson MH, Csibra G, Grant J, Karmiloff-Smith A. ERP abnormalities of illusory contour perception in Williams syndrome. Neuroreport 2003;14(14):1773-7.

Levitin DJ, Menon V, Schmitt JE, Eliez S, White CD, Glover GH, et al. Neural correlates of auditory perception in Williams syndrome: an fMRI study. Neuroimage 2003;18(1):74-82.

Morris CA, Demsey SA, Leonard CO, Dilts C, Blackburn BL. Natural history of Williams syndrome. J Pediatr 1988; 113: 318-26.

Reiss AL, Eliez S, Schmitt JE, Staus E, Lai Z, Jones W, Bellugi U. Neuroanatomy of Williams syndrome: a high-resolution MRI study. J Cogn Neurosci. 2000;12 Suppl 1:65-73.

Age-Related Effects of Priming in Auditory Association Cortex

C. Aine[1], J. Adair[1], J. Knoefel[1], D. Hudson[2], C. Qualls[1], W. Cobb[2], D. Padilla[2], S. Kovacevic[3], J. Stephen[3]
[1]Albuquerque VA Medical Center, [2]BRINM, Albuquerque, [3]University of New Mexico SOM, NM USA

The encoding aspect of an implicit auditory verbal memory task was used to examine age-related effects of repetition priming (i.e., individuals perform faster and more accurately, along with concomitant reduction in activity in posterior regions, upon repetition of stimuli). Two groups of healthy normal subjects (20-40 and ≥ 65 years) listened to a list of 105 words representing common objects 3 times. The subjects' task differed upon each presentation: 1) is the object larger than a television set; 2) is the object used in daily living; and 3) after 20 minutes, the original list of words was embedded within a new list of words and subjects had to decide if each word was one they heard previously. Multi-start, a multi-dipole, spatio-temporal algorithm was used for characterizing source locations and timecourses. The figure at the left shows examples of Superior Temporal Gyrus (STG) timecourses from two young males (top and bottom rows). The largest amplitude tracing in both plots was evoked by the first presentation of the words and the smaller amplitude tracing was evoked during the third presentation of the words (delayed recognition condition). Differences between Trials 1 and 3 can be seen as early as 50 ms (i.e., greater amplitudes associated with the 1st trial) and age-related differences between 10 elderly and 8 young were statistically significant at 50 ms (i.e., peak amplitude did not differ according to task in the elderly). In agreement with Näätänen and colleagues (2001), it appears that a "primitive" form of intelligence exists in STG. This work was supported by VA Merit Review and The MIND Institute grants.

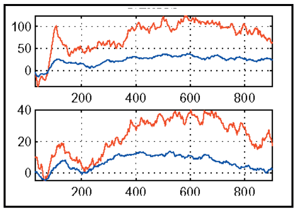

Näätänen, R, Tervaniemi, M, Sussman, E, Paavilainen, P, Winkler, I. (2001) "Primitive" intelligence in the auditory cortex. TINS 24:283.

Can MEG be used to monitor multiple sclerosis?

K.S. Cover, H. Vrenken, J. J.G. Geurts, B. van Oosten, B. Jelles, C.H. Polman, C.J. Stam MD,
B.W. van Dijk PhD
VU Medical Centre, Amsterdam, The Netherlands

Purpose: In this pilot study, we investigated the possible usefulness of MEG assessment of interhemispheric connectivity in MS. Currently, monitoring the course of the disease in multiple sclerosis (MS) patients is based on a combination of clinical measures and MRI measures. Loss of interhemispheric connectivity in MS patients has been assessed by other means including neurophysicological testing, functional and structural MRI, EEG and transcranial magnetic stimulation. However, none of these assessments indicated a promising marker for MS. **Method:** Five minutes of eyes closed data was acquired while each subject was seated in a 151 channels CTF (Vancouver, Canada) MEG scanner. Ten MS patients (EDSS 1.0-3.5 RR) and 11 healthy controls were scanned for the pilot study. We selected an artefact free 16s interval from each subject's data set. We then calculated the interhemispheric correlation measure over each 16s interval for each of 5 frequency bands (1-4Hz, 4-8Hz, 8-12Hz, 12-30Hz, 30-48Hz). **Results:** When ranked by interhemispheric correlation measure in the alpha band (8-12Hz), of the 21 subjects the highest 9 were all healthy controls and the lowest 7 were MS patients. By this ranking, there was a highly significant (p=0.00011 (Mann-Whitney-Wilcoxon 2 sided test)) difference between the two groups. **Conclusion:** Most likely, the loss of interhemispheric correlation in MS patients reflects widespread white matter dysfunction including connectivity loss, in particular of transcallosal commissural fibres. Determination of interhemispheric correlation with MEG is a promising marker for overall assessment of brain function in MS.

Somatosensory Evoked Magnetic Fields In Mild And Moderate Head Trauma

Jeffrey David Lewine [1,2]. John Davis [1], James Pingree [1], Robert Thoma [1], Robert Burr [1], Dina Hill [1], Michael Funke [1], Greg Jones [1], Erin Bigler [1]
[1] Functional Brain Imaging Program, University of Utah School of Medicine [2]. Hoglund Brain Imaging Center, The University of Kansas Medical Center

Introduction: This study sought to determine the extent to which mild/moderate head trauma alters somatosensory evoked fields. *Materials and Methods*: Two studies were performed, in the first, somatosensory evoked fields were recorded from 30 normal control subjects, 13 patients with a history of head trauma but no persistent post-concussive symptoms, and 17 patients with post-concussive symptoms subsequent to mild or moderate head trauma 6+ months earlier. In the second study, 14 persons underwent somaotosensory evaluations at 1 week, 4-6 weeks, and 6 months post head trauma.

Results: In study one, it was found that the M30 component of the median nerve somatosensory evoked field was abnormally small in more than 60% of subjects with persistent post-concussive problems. Immediately following head trauma 65% of subjects showed low amplitude M30 responses. By 6 weeks, this number dropped to 35%. Importantly, all 5 subjects with abnormal SEFs at 4-6 weeks, showed persistent cognitive compromise at 6 months. Of the 9 subjects with normal SEFs at 4-6 weeks, only one showed cognitive compromise at 6 months. It should also be noted that MEG was more predictive of long term outcome than either structural MRI or neuropsychological testing.

Discussion and Conclusions: The data indicate that SEFs may be a sensitive correlate of cognitive compromise following head trauma and that measurements taken at 4-6 weeks post trauma have high positive and negative predictive value with respect to long-term outcome.

Temporo-Parietal Theta Rhythm in Hemisphere with Carotid Artery Occlusive Disease

N.Nakasato, S. Seki*, S. Ohtomo, A. Kanno, H. Shimizu, T. Tominaga*
Department of Neurosurgery, Kohnan Hospital and *Tohoku University, Sendai, Japan

Background: Previous scalp EEG studies have detected unilateral upper theta rhythm in patients with erebrovascular diseases, but the incidence was small. Magnetoencephalography (MEG) may have higher sensitivity and spatial resolution than scalp EEG to detect the theta rhythm in patients with internal carotid artery (ICA) occlusive disease. Methods: Simultaneous EEG and MEG were performed in 48 patients with unilateral (n=39) or bilateral (n=9) stenotic lesions (more than 50% or occlusion) of the ICA (n=50) or middle cerebral artery (n=7) at least 30 days after the last stroke event, and in 27 age-matched healthy normal subjects. No subject had large infarct foci or severe neurological deficits. Results: MEG detected the theta rhythm (6-8Hz) in 14 of 48 patients: ipsilateral to the stenotic or occluded side in 13 hemispheres and bilaterally in 1 patient with unilateral lesion. The source of the MEG theta rhythm was estimated in the dorsolateral temporo-parietal area, regardless of the location of small infarct foci or the stenotic portion of the ICA system. The temporo-parietal theta rhythm (TPTR) was separated from the occipital alpha rhythm by frequency and distribution in MEG. In 2 of 14 patients, the TPTR was also found in EEG, but MEG provided better separation from the alpha rhythm. Neither MEG nor EEG detected TPTR in the normal subjects. Conclusion: Unilateral TPTR is correlated with the hemisphere with ICA occlusive disease. The TPTR may indicate mild, or subclinical, hemodynamic abnormalities in the ICA system. MEG is superior to EEG for the detection and localization of TPTR.

Altered generation of spontaneous neuromagnetic oscillations in Alzheimer's disease studied with minimum current estimates

Daria Osipova[1,2,3], Jyrki Ahveninen[1,2,4] Ole Jensen[5], Ari Ylikoski[6], and Eero Pekkonen[1,2,7]
[1]Cognitive Brain Research Unit, Department of Psychology, University of Helsinki, Finland;[2]BioMag Laboratory, Engineering Centre, Helsinki University Central Hospital, Finland;[3]Helsinki Brain Research Center, Helsinki, Finland;[4]Massachusetts General Hospital-NMR Center, Harvard Medical School, Charlestown, Massachusetts, USA;[5]F.C. Donders Centre for Cognitive Neuroimaging, Nijmegen, the Netherlands;[6]Department of Neurology, Koskela Hospital, Helsinki University Central Hospital, Finland; [7]Department of Neurology, Helsinki University Central Hospital, Finland

The abnormalities in the sources of spontaneous brain activity in Alzheimer's disease (AD) were estimated with minimum current estimates (MCE) calculated in the frequency domain. 306-channel MEG was recorded from non-medicated AD patients with mild to moderate cognitive impairment and age-matched controls in the eyes-closed condition. MCE, which is based on minimum L1-norm estimates and requires no assumptions about the number of sources, was calculated for the individual peak frequencies (7-11 Hz) in the power spectra. Activation within the regions of interest (ROIs) medially placed in parieto-occipital area was compared between the AD patients and the controls. Overall, oscillatory sources appeared to be less focal and displayed greater variability in AD patients, as compared with controls who demonstrated fairly robust activation near parieto-occipital sulcus. Activation within the parieto-occipital ROIs was significantly weaker in the AD patients. These preliminary results suggest abnormalities in oscillatory sources in AD, supporting the existing evidence of deficits in spontaneous EEG/MEG activity. MCE that provides simultaneous mapping of several oscillatory sources in the same frequency band might be a useful tool for detecting neurophysiological abnormalities associated with AD.

Acknowledgements: We thank Dr. Kimmo Uutela for technical discussions.

Brain sensorimotor hand area organization and functionality in acute stroke: insights from MEG

F. Tecchio[1], F. Zappasodi[1], P. Pasqualetti[2], A. Oliviero[2], C. Salustri[1], D. Lupoi[3], M. Ercolani[2], G-L Romani[4], V. Pizzella, P. M. Rossini[1-4-5]

1.Istituto di Scienze e Tecnologie della Cognizione (ISTC), CNR, Rome, Italy; 2. AFaR, Ospedale "Fatebenefratelli", Dipartimento di Neuroscienze, Isola Tiberina, Rome, Italy; 3. AFaR, Ospedale "Fatebenefratelli", Dipartimento di Radiologia, Rome, Italy; 4. Dip. Scienze Cliniche e Bioimmagini ed ITAB, Università "G. D'Annunzio", Chieti, Italy.5. Neurologia Clinica, Università Campus Biomedico, Rome, Italy.

A 'snapshot' of the acute phase following a cerebral stroke is fundamental to understand the brain's adaptation potential, which plays a key role in clinical recovery. In the present study, the characteristics of the spontaneous cerebral activity of the rolandic region and the evoked response following the stimulation of the median nerve have been studied trough magnetoencephalographic (MEG) recordings in 32 patients admitted to neurological ward for first-ever acute ischaemic stroke involving upper limb and hand. Both in affected (AH) and un-affected hemispheres (UH) spontaneous activity evaluation was performed by analysis of total power and spectral properties, individual alpha frequency and spectral entropy. Evoked activity was evaluated by characterization of the cortical sources activated by stimulation of the median nerve, in terms both of absolute values in each hemisphere, and of interhemispheric differences. Interhemispheric waveshapes cross-correlations were also carried out. Neurophisiological findings were correlated with neuroradiological ones and clinical scores. In the acute phase after an ischemic attack, the rest activity showed signs suggesting: a reduction of spectral richness; an increase of the intra-regional neural synchrony; an increase of the lower with respect to the higher frequency powers. Signs of enhanced excitability were present in the AH following a cortical lesion, usually in combination with preserved hand functionality. An enhanced excitability of the UH was paired with larger lesions with cortical involvement; signs compatible with an abnormal transcallosal transmission and intracortical function of inhibitory GABAergic inter-neurons in the AH were found subtending UH enhancement. Spared responsiveness from Brodmann's area (BA) 2 and posterior parietal areas despite an altered response from BA 3b was found in six patients, combined to high hand functionality. Present results in acute phase increase the knowledge of the mechanisms governing brain adaptation/reaction capabilities, for future efforts to establish therapeutic and rehabilitative procedures.

This poster will be also presented in Symposium 10. For the full paper, see Page 42.

P6-4

Inherited auditory-cortical abnormalities in twins discordant for schizophrenia

J. Ahveninen [1,2,4,5], I.P. Jääskeläinen [1,5], D. Osipova [2,4], M.O. Huttunen [6], R.J. Ilmoniemi [4], J. Kaprio [3], J. Lönnqvist [6], M. Manninen [6], S. Pakarinen [2,4], S. Therman [6], R. Näätänen [2,4], T.D. Cannon [7]
[1]MGH/MIT/HMS–Martinos Center, Charlestown, MA; [2]Cogn. Brain Res. Unit, and [3]Dept. Publ. Health, Univ. Helsinki, FINLAND; [4]BioMag Lab., Helsinki Univ. Centr. Hosp., FINLAND; [5]Lab. Comput. Engin., Helsinki Univ. Technology, FINLAND; [6]Dept. Mental Health and Alc. Res., Natl. Publ. Health Inst. Finland, FINLAND; [7]Depts Psychol., Psychiatry and Biobehav. Sci., and Human Genet., UCLA, CA

Information on the inheritance of neurophysiological abnormalities might help to elucidate the molecular genetic basis of schizophrenia. Here, we used MEG and EEG to determine inherited *vs.* state dependent auditory-cortical deficiencies in schizophrenia. Mono- and dizygotic (MZ and DZ) twin pairs discordant for schizophrenia, recruited from a total population cohort, were compared with a demographically balanced sample of healthy control twin pairs from Finland. EEG/MEG responses were measured to frequent standard and “rare” deviant tones. Neurophysiological measures were regressed against the degree of genetic relatedness to patients with schizophrenia. As expected, the EEG responses P50, N1, and mismatch negativity (MMN), as well as the source amplitude of the MEG response P50m, were reduced in the schizophrenic patients. P50/P50m and N1 were significantly decreased also in their unaffected co-twins, as compared to the controls. Interestingly, in the unaffected subjects, the decrease of P50 and N1 amplitude correlated significantly with the degree of genetic resemblance to the subjects having schizophrenia. Genetic modeling of variance components suggested that the P50 and N1 amplitude measures have high heritability. Our results suggest that schizophrenia may be associated with inherited abnormalities in early cortical auditory processing, reflected by the decreased P50 and N1 amplitudes. MMN deficits, previously shown to progress with disorder per se, might reflect mainly disease-specific changes.

This poster will be also presented in Symposium 13. For the full paper, see Page 58.

Impoverished Working Memory Network in Schizophrenia

C.J. Aine[1,2], D. Hudson[3], J. Bustillo[2], J. Lauriello[2], L. Rowland[2], R. Lenroot[2], S. Kovacevic[2], J. Stephen[2]
[1]Albuquerque VA Medical Center, [2]University of New Mexico SOM, [3]BRINM, Albuquerque, NM USA

A spatial working memory task was used to test the integrity of brain regions in chronic schizophrenic patients involved in encoding and recognition. It was hypothesized that schizophrenic patients, relative to normal control subjects, experience difficulty in sustaining activity across the multiple association areas during encoding, which can be characterized by cross-correlating the timecourses from these brain regions. The stimuli consisted of 16 nonsense shapes embedded in a 4x4 cell matrix. Subjects were to encode the location of the red shape among 15 green shapes in a Sternberg fashion (memory set sizes of 1 and 3). MEG data were analyzed using Multi-start, i.e., the average of the 5 best fits out of 10,000 unconstrained multi-dipole, spatio-temporal fits were used in MANOVAs and Pearson correlations. Hypofrontality was evident in patients during the encoding stage, as shown in the figure at the left. The higher-amplitude timecourse is an average across 6 normal controls. The lower-amplitude timecourse is an average from 6 chronic schizophrenia patients. In contrast, the patients exhibited hyperfrontality (i.e., greater amplitude around 300-600 ms which then quickly subsided) during the delayed recognition task (not shown). In general, normal control subjects revealed strong correlations between frontal and posterior brain regions which correlated with good performance. The poorer performing schizophrenic patients did not reveal similar correlations. Coordinated activity between frontal and posterior brain regions appears to help assure performance efficiency which was deficient in the schizophrenia patients. This work was supported by The MIND Institute.

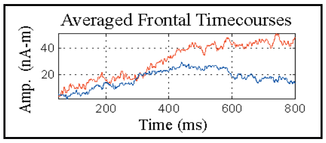

Paroxysmal MEG Activity in Psychiatric Disorders

C. Amo 1, LF Quesney 1-2, F. Maestu 1, A. Fernández 1, T Ortiz 1.
1Centro de Magnetoencefalografía Universidad Complutense de Madrid, España
2 McGill University, Dept. Neurology and Neurosurgery., Montreal, Canada

Introduction: Functional neuroimaging in psychiatric disorders helps identifying hypo-metabolic or hypo-perfusion changes in specific brain regions. We studied MEG´s diagnostic contribution in patients with Obsessive Convulsive (OCD) and Bipolar disorders. Method : Simultaneous MEG (144 channels) and EEG recordings (20 channels were performed in 14 patients with Obsessive-Compulsive disorders (OCD , mean age 33 years) and in 18 patients with bipolar disease (mean age 39 years). Dipole selection criteria included: correlation >0.95, RMS= at least 400fT, GOF >0.95, confidence volume <15 cm3 and ||Q|| < 400nAm. MEG was performed in 12 normal subjects matched according to age and sex. Results :1) OCD : Paroxysmal MEG activity (PMA) consisting of spikes and polyspikes, were exclusively seen in MEG tracings of 13/14 patients (93 %). This activity was not followed by a slow wave . PMA´s intensity measured in dipoles/min. correlated with disease severity. A predominant distribution of PMA was seen in : cingular cortex (11/12 patients), insula (7/12 patients) and orbito-frontal cortex (4/7 patients).None of the control subjects showed MEG paroxysmal activity.2) Bipolar Disorder : In 13/18 patients (72%) presented with PMA predominating in : mid and posterior cingular cortex (7/13 patients) and posterior insular region (10/13 patients). Seventeen patients were in a depressive phase and one was in a manic state. Conclusions :MEG confirms an anterior cingular, orbito-frontal and anterior insular network dysfunction in OCD. Since serotonin neurotransmission is deficient in OCD, we propose that PMA represents a state of increased cortical excitability due to reduced cortical serotoninergic inhibition, which also explains the lack of slow wave activity following the paroxysmal transients. As a new finding, a posterior cingular –insular network dysfunction was documented in bipolar disorder.

Low Modulation of MEG Alpha Band in OCD during Visual Working Memory Task Suggests Abnormally Active "Baseline Mode"

K.T. Ciesielski[1,2,3], M.S. Hämäläinen[1], P.G. Lesnik[1,3], D.A Geller[2], L. Parks[3], S.L. Lundy[3], S.P. Ahlfors[1]
[1]MGH/MIT/HMS Athinoula A. Martinos Center for Biomedical Imaging, Charlestown, USA. [2]Dept. Psychiatry, MGH, Boston, USA.
[3]Dept. of Psychology, Univ. New Mexico, Albuquerque, N.M., USA

"Baseline Mode" [1] refers to EEG/MEG alpha rhythm reflecting "idling" activation within attentional system. Alpha is suppressed during processing of external task demands and during intrinsic mental operations with a high cognitive load. Patients with obsessive-compulsive disorder (OCD), who experience obsessive thoughts and mental rituals, were hypothesized to show abnormal suppression of alpha when performing a working memory task. Furthermore, we expected a more normal pattern of alpha when the demands from an external distractor was presented, as it may dampen the effect of obsessive thoughts. We recorded whole-head MEG (Neuromag Ltd) from OCD patients (Y-BOCS: obsessive items above 12, compulsive above 10) and pair-matched controls, while they were performing 2 versions of a visual-spatial delayed matching-to-sample task (DMST; without or with a distractor in the Delay period). Temporal-Spectral Evolution measure of event-related-alpha activity (8-13 Hz, parieto-occipital and frontal) was computed within four 400 ms windows: Baseline, Post-Encoding (PE), Post-Distractor (PD) and Post-Retrieval (PR). No group differences were found in the accuracy of task performance. Event-related alpha was significantly more suppressed (more cognitive effort) during PD in OCD and during PR in Controls; no group difference was found during PE. The pattern of alpha suppression during Delay was more similar between the groups when a Distractor was present. The abnormal pattern of alpha suppression in OCD, in conjunction with their normal accuracy of performance, suggests that there is a cerebral mechanism related to performance compensating for abnormally active "baseline mode".

Supported by The MIND Institute.

[1] Laufs, H. et al. 2003. PNAS 100, 11053-11058.

A Specific Hippocampal Deficit in Schizophrenia

[1,2]F.M. Hanlon, [1,2,3]M.P. Weisend, [2]R.A. Yeo, [6]M.X. Huang, [1,4]R.J. Thoma, [6]R.R. Lee, [2]S.N. Moses, [1]K.M. Paulson, [5]H. Petropoulos, [4,7]G.A. Miller, [1,4]J.M. Cañive
[1]New Mexico VA Health Care System; [2]Department of Psychology; [3]Department of Radiology; [4]Department of Psychiatry; and [5]Mental Illness and Neuroscience Discovery Institute, Alq, NM; [6]Department of Radiology, UCSD and VA, San Diego, CA; [7]Departments of Psychology and Psychiatry and Beckman Institute Biomedical Imaging Center, University of Illinois, Urbana-Champaign, Illinois

Numerous studies have shown hippocampal abnormalities in schizophrenia. Despite these reports, schizophrenia patients have not been systematically evaluated on a task that has been shown to be specifically dependent on the hippocampus. The transverse patterning task (TP) is sensitive to the relational mnemonic capabilities of the hippocampus. In TP, subjects choose between stimuli presented in pairs, with the correct choice being a function of the specific pairing. Schizophrenia patients and controls performed a non-verbal version of TP as well as control tasks that are not hippocampal-dependent. Magnetoencephalography (MEG) data was done with a 122-channel, whole-cortex biomagnetometer and analyzed using multi-dipole spatial temporal analysis. Consistent with predictions, patients displayed a behavioral impairment in TP. No group differences were obtained for the non-hippocampal-dependent tasks. MEG showed controls activating right hippocampus during TP performance, and MRI volumetric analyses found right hippocampal volume correlated with TP performance during training. Patients showed more bilateral or left hippocampal activation during TP and greater left lateralization predicted better performance on TP. Hippocampal activation was seen in a small percentage of control subjects during the control tasks, with no group differences in lateralization. Schizophrenia patients' abnormal hippocampal lateralization addresses the mechanism for the behavioral deficit and furthermore demonstrates the feasibility of recording hippocampal activity with extracranial MEG.

Neuromagnetic Correlates Of Auditory Hallucinations

Jeffrey D Lewine, Ph.D[1,3], Jose M. Canive, M.D[2], Christopher J. Edgar, M.A.[2], John T. Davis, Ph.D[1]
[1] Functional Brain Imaging Program, University of Utah School of Medicine; [2] Department of Psychiatry, Albuquerque Veterans Administration Medical Center; [3] Hoglund Brain Imaging Center, Departments of Neurology and Psychiatry & Behavioral Sciences, KUMC.

Introduction: This study sought to elucidate the neurobiological substrates of auditory hallucinations in schizophrenia. *Materials and Methods:* Six minutes of spontaneous MEG data were collected from each of 4 patients with schizophrenia who reported auditory hallucinations during the MEG examination [group AH+], 4 schizophrenic patients with histories of hallucinations, but with none during MEG [group AH0], 4 schizophrenic patients without a significant history of hallucinations and with none during MEG [AH-], and 12 sex and age-matched normal comparison subjects. Quantitative spectral analyses were performed and the patient data were compared to the data from normal comparison subjects. *Results*: Patients with histories of significant hallucinations (AH+ and AH0) demonstrated increased left inferior frontal theta activity relative to normal comparison subjects and schizophrenic patients without a significant history of hallucinations (AH-). Active hallucinations during the MEG examination were characterized by the additional presence of bursts of 7.5-9.5 Hz activity over one or both superior temporal regions. Source modeling showed this activity to arise predominantly from primary and secondary auditory processing areas of the temporal lobe. Active hallucinations were seen only when both left inferior frontal and superior temporal abnormalities were present. *Discussion and Conclusions*: The data are consistent with the hypothesis that auditory hallucinations reflect abnormal monitoring of inner speech under conditions where the auditory cortex of the superior temporal plane is abnormally active. The abnormal auditory activity is postulated to impart to inner speech a brain activity profile that is normally associated with the monitoring of external speech.

Epileptiform Activity And Steroid Responsivity In Autism

Jeffrey David Lewine [1,2], Michael Chez [3], Richard Andrews [4], Stephen Mott [5], James Riviello [6], Michael Funke [2], John T. Davis [2], Sherri L. Provencal [2], Dina Hill [2],
[1] Hoglund Brain Imaging Center The University of Kansas Medical Center [2] Functional Brain Imaging Program, University of Utah School of Medicine [3] Pediatric Neurology, Lake Forrest, Illinois. [4] RA Neurological, Omaha, Nebraska. [5] Developmental Pediatrics Program, Children's National Medical Center [6] Department of Neurology, Children's Hospital of Boston

Objective: The goal of this study was to determine if specific patterns of epileptiform activity are predictive of the quality of clinical response to high-dose steroid therapy in the autism spectrum disorders (ASDs).
Design: MEG and EEG data, along with clinical data, were retrospectively reviewed for 36 children with autism spectrum disorders who had been treated with high-dose prednisone, each child known to have had an epileptiform EEG -- a pre-requisite for treatment with steroids. Based upon review of clinical notes and parental interview, 20 of the children were classified as steroid responders. In nine of these cases there was additional, explicit documentation that steroid therapy had led to improved language skills, as assessed by standardized expressive and receptive language tests. There were 16 cases where the child was classified as non-responsive to steroids. *Results*: MEG revealed peri-sylvian epileptiform activity in 32 of the 36 subjects, with the majority of subjects (n=25) showing multifocal patterns of epileptiform activity. For both MEG and EEG, the best rule for predicting steroid responsivity was: 'a subject will respond well to steroids if epileptiform activity is restricted to peri-sylvian, peri-rolandic, and inferior frontal regions'. Using this rule, EEG alone correctly classified 13 of the 16 non-responders (81%), and 13 of the 20 responders (65%). MEG was more informative, providing correct classification of 15 of 16 non-responders (94%), and 17 of the 20 responders (85%). *Conclusions*: A sub-set of children with regressive autism spectrum disorders and epileptiform MEG and EEG show a positive response to high-dose steroid therapy, especially in the language domain. Good responsivity is associated with a restricted epileptiform profile involving only peri-sylvian, peri-rolandic, and inferior frontal regions. When other brain regions are epileptiform, it is unlikely that a positive steroid response will be seen.

Spectro-temporal neuromagnetic and hemodynamic correlates of impaired P50 suppression in schizophrenia

K. Mathiak, H. Ackermann, A. Rapp, U. Klose, T.T.J. Kircher
University of Tübingen, Germany

Long standing observations on schizophrenia reveal several measures of stimulus adaptation to be impaired. The P50 suppression paradigm assesses the decrease of auditory evoked responses to a second stimulus S2 shortly (500 ms) after the first S1. Dysfunctions at the thalamus as well as cortical networks have been suggested as cause for impaired P50 suppression in schizophrenia. We studied 12 subjects with schizophrenia according to DSM-IV and a group of matched controls with P50 suppression paradigms in fMRI and whole-head MEG. Spectro-temporal analysis of evoked and induced neuromagnetic fields over the left and the right auditory cortex revealed reduced overall activity and a reduction of energy in the beta frequency range at later frequency ranges most pronounced over the right hemisphere. Moreover, the BOLD measure of suppression correlated most highly at the right hemisphere with its neuromagnetic equivalent across all subjects (cc = 0.5). Finally, coherences between the left and the right hemisphere of induced oscillations were significantly reduced in the patient group. The study reproduced stimulus suppression deficits in schizophrenia with localized BOLD responses and in neuromagnetic oscillation at the left and the right auditory cortex. Moreover, both measures were found to be linked by cross-subject regression. The data support models of impaired local network functions across primary and higher order auditory cortex in schizophrenia. These disturbances might contribute to the emergence of auditory hallucinations and formal thought disorders.
Acknowledgments: Supported by DFG SFB 550/B1.

MEG Reveals Rapid Temporal Processing Impairment In Autism

J. Oram Cardy[1], E. Flagg[1], P. Ferrari[1], W. Roberts[1,2], & T. P. L Roberts[1]
University of Toronto[1] & Hospital for Sick Children, Toronto[2], Canada

Goals: We applied a novel MEG approach to examine Rapid Temporal Processing (RTP) in children with Autism. Deficient RTP may contribute to the debilitating language impairments in Autism by interfering with processing of brief acoustic transitions crucial for speech perception [1]. Behavioral RTP paradigms used to date have been confounded by attention and memory demands. MEG offers the opportunity to acquire neural measures of RTP within a passive experimental paradigm, and critically, the submillisecond temporal resolution needed to examine the cortical activity associated with RTP. We measured the auditory M100 in response to rapid tone pairs as a potential neural correlate of RTP. *Methods:* 8 adults, 7 children and adolescents with Autism, and 6 typically developing controls were passively presented 120 trials of a rapid tone pair (40ms 1kHz tones separated by a 150 ms silent gap). Evoked neural activity was recorded using a whole cortex, 151-channel MEG system (CTF Systems) and examined, after averaging all trials, for identification of an auditory M100 response to each tone; latency and amplitude of each identifiable M100 peak was recorded. *Results:* The first tone elicited an identifiable M100 in all adults and controls, and 5/7 subjects with Autism (χ^2, n.s.). The second tone, which presented RTP demands, elicited an identifiable M100 in most adults (7/8) and controls (4/6) but only one subject with Autism (χ^2, p=.01). Analysis of identifiable responses to the first tone revealed that adults showed greater M100 peak amplitude than both child groups (p=.002), who did not differ. No latency effects were found. *Conclusion:* Findings provided support for and suggested a possible neural correlate of dysfunctional RTP in Autism.

Supported by the *National Alliance for Autism Research* and the *Canadian Institutes of Health Research*.

[1] Tallal, P. et al. 1996. Language comprehension in language-learning impaired children improved with acoustically modified speech. Science 271, 81-84.

A specific reduction in the sustained 40Hz magnetic field power in schizophrenia

S. M. Stufflebeam, T. Witzel, F. H. Lin, D.M. Foxe, K. Spencer, and R. C. McCarley
HST/MIT/MGH Athinoula A. Martinos Center for Biomedical Imaging, Boston, MA, USA

Purpose: To quantify and localize the neuromagnetic 40Hz sustained response in schizophrenia. **Methods**: *Subjects*: 5 medicated chronic schizophrenic subjects and 5 neurologically normal subjects were studied. *Stimuli*: Blocks of 500ms trains of 1msec auditory clicks were presented at 75dB HL, bilaterally. MEG: 306-channel VectorView; MRI: 3T fMRI using a sparse auditory imaging technique (sounds presented in 8 sec of silence). *Analysis*: Welch-method PSD using a 2-dipole ECD; Inflated cortex (FreeSurfer) constrained, wavelet-transformed minimum norm estimate with fMRI-weighting (Dale et al, Neuron 2000) to calculate current distributions on the cortical surface. **Results**: The 40Hz response was significantly reduced in the SZ subjects ($P<0.05$), but the 20 Hz and 30Hz response were not significantly different from the control subjects ($P>0.7$). fMRI demonstrates activation of the entire Heschl's gyrus with variable response in the planum temporally. There was a trend towards a correlation between the cortical thinning in the left posterior STG and the power reduction in the left 40Hz power, but did not reach statistical significance with our small pilot sample size. **Conclusion**: A specific reduction of the 40Hz sustained neuromagnetic response power in schizophrenic patients appears to originate in Heschl's gyrus, most prominently on the left side. This supports findings in EEG [1] and suggest abnormal gamma processing the auditory cortex of schizophrenics.

Supported by the MIND Institute.

[1] Kwon *et al.* Gamma frequency-range abnormalities to auditory stimulation in schizophrenia. Arch Gen Psychiatry. 1999 Nov;56(11):1001-5.

Auditory Sensory Gating Deficit and Cortical Thickness in Schizophrenia

[1,2]RJ Thoma, [2]N Sanchez, [1,2]FM Hanlon, [1,2]MP Weisend, [2]M Huang, [1,3]GA Miller, [1,2]JM Canive,
[1] Departments of Psychiatry and Radiology, University of New Mexico, USA; [2]New Mexico VA Health Care System; [3]Department of Psychology and Beckman Institute, University of Illinois at Urbana-Champaign, USA

A P50 sensory gating deficit is considered characteristic of schizophrenia. Abnormalities of temporal lobe structure are also common attributes of the disorder. While the standard EEG P50 sensory gating measure does not foster differential assessment of left- and right-hemisphere contributions, its analogous MEG measured M50 component may be used to measure gating of auditory source dipoles localizing to left and right hemisphere primary auditory cortex. We sought to determine how sensory gating ratio may relate to cortical thickness at the site of the auditory dipole localization. A standard paired-click paradigm was used during simultaneous EEG and MEG data collection for groups of 22 patients and 11 normal control subjects. Sensory gating ratios were determined by measuring the strength of the 50ms response to the second click, divided by the first click (S2/S1). Cortical thickness was assessed by two reliable raters (intraclass correlation > .90) using 3D sMRI. (1) Patients had a P50 and left M50 sensory gating deficit; (2) Cortex in both hemispheres was significantly thicker in the control group; (3) In the schizophrenia group: Left M50 gating ratio negatively correlated with left cortical thickness; and (4) there was a trend for right M50 gating ratio to correlate with right cortical thickness. MEG assessed hemisphere specific auditory sensory gating ratio may reflect cortical abnormality in schizophrenia.

This poster will be also presented in Symposium 13. For the full paper, see Page 54.

Determination of multi-coil currents considering mutual coupling effects in transcranial magnetic stimulation

Han, B. H.[1], Jeon, C. I. [1], Jin, S. O. [1], Kim, K. U. [1], Huh, Y. [1], and Lee, S. Y. [2]

[1]Electromagnetic Medical Device Research Center, Korea Electrotechnology Research Institute, Korea
[2]Department of Medical Engineering, Kyung Hee University, Korea

ABSTRACT

The multi-channel magnetic stimulation with a number of coils is indispensable for transcranial magnetic stimulation (TMS). A multi-channel magnetic stimulator is able to increase the localization of stimulation sites and the intensity of magnetic stimulation in comparison with a single-channel magnetic stimulator. During the stimulating of target sites, the factors of the determining of a stimulating form are the physical factors of coils, the coil currents, and the electrophysiological properties of the stimulated sites. The stimulating points and the stimulating shapes are determined by only the adjustment of the coil currents because the physical specifications of the stimulating coil have been already determined before the mounting to the system, and the electrophysiological properties of the human body could not be changed. The frequency and the strength of the magnetic stimulation are changed due to the mutual inductance among the adjacent coils during the time-varying coil currents. Therefore, a multi-channel magnetic stimulation system has to be designed with consideration of the mutual inductance among the adjacent coils. In this paper, the multi-coil array of the multi-channel magnetic stimulation is proposed for the use of TMS. Precise spatial localization of stimulation sites without any movements of the stimulation coils is very important for the efficient TMS. The optimal coil currents are computed to stimulate the specific target sites and the mutual inductance among the adjacent coils is measured through the multi-channel magnetic stimulating coil model.

KEY WORDS

Multi-coil, mutual coupling, optimal coil current, multi-channel stimulation.

INTRODUCTION

The determination factors of magnetic stimulation shape are divided into the material parts and the immaterial parts. The material parts fixed during the design and manufacturing of a magnetic stimulator are the physical factors of magnetic stimulation coil such as 3 dimensional structure, size, and inductance. The immaterial parts are the intensity of the coil current and the current waveform. The physical factors of stimulation coil determine the wide areas of the desired stimulation site and the character of magnetic stimulation, while the coil current and the current waveform determine the stimulation shape within the previously fixed physical areas. Recently, theories of multi-channel magnetic stimulation have been introduced [Han, 2004] [Ruohonen, 1999]. By using multi-coil with which separate channels are connected and by the adjustment of coil current, the stimulation site can be moved without any physical movements of the coils and the spatial localization in the stimulation can be achieved more precisely than by a conventional single coil based system. For this, the multi-channel magnetic stimulator can be greatly utilized in TMS and brain studies in conjunction with anatomical CT or MRI head images for precise targeting of cortex stimulations [Bohning, 1999]. In the multi-channel TMS system, the mutual coupling effect among the adjacent stimulation coil has to be inevitably considered. When the coil current flows into the stimulation coil array, the mutual inductances that can induce the undesired stimulation shape existed in the multi-coil array. In this paper, we proposed the multi-coil structure for multi-channel magnetic stimulation. When the coils are approached to the adjacent coils, we measured the coupling coefficient through the multi-channel magnetic stimulating circuit model and calculated the multi-coil currents and voltages.

METHODS

The intensity and frequency of the coil currents are transformed with respect to the mutual coupling grade in the multi-coil array when the coil currents of the multi-channel magnetic stimulator flow into the stimulation coil array. In order to measure the mutual inductances of multi-coil array, the stimulation coil array has been fabricated with circular type for the convenience of fabrication. The mutual inductance has been measured as the distance *d* between the center of a coil and the center of another coil changed. For the purpose of the calculation of the mutual inductance *M* and the coupling coefficient *K* as $M=K(L_1L_2)^{1/2}$, firstly we measured the inductance of a single coil like L_1, L_2, respectively, and measured the total inductance after the coupling the two coils. The coil model of two-channel is the base of the multi-coil array. The coil current of each channel can be calculated by Equation (1), where the capacitance, resistance, inductance, and current of the channel 1 are C_1, R_1, L_1, i_1, respectively, those of the channel 2 are C_2, R_2, L_2, i_2, respectively.

$$\left(L_1-\frac{M^2}{L_2}\right)i_1''+R_1i_1'-\frac{MR_2}{L_2}i_2'+\frac{1}{C_1}i_1-\frac{M}{L_2C_2}i_2=0\ ,\ \left(L_2-\frac{M^2}{L_1}\right)i_2''+R_2i_2'-\frac{MR_1}{L_1}i_1'+\frac{1}{C_2}i_2-\frac{M}{L_1C_1}i_1=0\ . \tag{1}$$

The 9-channel model shown in Figure 1 can be extended from the model of the two-channel. The 9-channel model is the basic unit of the coil array of magnetic stimulation that a coil affects the inductance of an adjacent coil. When the driving current of magnetic stimulator in the 9-channel model is injected into the channel 5, the coils situated in the cross line, such as channel 2-5, 4-5, 5-6, and 5-8, have the non-negligible coupling coefficients. The coils situated in the diagonal line, such as channel 1-5, 3-5, 5-7, and 5-9 have the small coupling coefficients than those of the cross line. In Figure 2, we have shown a planar coil array consisting of 6 by 6 as the extended model of Figure 1, and each coil has the outer diameter of 20mm, the inner diameter of 16mm, and the thickness of 2mm.

It was reported that the numerical methods were used to find the optimal coil current of each channel in multi-channel magnetic stimulation [Ruohonen, 1999]. There are the least square method (LSM) using the pseudo-inverse matrix and the conjugate gradient method (CGM) using the iteration of calculation in the numerical method. In this paper, we used the CGM for the calculation of the optimal coil current of the multi-coil array. We define the cost function *f* written by Equation (2),

$$f=\int_{\mathrm{v}}\left|\vec{P}-\vec{E}\right|^2 d\mathrm{v}\ =\int_{\mathrm{v}}\left|\vec{P}+\sum_{i=1}^{N}\left(I_i^{peak}\frac{du_i}{dt}\right)\vec{L}_i(\vec{r})\right|^2 d\mathrm{v}\ , \tag{2}$$

where P is the pre-defined field, E is the induced field by magnetic stimulation, L_i is the lead field of coil i, I_i is the current of coil i, N is the number of channel, i is the number of coil, r is the distance vector from origin, I_i^{peak} is the peak value of the first period of a coil current calculated by Equation (1), u_i is the unit current of coil i, and v is the 3 dimensional volume. We can find the optimal coil current on the restriction of minimization of the cost function. Also, the corresponding voltages with the optimal currents can be found using Ohm's law considering the mutual couplings.

RESULTS

As the results of the measurement of inductance with the fabricated multi-coil array, the coupling coefficient K has been changed in respect to the change of distance d between the centers of coil as shown in Figure 3, where L=35μH. The inner diameter and the outer diameter are 70mm and 142mm, respectively. The direction of coil current was equal to each other. The coupling coefficient K has been changed from -0.08 to 0.77. The negative polarity is caused by the opposite direction of coil current in the overlap site during the edges of coils are approached to each other. The K =0.08 has been measured when the two coils were contact with each other like channel 1-2 of Figure 1. When the two coils were apart from each other as much as channel 1-5 of Figure 1 situated in diagonal line, K has been measured at 0.01. In Figure 2, the coupling coefficients of this model were considered as the same values because this model was the extended that of Figure 1.

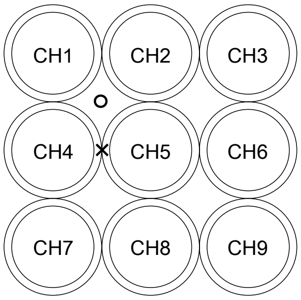

Figure 1. The 9-channel model of multi-channel coil array.

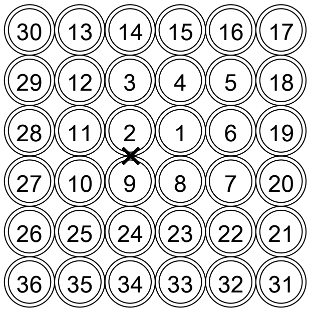

Figure 2. The 36-channel coil array model.

For the calculation of the optimal currents, we considered X-mark represented in Figure 2 as the desired stimulation site. The desired site is 20mm below the coil array and the direction of the desired field is assumed to be along the parallel plane. The desired fields represented by the pre-defined fields P in Equation (2) were calculated using the commercial FEM electromagnetic solver (OPERA, Vector fields Inc.). In the FEM calculation, a cylindrical current dipole of 1mA was located along the pre-defined direction at the desired site. Using the lead fields and the conjugate gradient method for the optimization, we have found the optimal coil currents as shown in Table 1. Positive and negative currents mean counter clockwise and clockwise currents, respectively, and we have found the corresponding voltages.

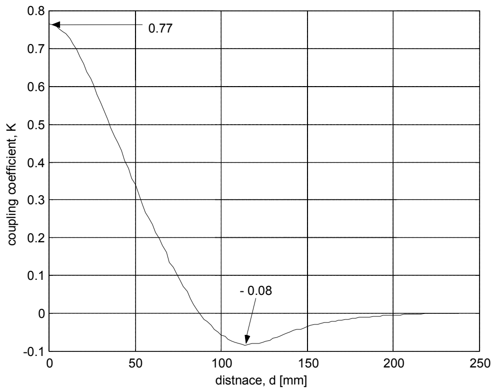

Figure 3. The measurement of coupling coefficients.

Table 1. The optimal currents with the corresponding voltages.

Coil number (current, voltage) (arbitrary unit)

30(13,7)	13(-31,-15)	14(124,67)	15(-30,-15)	16(8,4)	17(3,2)
29(-25,-12)	12(97,48)	3(-391,-213)	4(112,56)	5(-35,-17)	18(8,4)
28(66,34)	11(-258,-132)	2(989,567)	1(-316,-164)	6(115,61)	19(-34,-18)
27(-60,-31)	10(249,127)	9(-1000,-573)	8(346,182)	7(-139,-75)	20(45,24)
26(3,0)	25(-56,-24)	24(376,205)	23(-129,-66)	22(53,28)	21(-19,-10)
36(-2,-1)	35(9,3)	34(-114,-62)	33(37,18)	32(-17,-9)	31(2,1)

DISCUSSION

We proposed the model of multi-coil array analyzing the mutual coupling effects in multi-channel TMS. The coil arrays composed of multi-coil have variable structures such as a planar type, a cylindrical type, and a spherical type. The model of a planar type can be used to apply the numerical analysis without difficulty and provide the basis of the real model like as a cylindrical model or a spherical model. Because of the mutual coupling in multi-coil array, the error will be produced in the desired stimulation at the target point during the design of a multi-coil array without the considering of mutual coupling effect. According to the results of this paper, the multi-channel magnetic stimulator must be designed with the consideration of mutual inductance. For the more effective localization of taget point, also, the structure of a double-layer overlapped by two single-layers can be considered, but the trade-off is requested because the fabrication cost of a double-layer coil array is more expensive than that of a single-layer.

ACKNOWLEDGEMENTS

This work was supported by the grant from the next-generation new technology development program of the Ministry of Commerce, Industry and Energy, Republic of Korea.

REFERENCES

Bohning DE, Shastri A, McConnell KA, Nahas Z, Lorberbaum, Roberts DR, et al. A combined TMS/fMRI study of intensity-dependent TMS over motor cortex. Biol Psychiatry 1999;45:385-94.

Han BH, Chun IK, Lee SC, Lee SY. Multichannel magnetic stimulation system design considering mutual couplings among the stimulation coils. IEEE Trans Biomed Eng 2004;51:812-7.

Ruohonen J, Ravazzani P, Grandori F, Ilmoniemi R. Theory of multichannel magnetic stimulation: Toward functional neuromuscular rehabilitation. IEEE Trans Biomed Eng 1999;46:646-51.

Quantitative Results concerning Effects of Repetitive Transcranial Magnetic Stimulation on Mesoscopic Brain Activity

Holzner, O.T. and Schöll, E.

Institute of Theoretical Physics, Technical University Berlin, Germany

ABSTRACT

Phase transitions in the behavior of neuron populations depending on electromagnetic input as in repetitive transcranial magnetic stimulation ("rTMS") are calculated, based on mesoscopic evolution equations, which are generated from stochastic single neuron models capturing a variety of inputs. Wherever synchronization of firing in neuron populations is measurable, thereby model-based quantitative predictions of effects of rTMS on brain activity can, for the first time, be tested experimentally.

KEY WORDS

Quantitative rTMS modeling, mesoscopic density evolution, observable phase transition

INTRODUCTION

We consider the time, when a neuron fires, as essential information about this neuron, and assume that it takes mesoscopic pools of neurons firing in synchrony to generate in-vivo observable electromagnetic activity. We consider a pool as homogenous, and consisting of a multitude of spatially adjacent neurons. Therefore we can approximate transmission delays within the pool as zero, and describe coupling between members of the pool as mean-field-coupling (in a system with many constituents interacting with each other, the aggregate of these mutual interactions is replaced by a field, to which each constituent responds). We assume that, under a certain input, the firing behavior of a single neuron is adequately described by a phase oscillator model, in which a particular phase is identified with the firing of the neuron (e.g. Winfree model, see Ariaratnam & Strogatz 2001).

METHODS

$$d\theta_j = \left\{ \omega + \left[(\alpha / N) \sum_{k=1}^{N} \delta(\theta_k - 1) + \beta(t) \right] S(\theta_j) \right\} dt + c dB_j$$

We first slightly simplify the Winfree-model by considering one average firing frequency ω for all neurons in the pool, then enhance it to the single-neuron Ito-equation shown by allowing for input $\beta(t)$ from outside the pool considered, and adding white noise with a noise-level c. θ_j is the phase of a neuron j at time t. Phase is a real number between 0 and the firing event 1. N is the total number of neurons in the pool, α the mean-field-coupling-constant. $\delta(\theta_k\text{-}1)$ models the contribution of the k-th neuron to the mean field. S models phase-dependent sensitivity of the j-th neuron to any input whichever. We choose a unit-step function, i.e. $S(\theta_j)=0$ for $0<\theta_j<\varepsilon$ and $S(\theta_j)=1$ for $\theta_j>\varepsilon>0$, as an approximation to refractory behavior. We sometimes assume $\beta(t) = C$ (C called background) based on the assumption that a pool might be weakly coupled to a large number of other pools, and that memorized changes of the weighted sum of the inputs of these pools into the pool under consideration are slow compared to changes in pool density / firing function under consideration. $\beta(t)$ may include a term $b \cdot \eta(t)$. $\eta(t)$ is exogenous input, which is assumed to enter the Ito-equation multiplied with a fixed translation parameter b (for the respective pool). Arbitrary input can either be simulated directly, or decomposed into a sequence of constant inputs. To explore the onset of observable rTMS effects, we mostly vary intensities (starting from zero) for some fixed prototypical intervention frequency (e.g. 20 discharges / time unit). The capacitors used in rTMS create induction-related phase shifts which are small compared to the time-scale of single-neural firing. Therefore we take η to be proportional to the coil current, the latter assumed to be biphasic as in Reilly 1998, p.398, fig. 9.24.

Aggregating the Ito-equation over the pool, and including memory effects via an impact function v (determined by the second equation) we obtain:

$$\frac{\partial}{\partial t} u(\psi,t) = \frac{c^2}{2} \frac{\partial^2}{\partial \psi^2} u(\psi,t) - \omega \frac{\partial}{\partial \psi} u(\psi,t) - v(t) \frac{\partial}{\partial \psi} [S(\psi) \cdot u(\psi,t)] \qquad \frac{dv}{dt} = -\lambda [v(t) - \alpha f(t) - \beta(t)]$$

$u(\psi,t)$ is the number density of neurons at a phase ψ at time t. $f(t) := u(1,t)$ is called firing function (percentage of oscillators infinitesimally close to the firing event) and assumed to be observable. λ is a decay constant. For two and more pools we replace $\beta(t)$ by background, weighted inputs from other pools, and weighted exogenous input, and allow for transmission delays τ between pools (w_{ij} is the weight for input from pool i to pool j):

$$\frac{\partial}{\partial t} u_{1,2}(\psi,t) = \frac{c^2}{2} \frac{\partial^2}{\partial \psi^2} u_{1,2}(\psi,t) - \omega_{1,2} \frac{\partial}{\partial \psi} u_{1,2}(\psi,t) - v_{1,2}(t) \frac{\partial}{\partial \psi} [S_{1,2}(\psi) \cdot u_{1,2}(\psi,t)] \qquad \frac{dv_{1,2}}{dt} = -\lambda_{1,2} [v_{1,2}(t) - \alpha_{1,2} f_{1,2}(t) - C - b_{1,2} \eta(t) - w_{21,12} f_{2,1}(t-\tau)]$$

The solution of these equations was simulated numerically (forward Euler, step size 10^{-6}, phase mesh width 10^{-3}), starting from a normalized superposition of Gaussian initial densities. We use dimensionless units throughout, scaling is performed as part of local calibration (see discussion). From firing functions of two different pools their phases ϕ_1, ϕ_2 are calculated via Hilbert transform. For small integers m, n m:n phase locking is defined by boundedness of the generalized phase difference $\Delta_{m,n} := m\phi_1 - n\phi_2$ (Tass et al 1998).

RESULTS

The behavior of a pool under various constant inputs (e.g. backgrounds) C is shown in figure 1: For positive input in the range displayed, periods between two subsequent maxima of the firing function decrease hyperbolically with increasing C, i.e. the frequency response is linear in C.

For fixed background and intervention frequency, period changes are linear with respect to intensity of rTMS pulses (for the parameter regions explored). The period changes achieved under otherwise equal conditions depends strongly on the background C (factors of up to 5 were simulated). Intervention frequency also has a background-dependent effect on period responses. A prototypical response to rTMS is shown in figure 2.

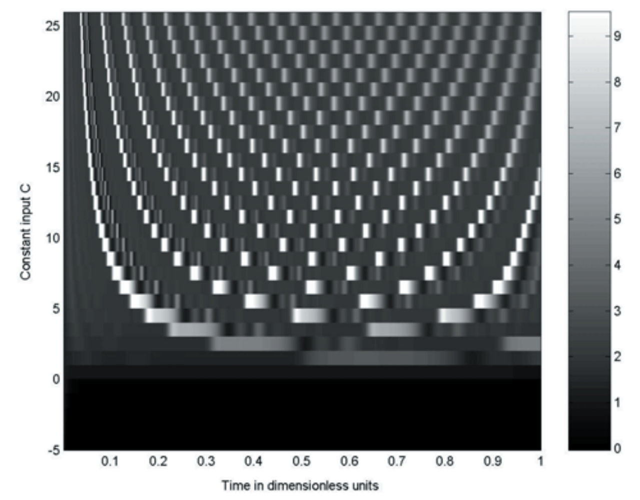

Figure 1. Firing function f for C = $\beta(t)$, greyscale = amplitude of f
Pool parameters: $\lambda = 100$, $\omega = 1$, $\alpha = -1$, c=0.03, $\varepsilon = 0.005$

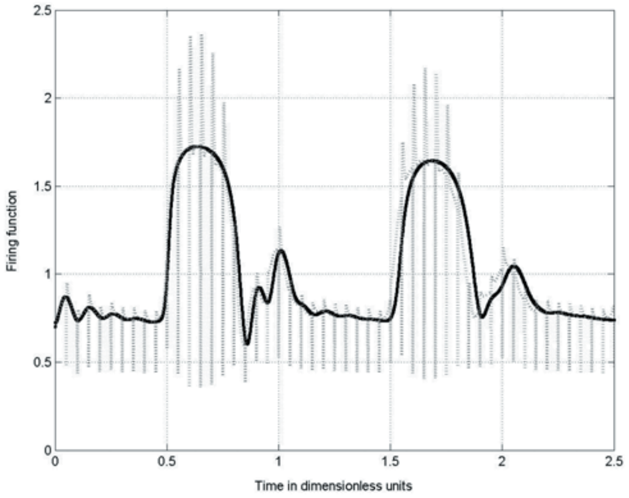

Figure 2. Firing function f for C = 1, solid line: no rTMS, dotted line: rTMS (20 pulses /unit), pool parameters as in fig. 1

rTMS can induce phase transitions in connected multi-pools at much lower intensities than necessary for single-pool frequency shifts. As an example, we consider two dissimilar pools, linked with a transmission delay, and provided with different connection weights. For the parameters given, without rTMS, pools 1 and 2 display 1:2 phase-locking (solid black line in fig. 3). For rTMS at 25% of the intensity used in fig. 2, at the same intervention frequency, the 1:2 generalized phase difference is kicked from the orbit, and finally drifts away (grey dotted line). Figure 3 shows these effects in delay coordinate representation of $\Delta_{1,2}$.

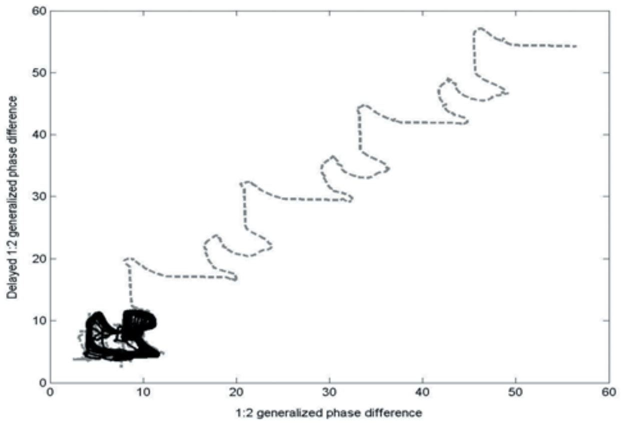

Figure 3. Embedded generalized phase difference. Pool parameters: C =4, c=0.03, λ_1=100, $3\omega_1=3=3\omega_2$, $3\alpha_1=-3=\alpha_2$, λ_2=300, ε_1= 0.005, ϵ_2 = 0.003, Connection parameters: $\tau = 0.005$ 4 $w_{21} = w_{12} = 2.0$, Translation parameters: $b_1 = 1.05$, $b_2 = 0.95$

DISCUSSION

Time scaling and knowledge of (in-vivo not observable) pool parameters can be obtained by local calibration (see Holzner 2004), during which the pool responses to test signals are measured and used for inferring pool parameters, as well as translation parameters of rTMS signals (determined by e.g. coil location, geometry, orientation, polarity, amplitude, intervention frequency). For example knowledge of the background considerably improves intervention efficiency with respect to one pool. Analogously translocal calibration (Holzner 2004) will use the impact of test signals on groups of pools to gauge their connection parameters (e.g. weight ratio, transmission delays). As one effect of different translation parameters (because e.g. pool locations have a different distance to the coil, or neural orientations differ) in connected mesoscopic pools, rTMS-induced break-up of phase locking has been demonstrated. Once relevant local, translation, and connection parameters have been calibrated, effects of rTMS on a network of pools can be predicted quantitatively. As pool responses are asumed to be measurable, these predictions allow for experimental testing of models, calibrations, intervention strategies, thereby opening the road to optimizing practically every application of TMS on neural pools.

ACKNOWLEDGEMENTS

We gratefully acknowledge stimulating discussions with Kevin Dolan, Peter Tass (both Institute of Medicine, Research Centre Juelich), and Andreas Amann (Institute of Theoretical Physics, Technical University Berlin).

REFERENCES

Ariaratnam JT, Strogatz SH. Phase Diagram for the Winfree Model of Coupled Neural Oscillators. Physical Rev. Letters 2001; 86(19): p. 4278-81.

Holzner OT. Model-based modification of brain activity. Master thesis, Berlin 2004, available from http://wwwnlds.physik.tu-berlin.de/~holzner.

Reilly JP. Applied Bioelectricity. Berlin: Springer; 1996.

Tass P, Kurths J, Rosenblum MG, Weule J, Pikovsky A, Volkmann J, et al. Complex Phase Synchronization in Neurophysiological Data. In Uhl C, editor. Analysis of Neurophysiological Brain Functioning. Berlin: Springer; 1998.

Optimum Coil Configuration in Magnetic Stimulation Therapy for Urinary Incontinence

M. Odagaki, K. Suga, T. Sasaki, H. Hosaka

Graduate school of Science and Engineering, Tokyo Denki University, Japan

ABSTRACT

It has been reported that magnetic stimulation effectively eliminates urinary incontinence. However, this type of therapy has not been established as a practical treatment for urinary incontinence because of its poor power conversion efficiency and the leakage of current to regions other than that of the target of stimulation. It is therefore necessary to develop magnetic stimulators that are more efficient in stimulating the sphincter muscles and the peripheral nerves, and are more convenient than those presently available. By using a large-diameter coil, the magnetic stimulation method offers a larger current distribution over a wider area of the target region than electrical stimulation method, and the placement of the coil can be relatively easily changed to obtain better therapeutic results. We attempted, with a computer simulation model of the female abdomen, to simulate the distribution of the induced current density on the basis of biological tissue conductivity. Finally, we determined which method of stimulation is the most efficient by varying the stimulator coil location and size. A genetic algorithm (GA) was used for optimization.

KEY WORDS

Magnetic stimulation, Genetic algorithm, Finite element method, Urinary incontinence

INTRODUCTION

The authors have reported that comparisons of the current distributions resulting from electrical and magnetic stimulation, and calculations based on the relevant data showed that the magnetic stimulation method using a large-diameter coil offers a current distribution over a wide area of the target region. The stimulating coil can be relatively easily shifted to obtain better therapeutic results. In this paper, we consider how to optimize stimulation by changing the coil placement and diameter in the treatment of urinary incontinence, and how to get the best result.

METHODS

Computer models are used in some basic studies of magnetic stimulation, and they provide for more quantitative and detailed analyses of the spatial distribution of current density. Model studies have been used to find out how currents are induced in the living body by time varying magnetic fields.

A three-dimensional inhomogeneous abdomen model is shown in Figure 1. The conductivities of biological tissues are known to be as follows: Muscle, 0.04 S/m; fat and bone, 0.04 S/m, and rectum, 0 S/m. Since the rectum is filled with gas, its conductivity is lower than those of other regions. In our computations, the conductivity of the rectal region was defined as 0. The totals of nodes and elements were 8894 and 53032, respectively.

The genetic algorithm (GA) is a machine learning model of an effective resolution algorithm for optimization problems, that is based on the evolutionary patterns of nature. In this paper, the genetic algorithm was combined with the finite element method. Figure 2 shows a drawing of a cross section of a female abdomen, prepared from a simulation model and representing only muscle, bone, fat. The circled and shaded areas indicate regions of pelvic floor musculature, in particular, the sphincter muscles around the anus and vagina. It is known that stimulation of the pelvic floor muscles lying between the pubis and the coccyx illustrated in Figure 2 is an efficient technique for improving urinary incontinence. Magnetic stimulation can be used for this purpose, and can eliminate this type of incontinence. It is desirable to carry out the stimulation on a focal area of the pelvic floor muscle. The stimulation index was defined as follows for investigation of the current density distribution in the pelvic floor muscles. Estimation of the stimulation efficacy for a given coil configuration can be made using Equation 1.

$$Stimulation \quad index == \frac{\sum_{i=1}^{M}\left|J_i\right|}{\sum_{j=1}^{N}\left|J_j\right|} \qquad (1)$$

where the numerator indicates the summation of current density in the pelvic floor muscle, and the denominator, the summation of current density in the three transverse slice images examined immediately above the lowest image (that is, between 10 and 30 mm above the lowest image). The stimulation index indicates the current distribution efficiency. This index can be useful for improving the localization of current distribution in the target

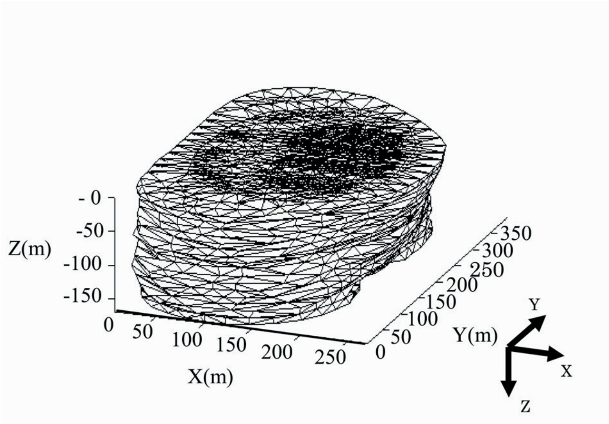

Fig. 1 Computer simulation model.

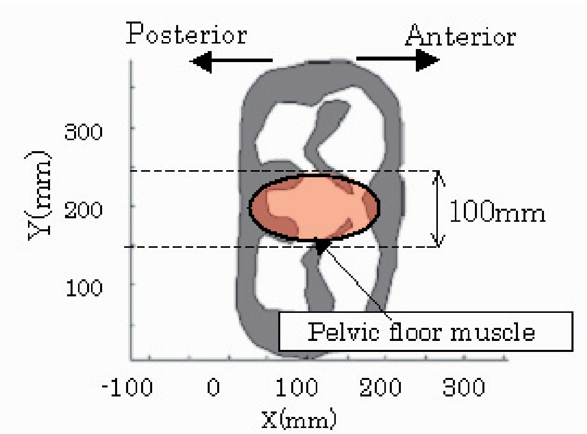

Fig. 2 Stimulation target.

plane by adjusting the placement of the mounted coil and the finite element model.

RESULTS

Figure 3 shows the results of the calculation of GA as far as the 100 th generation. The abscissa represents the generation number, while the ordinate indicates the average value of the stimulation index for each generation and the maximum value up to that generation. Examination of Figure 3 reveals both the rapid rise of the of the average stimulation index by about the tenth generation, and a tendency, with each subsequent generation, for the current to become more concentrated in the muscle groups of the pelvic floor. With further computation, it was possible to confirm that the average and maximum values had both stabilized, and that the stimulation indices from the 34th generation to the 100th generation had a maximum value of 0.428. At that time, the coil diameter, R, was 56.4 mm and the location, X, of the coil was 143 mm posterior to the front border of the mode. The distribution of current is shown in Figure 4, together with the idealized location of the coil. It is clear from Figure 4 that there is an extensive distribution of current in the musculature of the pelvic floor. In the conditions shown, the stimulating coil had 24 turns, and during magnetic stimulation the current was 1 kA, with a frequency of 1.5 kHz.

Ideal coil shape and size were determined from the effects of the low electric conductivity of the pelvis and the rectum. Since the pelvic floor musculature is relatively close to the surface of the body, a small coil diameter reduces the degree of penetration of the magnetic field, but it is possible for the current distributed through the pelvic floor muscles to surpass the threshold value.

DISCUSSION

Changing the coil placement and diameter with the help of GA improved the stimulation index, and the conditions for maximum stimulation were determined by the efficiency of current distribution in the muscles of the pelvic floor. As seen in Figure 4, this method of stimulation offered an extensive current distribution over the pelvic floor musculature.

In order to determine in a similar manner, for simulation models other than the present one, whether optimization of coil placement is possible, the sizes of the models have been changed, and similar calculations have been tried. The size in the direction (anterior - posterior) of the X axis of the simulation model was increased by approximately 140%. The result was that the maximum value of the stimulation index up to the 100 th generation was 0.487. In two simulation models, the maximum values of the stimulation indices and the coil placements and diameters at the same times are shown in Table 1. The coil placements for the figures in Table 1 were 165 mm. Similarly to the results shown in Figure 4, the positioning was almost at the center, and the coil diameter was 66% of the extent of the pelvic floor musculature, a little larger than is shown in Figure 4. It was realized that, when individual differences were taken into account in this way, the application of GA was possible.

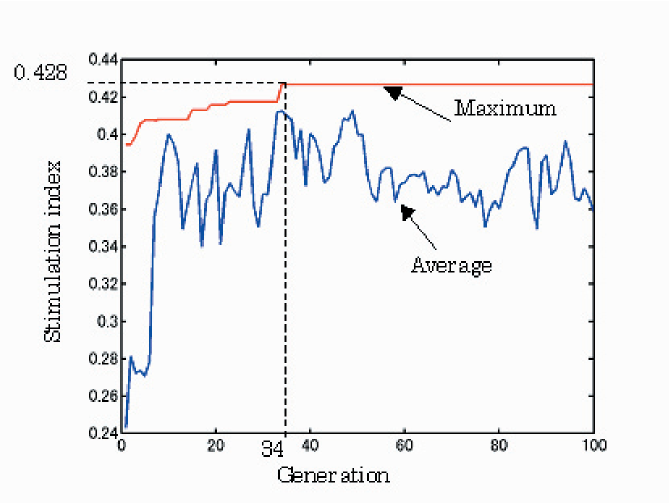

Fig. 3 The process of calculations.

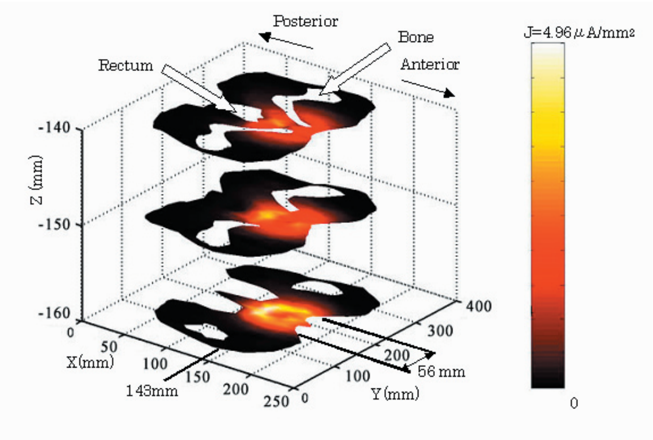

Fig. 4 Current distribution induced by magnetic stimulation using a circular coil of diameter 56 mm.

Table. 1 Comparison of simulation results

Body size ratio	1	1.4
Stimulation index	0.428	0.487
Coil diameter (mm)	56	66
Coil location (mm)	+4	+32

REFERENCES

Ishikawa N, Suda S, Sasaki T, Ymanishi T, Hosaka H, Yasuda K, Ito H. Development of a non-invasive treatment system for urinary incontinence using a functional continuous magnetic stimulator (FCMS). Med. Biol. Eng. Comput. 1998; 36: p. 704- 10

Odagaki M, Suga K, Sasaki T, Cohen D, Hosaka H. Comparison of current distributions between electrical and magnetic stimulation for treatment of urinary incontinence using a computer model. Proceeding of IEEE EMBS 24th International Congress; 2002 U. S. A. Houston; 2002

Odagaki M, Suga K, Sasaki S, Yunokuchi K, Hosaka H. Efficiency of electrical and magnetic stimulation for treatment of urinary incontinence. Transactions of the Japanese Society for Medical and Biological Engineering 2003; 41: p. 213-220

P6-5

Numerical Calculation of Eddy Currents in Transcranial Magnetic Stimulation for Psychiatric Treatment

Sekino, M. and Ueno, S.

Department of Biomedical Engineering, Graduate School of Medicine, University of Tokyo, Japan

ABSTRACT

In this study, current distributions in transcranial magnetic stimulation (TMS) were calculated under various conditions and compared with the current distribution in electroconvulsive therapy (ECT) in order to find an optimum condition of TMS as an alternative to ECT. Current distributions in TMS were obtained for the following coil shapes and coil diameters: circular coils of 50 mm, 75 mm, 100 mm, 125 mm, and 150 mm, and figure-eight coils of 50 mm, 75 mm, 100 mm, and 125 mm. Evaluative performance function F increases with the difference in current distributions between ECT and TMS. The minimum value of F decreased with an increase in the coil diameter. In the case of a 150-mm circular coil, the performance function had a minimum value of 6.3 A^2/m^4 at a coil current of 29 kA, which corresponded to a magnetic flux density of 0.24 T. A coil position on the forehead and the use of a large circular coil gave better results.

KEY WORDS

Transcranial magnetic stimulation, electroconvulsive therapy, finite element method

INTRODUCTION

Electroconvulsive therapy (ECT) is a treatment method for severe mental illnesses, such as depression, by an application of electric current to the brain. Transcranial magnetic stimulation (TMS) is a method for stimulating the brain by applications of a pulsed magnetic field and a resulting eddy current [Barker, 1985] [Ueno, 1990]. Though psychiatric treatments by TMS have been tried in numerous studies, the effect of TMS is still not clear. An appropriate approach to the initial attempt of TMS therapy is to find a stimulus condition which gives a current distribution in the brain similar to ECT. In previous studies, current distributions in ECT and TMS were compared using numerical simulations [Sekino, 2002] [Nadeem, 2003] [Sekino, 2004]. However, all of these simulations used only the figure-eight coils in TMS. In the present study, we obtained current distributions in TMS for circular coils and figure-eight coils under various stimulus parameters. Current distributions in ECT and TMS were compared to find the optimum conditions of TMS as an alternative to ECT.

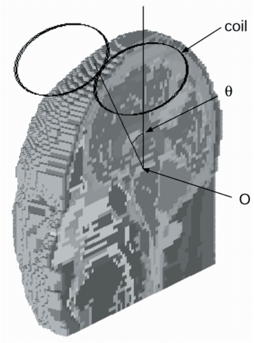

Figure 1. Numerical model of transcranial magnetic stimulation (TMS) with a 75-mm figure-eight coil.

METHODS

We used the three-dimensional human head model shown in figure 1 [Brooks Air Force Laboratory]. Electrical conductivities of the tissues were determined using the 4-Cole-Cole model [Cole, 1941] and Gabriels' database of dielectric properties [Gabriel, 1996]. Though the original model had a spatial resolution of 1 mm, we reconstructed the model with a resolution of 3 mm to reduce the computation time. The numbers of nodes and elements were 189975 and 177649, respectively. Numerical solutions were obtained using the finite element method, as described in a previous paper [Sekino, 2004]. As a typical condition of ECT, a voltage of 100 V was applied between a pair of electrodes place on the tempora. Electric potentials were set to 137 nodes for each electrode, which corresponded to an electrode area of approximately 13 cm^2. Current distributions in TMS were simulated for the following coil shapes and diameters: circular coils of 50 mm, 75 mm, 100 mm, 125 mm, and 150 mm, and figure-eight coils of 50 mm, 75 mm, 100 mm, and 125 mm. Figure 1 shows the TMS model with the 75-mm figure-eight coil. To investigate the dependence of eddy current distributions on the coil position, the coil was rotated around the center of the head, O, at angle θ, from the vertex toward the forehead ($\theta = 30^o$ in fig. 1(b)). The pulse duration of TMS was 240 μs. The difference in current distributions between ECT and TMS was evaluated using a performance function,

$$F = \frac{1}{V_0}\int_{\text{cerebrum}} \left(|\mathbf{j}_E| - |\mathbf{j}_T|\right)^2 dV \tag{1}$$

where V_0 is the volume of the cerebrum, $\mathbf{j}_E$ is the current density in ECT, and $\mathbf{j}_T$ is the current density in TMS. Integration was performed covering the elements included in the cerebrum. Because this function increases with the difference in current distributions between ECT and TMS, the optimum condition of TMS gives a minimum value of the function.

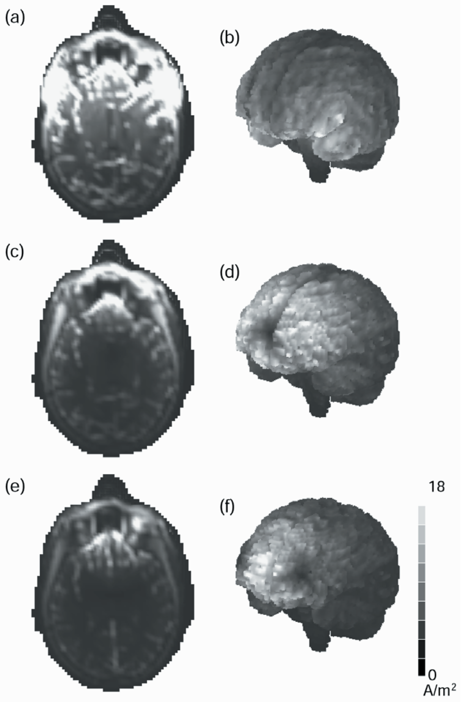

Figure 2. (a)(b) Current distributions in ECT. (c)(d) Current distributions in TMS by a 100-mm circular coil. (e)(f) Current distributions in TMS by a 75-mm figure-eight coil.

RESULTS AND DISCUSSION

Figures 2(a)(b) show current distributions in ECT on a transversal slice and the brain surface. The scalp under the electrodes located on the temora exhibited the maximum current density of 543 A/m^2. Because the skull had a relatively low conductivity, a significant amount of the current flowed along the scalp and did not penetrate the skull.

Because the electrodes were located on opposite sides of the brain, the injected currents were distributed across the brain and extended to the deeper regions. The white matter tissues at the center of the brain exhibited current densities of approximately 5 A/m^2, while the frontal cortex exhibited higher ones, and the maximum current density within the brain was 22 A/m^2.

Figures 2(c)(d) show current distributions in TMS on a transversal slice and the brain surface. The stimulation was applied by a 100-mm circular coil at the position $\theta = 60^{o}$ with a coil current of 45 kA. Figures 2(e)(f) show current distributions in TMS by a 75-mm figure-eight coil. Maximum current densities in the whole model for the circular coil and the figure-eight coil were 53 A/m^2 and 64 A/m^2, respectively. The two coil elements of the figure-eight coil induced eddy currents in the same direction under the intersection. The brain surface under the intersection of the coil exhibited high current density values. The circular coil induced more widespread eddy currents compared to the figure-eight coil. Maximum current densities in the brain for the circular coil and the figure-eight coil were 26 A/m^2 and 27 A/m^2, respectively, which were comparable to the current densities in ECT. The current densities at the center of the brain were below 2 A/m^2, which was much smaller compared to the case of ECT. Coils with smaller diameters induced more localized eddy currents and exhibited less extension to deep regions.

Figures 3(a)(b) show the dependence of the performance function F on the coil current and the coil position. The stimulations were applied from a 100-mm circular coil and a 75-mm figure-eight coil at coil angles θ varying from 0^{o} to 60^{o}. The minimum value of F decreased with an increase of the coil angle. At larger coil angles, the coil approached the electrode positions in ECT, and generated currents in the forehead. The coil angle was limited to 60^{o} in order to avoid interference between it and the nose. In the case of the 100-mm circular coil at $\theta = 60^{o}$, the performance function had a minimum value of 6.9 A^2/m^4 at a coil current of 41 kA, which corresponded to a magnetic flux density of 0.52 T at the center of the coil. In the case of the 75-mm figure-eight coil at $\theta = 60^{o}$, the performance function had a minimum value of 9.5 A^2/m^4 at a coil current of 53 kA.

Figures 4(a)(b) show the dependence of the performance function F on the coil current and the coil diameter. Data were presented for circular coils of 50 mm, 75 mm, 100 mm, 125 mm, and 150 mm, and figure-eight coils of 50 mm, 75 mm, 100 mm, and 125 mm with a constant coil position of $\theta = 60^{o}$. The minimum value of F decreased with an increase in the coil diameter, which was because eddy currents induced by larger coils were distributed in larger and deeper areas. Thus, the use of larger coils is desired to obtain current distributions similar to ECT. The 150-mm circular coil gave the best result in our simulation. In the case of the 150-mm circular coil, the performance function had a minimum value of 6.3 A^2/m^4 at a coil current of 29 kA, which corresponded to a magnetic flux density of 0.24 T. The coil current corresponding to the minimum value of F was significantly affected by the coil diameter, so the coil current should be carefully determined for coils with different diameters. The coil current giving the minimum value of F decreased with an increase in the coil diameter because large coils produced higher current densities in the side of the brain.

In this study, stimulus conditions of TMS were optimized based on numerical simulations. In conclusion, a coil position on the forehead and the use of a large circular coil gave the best result.

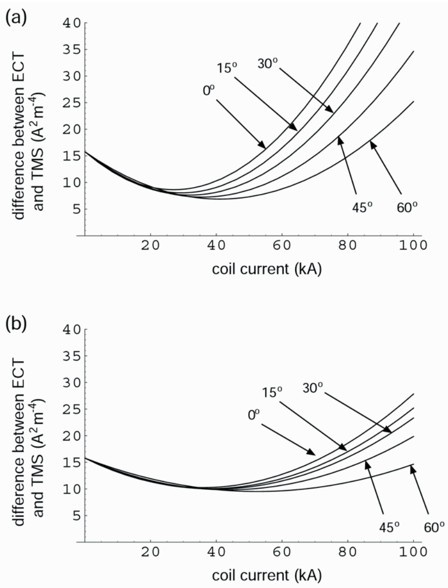

Figure 3. Dependence of the performance function F (equation (1)) on the coil current and the coil position for (a) circular coils and (b) figure-eight coils. The coil position is represented by angle θ from the vertex.

ACKNOWLEDGEMENTS

This study was supported by a grant from the Magnetic Health Science Foundation, a Grant-in-Aid for Specially Promoted Research (No. 12002002) and a Grant-in-Aid for JSPS Fellows from the Ministry of Education, Culture, Sports, Science and Technology, Japan.

REFERENCES

Barker AT, Jalinous R, Freeston IL. Noninvasive magnetic stimulation of human motor cortex. Lancet 1985;2:1106-7.

Brooks Air Force Laboratory: www.brooks.af.mil/AFRL/HED/hedr/dosimetry.html

Cole KS, Cole RH. Dispersion and absorption in dielectrics: Alternating current characteristics. J Chem Phys 1941;9:341-51.

Gabriel C, Gabriel S, Corthout E. The dielectric properties of biological tissues: I. literature survey. Phys Med Biol 1996;41:2231-49.

Nadeem M, Thorlin T, Gandhi OP, Persson M. Computation of electric and magnetic stimulation in human head using the 3-D impedance method. IEEE Trans Biomed Eng 2003;50:900-7.

Sekino M, Ueno S. Comparison of current distributions in electroconvulsive therapy and transcranial magnetic stimulation. J Appl Phys 2002;91:8730-2.

Sekino M, Ueno S. FEM based determination of optimum current distribution in transcranial magnetic stimulation as an alternative to electroconvulsive therapy. IEEE Trans Magn 2004 (in press).

Ueno S, Matsuda T, Fujiki M. Vectorial and focal magnetic stimulation of the brain for the understanding of the functional organization of the brain. IEEE Trans Magn 1990;26:1539-44.

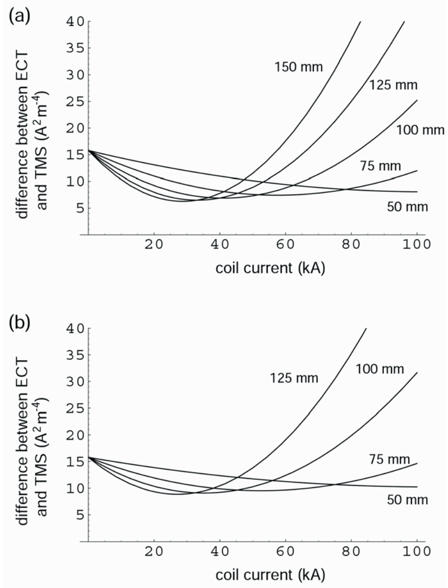

Figure 4. Dependence of the performance function F on the coil current and the coil diameter for (a) circular coils and (b) figure-eight coils.

Cutaneous Sensation Block Induced by Navigated Brain Stimulation of SI

H. Hannula[1,5], S. Ylioja[2,5], A. Pertovaara[3], A. Korvenoja[4,5], J. Ruohonen[1], R.J. Ilmoniemi[1,5], S. Carlson[2,5]
[1]Nexstim Ltd., Helsinki, Finland, [2]Neuroscience Unit, Institute of Biomedicine/Physiology, University of Helsinki, Finland,
[3]Department of Physiology, University of Turku, Finland, [4]Helsinki Medical Imaging Center, University of Helsinki, Finland,
[5]Helsinki Brain Research Center, Finland

Earlier transcranial magnetic stimulation (TMS) studies reporting blocking of cutaneous sensation have involved sensory-motor cortex stimulation, and it is unclear whether MI or SI mediates the TMS-induced block of sensation [1]. We demonstrate with Navigated Brain Stimulation (NBS) that it is possible to direct the TMS pulse selectively to the SI to produce block of sensations from the respective skin area. Real-time computation of the coil's intracranial electric field enabled accurate and reproducible cortical stimulation. EMG responses were recorded to ensure that TMS induced no motor response. The critical time window for blocking sensation was determined by varying the delays (20, 50, 100, 150, 250 ms) between cutaneous and TMS stimulation. Randomly ordered test sequences included real and sham TMS combined with real or sham cutaneous stimulus. Subjects rated cutaneous sensations using a three-category rating scale. Responses were analyzed using signal detection theory. Blocking was maximal when cutaneous stimulation occured 20 to 50 ms before the TMS pulse, delivered behind the precentral gyrus posterior to the corresponding motor area. TMS applied 150 ms after cutaneous stimulation could no longer block the sensation. The cortical area where TMS produced blocking of sensation was approximately 15 mm x 15 mm. It is concluded that NBS-controlled TMS of SI is sufficient for blocking sensation from the respective skin area.

[1] McKay D.R., et al., 2003. Magnetic stimulation of motor and somatosensory cortices suppresses perception of ulnar nerve stimuli. International Journal of Psychophysiology 48, 25-33.

Response Map of Evoked EEG by Transcranial Magnetic Stimulation

K. Iramina, T. Maeno, S. Ueno
Department of Biomedical Engineering, The University of Tokyo

The evoked potential induced by stimulating at cerebellum by TMS(transcranial magnetic stimulation) was measured and the reaction map of the TMS over the cerebellum for observing the neuronal connectivity in the brain were obtained in this study. An EEG measurement system to eliminate the electromagnetic interaction emitted from TMS was used. EEG activities 5 ms after TMS stimulation were successfully measured. There were several components of evoked potential after stimulation, at 10 ms, 25 ms and 50 ms. A large response of evoked potential appeared at about 10 ms after TMS when the cerebellum was stimulated. Reaction maps of the stimulation at the occipital area were obtained using the 9 ms evoked potential component. From the reaction map, it is possible to consider that the fast component of evoked signal by TMS to the cerebellum was conducted posteriorly to anteriorly along the pathways of the neuronal fiber exiting the cerebellum to cerebral cortex. The response at the right brain was large when the left cerebellum was stimulated. The response at the left brain was large when the right cerebellum was stimulated. The response map of the TMS gave information of the neuronal connectivity. TMS will become a useful tool for the study of cortical reactivity and neuronal connectivity of the brain.

Associative plasticity of the motor cortex induced by movement-related transcranial magnetic stimulation (TMS)

Yoshino Ueki, Tatsuya Mima, Mamdouh Ali Kotb, Keiichiro Toma, Hidenao Fukuyama, Takashi Nagamine
Human Brain Research Center, Kyoto University Graduate School of Medicine, Japan

An interventional paired associative stimulation combining the peripheral nerve and the cortical stimulation can increase the excitability of motor cortex beyond the period of stimulation. The aim of this study is to elucidate whether movement- related transcranial magnetic stimulation (TMS) over the primary motor cortex (M1) can induce the similar associative plasticity. In 9 healthy volunteers, two sets of TMS (0.2Hz, 20minutes) were applied combining with the visually-triggered movement of the right abductor pollicis brevis (APB) at the different timing on separate days. Subjects were instructed to contract their right APB, immediately after the visual stimulus presented at 0.2Hz. Suprathreshold TMS was given over the left M1 at pre- or post- 50ms of average reaction time. MEP amplitude, motor threshold and pinching power were measured before (baseline), immediately after, 15 minutes and 30 minutes after intervention. Pre-movement-related TMS produced an increase in the MEP amplitude of the right APB muscle (MEP amplitude ratio; 1.64 (immediately after), 1.26 (15 minutes after), 0.9 (30 minutes after)), whereas post-movement-related TMS had no significant effect on the MEP amplitude. Either pre- and post-movement-related TMS failed to alter the motor threshold and pinching power. Movement-related TMS can increase the motor excitability when TMS was given prior to the movement. This timing-dependent effect of movement-related TMS may be an another example of temporally asymmetric Hebbian rule.